Eel density analysis (EDA 2.2.1). Escapement of silver eels (Anguilla anguilla) from French rivers. 2018 report

Technical Report · August 2018

CITATIONS
3

READS
385

5 authors, including:

Cedric Briand
EPTB Vilaine
49 PUBLICATIONS **582** CITATIONS
SEE PROFILE

Laurent Beaulaton
Office Français de la Biodiversité (OFB)
59 PUBLICATIONS **648** CITATIONS
SEE PROFILE

Hilaire Drouineau
French National Institute for Agriculture, Food, and Environment (INRAE)
73 PUBLICATIONS **718** CITATIONS
SEE PROFILE

Patrick Lambert
French National Institute for Agriculture, Food, and Environment (INRAE)
90 PUBLICATIONS **882** CITATIONS
SEE PROFILE

Eel density analysis (EDA 2.2.1)

Escapement of silver eels (*Anguilla anguilla*) from French rivers

---

2018 report

Cédric Briand (1), Pierre-Marie Chapon (2), Laurent Beaulaton (2) , Hilaire Drouineau (3), Patrick Lambert (3).

(1) **EPTB-Vilaine** (2) **AFB-INRA** (3) **IRSTEA**

version 2.2.1, 29th September 2018

Abstract

Résumé

EDA (Eel Density Analysis) est un outil de modélisation qui permet de prédire les densités d'anguilles jaunes et l'échappement d'anguilles argentées à partir des données des réseaux de pêches électriques. La version 2018 d'EDA (version 2.2.1) est basée sur un jeu de données de 29 183 opérations de pêches électriques contre 24 541 pour la version de 2015 (version 2.2.0) et 9 556 pour la version EDA 2.1 de 2012. L'augmentation du jeu de données s'explique par l'intégration des pêches en milieu profond et des données des réseaux spécifiques anguilles. Le modèle se distingue également par la prédiction des densités par classes de tailles séparées par les bornes 150, 300, 450, 600 et 750 mm. Il donne une estimation des biomasses produites sur le territoire Français métropolitain à 1.724 ± (1.242, 2.27) millions d'anguilles argentées en 2015. Le modèle qui prédit les départs d'argentées permettra d'intégrer les impacts anthropiques liés aux turbines et à la pêche pour produire une estimation des indicateurs de stock Bcurrent, Bbest demandés pour le rapportage de 2018.

Mots clés: anguille, densité, anguille argentée, modèle de production, stock, France, UGA, modèle EDA, règlement CE 110/2007

Abstract

EDA (Eel Density Analysis) is a modelling tool which allows the prediction of yellow eel densities and silver eel escapement from electrofishing survey networks. The 2018 version of EDA (2.2.1) is based on a dataset of 29183 electrofishing operations compared to 24 541 for 2015 (version 2.2.0) and only 9 556 in the 2012 version (2.1). The larger dataset is explained by the inclusion of deep water electrofishing operations and the eel specific surveys. The model distinguishes from its 2012 (2.1) version by the prediction of eel abundance per size class, separated with boundaries 150, 300, 450, 600 and 750 mm. The model estimates the eel biomass on the French territory at 1.724 ± (1.242, 2.27) millions of silver eels in 2015.

Anthropogenic impacts corresponding to the glass eel fisheries, amateur and commercial yellow eel fisheries, silver eel fisheries and turbine mortalities, will be included in the model to produce stock indicators Bcurrent, Bbest mandatory for the 2018 postevaluation of the eel management plan.

Keywords: Eel, migration, Silver eel, production model, stock, France, EDA model, EU regulation 110/2007

Contexte

Depuis les années 1980, les arrivées de civelles d'anguilles européennes (*Anguilla anguilla*) ont diminué à un niveau entre 4 et 12 % de leur niveau de référence entre 1960-1979 (ICES, 2017). Pour enrayer le déclin de l'anguille européenne observé depuis la fin des années 70, le règlement européen 1100/2007, qui se décline dans des plans de gestion nationaux, fixe comme objectif global 'd'assurer un taux d'échappement d'au moins 40 % de la biomasse d'anguilles argentées [...] d'un stock n'ayant subi aucune influence anthropique'.
Le rapportage à la commission par les états membres de l'UE doit permettre d'évaluer le niveau actuel d'échappement en anguilles argentées et de fournir une estimation de la mortalité d'origine anthropique affectant le stock d'anguilles en France. Les dates de rapportage prévues dans le règlement sont 2012, 2015 et 2018. Le modèle EDA 1.3 a été utilisé pour produire une première estimation de la biomasse d'anguilles argentées s'échappant du territoire lors de la mise en place du plan de gestion répondant au règlement. En 2012, pour le premier rapportage, la version EDA 2.1 a été utilisée pour fournir une nouvelle estimation des biomasses produites. La version du modèle (2.2.0) a permis de mieux prendre en compte le calcul des impacts anthropiques et de limiter l'incertitude quand aux productions d'anguilles argentées pour les milieux profonds. Cette version du modèle 2.2.1 est simplement une mise à jour des données avec l'ajout de trois années de 2012 à 2015. Il a été traduit en anglais pour faciliter l'échange et l'évaluation du modèle dans le cadre du rapportage.

Les auteurs

- Cédric Briand, Responsable du pôle milieu naturel et animation bassin, cedric.briand@eptb-vilaine.fr, EPTB-Vilaine
  Calibration du modèle, construction des bases de données Postgres avec Pierre-Marie, rapport & figures. Cartes avec Benjamin Magand (EPTB Vilaine).
- Laurent Beaulaton, chef du pôle AFB-INRA, laurent.beaulaton@afbiodiversite.fr, AFB
  Modèle d'argenture, supervision, coordination et relecture.
- Pierre -Marie Chapon, pôle ONEMA-INRA, pierre-marie.chapon@onema.fr, ONEMA.
  Compilation des données, validation des étapes de la construction des jeux de données du modèle, construction des bases excel, centralisation et échanges avec les acteurs de terrain.
- Hilaire Drouineau, Ingénieur de recherches, hilaire.drouineau@irstea.fr, IRSTEA Bordeaux, pôle écohydraulique ONEMA-IMFT-IRSTEA.
  Assistance technique et évaluation, relecture.
- Patrick Lambert, Ingénieur de recherches, patrick.lambert@irstea.fr, IRSTEA Bordeaux, pôle écohydraulique ONEMA-IMFT-IRSTEA.
  Assistance technique et évaluation, responsable du développment du modèle EDA pour l'IRSTEA.

Contents

List of Figures

List of Tables

Première partie

Résumé opérationnel (en Français)

Le modèle EDA 2.2.1 prédit les abondances d'anguilles jaunes, puis argentées à partir des nombres d'anguilles mesurés lors des pêches électriques en France. Le réseau hydrographique théorique est utilisé pour appliquer le modèle à l'ensemble des segments hydrographiques et calculer la densité d'anguilles et les effectifs d'anguilles jaunes. Un modèle d'argenture (Beaulaton et al., 2015) est ensuite utilisé pour calculer la production d'anguilles argentées en effectif et en biomasse. Le modèle EDA ne s'applique qu'aux rivières, il ne donne pas d'estimation de production pour les lagunes, les marais, les lacs et les zones côtières.

L'approche de modélisation est basée sur un modèle delta-gamma (Stefánsson, 1996) qui permet d'expliquer une large proportion de la variabilité de données d'abondance principalement quand il y a une surreprésentation des valeurs nulles. Le modèle EDA combine un modèle de présence-absence (modèle Δ ou binomial) pour déterminer la probabilité d'une densité observée non nulle, et un modèle de densité (modèle Γ) pour déterminer le niveau des densités non nulles. La multiplication de ces deux modèles (modèle $\Delta\Gamma$) permet ensuite de calculer la densité d'anguilles prédite dans un tronçon.

Le modèle utilise les hauteurs d'ouvrage et la distance à la mer pour caractériser l'accessibilité des bassins versants pour l'anguille. Le cumul des hauteurs d'ouvrages est calculé depuis la mer, et les valeurs manquantes font l'objet d'une prédiction par modélisation qui prend en compte les caractéristiques locales (pente et débit), la zone géographique et le type d'ouvrage. D'autres variables décrivant les conditions au niveau du tronçon hydrographique : pente, débit, température, largeur, UGA ont été utilisées en plus de l'accessibilité pour caractériser les conditions au niveau des stations de pêche. Les autres variables décrivant les pressions anthropiques : pêche civellière, pêche d'anguille jaune, pollution n'ont pas été utilisées dans le modèle car les données n'ont pas été jugées comme suffisantes. Les variables concernant l'utilisation du sol (urbanisation, argriculture...) soit sur le bassin versant entourant le segment hydrographique, soit sur le bassin en amont, n'ont pas non plus été utilisées dans le modèle, car elles conduisent à des effets probablement factices.

La densité ou la présence d'anguille par opération ont été découpées par classes de taille, <150, 150-300, 300-450, 450-600, 600-750 et >750 mm et utilisées comme variable dépendante dans le modèle.

La meilleure calibration du modèle modèle Δ est obtenue en utilisant l'année (comme facteur), l'unité de gestion anguille (UGA), la température de juillet, le protocole de prospection (pêche complète, indice d'abondance anguille, pêche complète ciblée anguille, pêche grand milieu, pêche en berge), la largeur du cours d'eau, l'accessibilité, la surface de la station de pêche et la classe de taille. Des réponses différentes en fonction de la classe de taille sont introduites dans le modèle pour l'accessibilité, la largeur et l'évolution temporelle . Le modèle prédit correctement 87% des données du jeu de calibration.

Le pourcentage de déviance expliqué par le modèle est de 40.93% pour un Kappa de (K=0.580).

Le modèle Gamma explique 46% de la déviance. La meilleure calibration est obtenue en utilisant les mêmes variables que le modèle delta, avec l'altitude en plus et sans

utiliser la surface en eau de la station (déjà comprise dans le calcul de la densité).

Les prédictions du modèle permettent d'observer une répartition des anguilles à l'échelle du territoire conforme avec les connaissances disponibles sur l'anguille. Les anguilles sont présentes sur une bonne partie du territoire, mais la présence en forte densité (> 5 ind.100m^{-2} toutes tailles cumulées) reste confinée aux zones côtières (Figure 1).

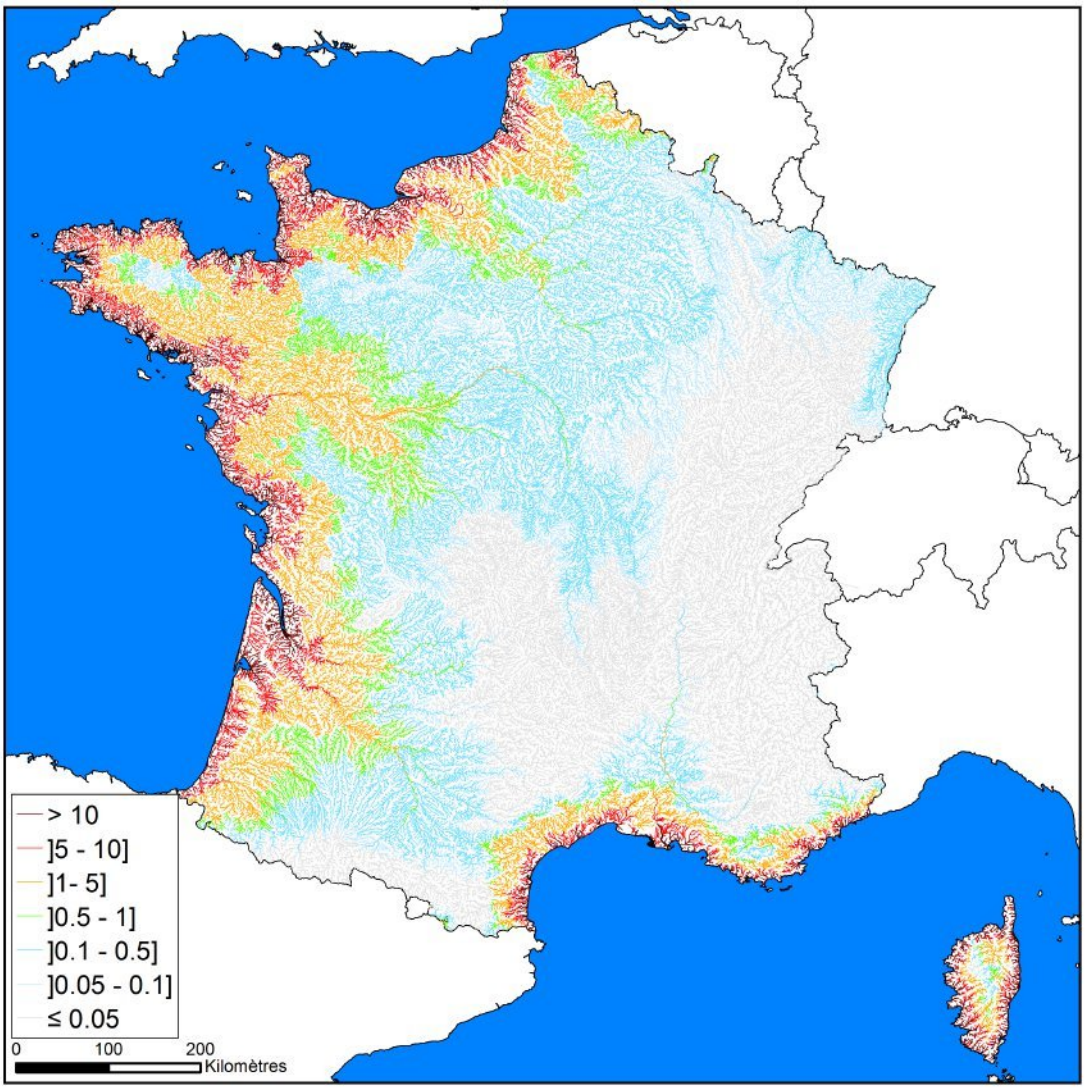

FIGURE 1 – *Densités d'anguilles jaunes (en anguille.100 m^{-2}) prédites en France Métropolitaine par le modèle EDA 2.2.1 en 2015.*

La multiplication par un modèle de probabilité d'argenture (Beaulaton et al., 2015) donne le nombre d'argentées des différentes classes de taille. Le nombre d'argentées est prédit pour chaque année. Depuis le maximum observé au début des années 1990, la tendance de production d'anguilles argentées du territoire est en baisse. Cette baisse n'est toutefois pas continue, et la phase de baisse la plus importante a été observée entre 1990 et 1995 (Figure 2).

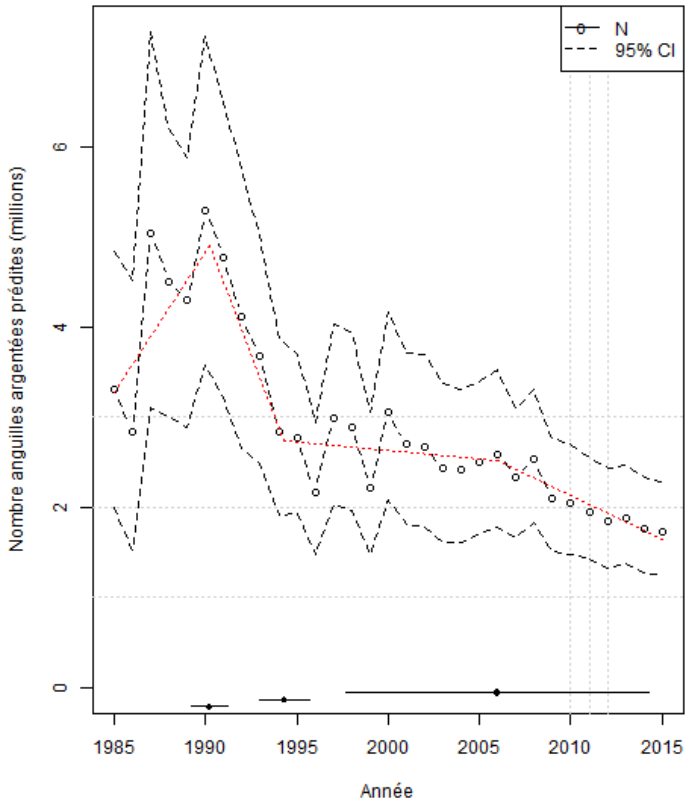

FIGURE 2 – *Estimation des effectifs d'anguilles argentées produites au niveau des cours d'eaux de France métropolitaine. La ligne rouge correspond aux quatre périodes d'une régression segmentée calée sur la courbe de tendance.*

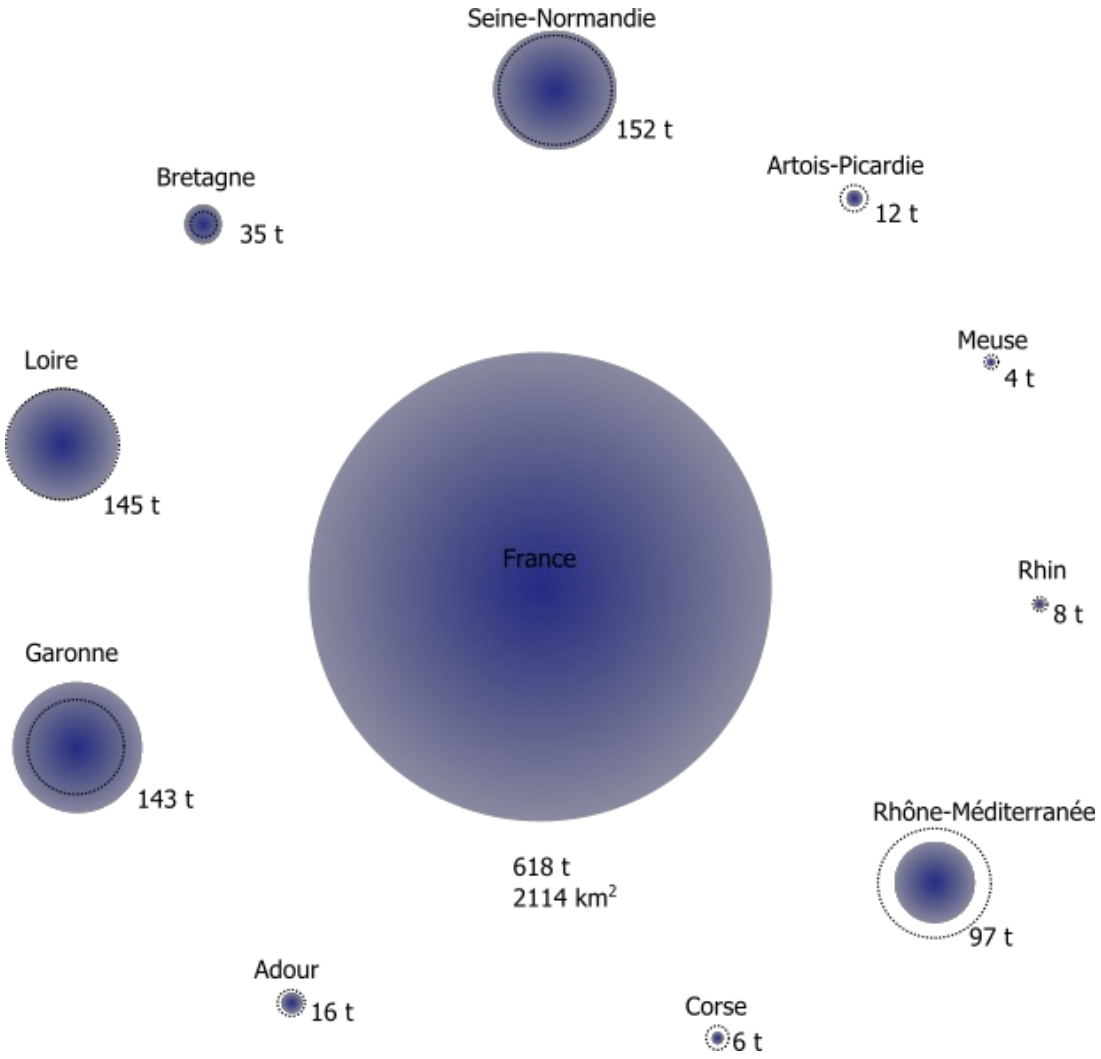

FIGURE 3 – *Production d'anguilles argentées, en biomasse, à l'échelle de la France, en 2015 et sa répartition par UGA. La taille des cercles pleins est relative à la biomasse, la taille des cercles en pointillés noirs à la surface en eau estimée à partir du RHT. Les UGA dont le cercle est à l'intérieur du cercle bleu ont une productivité plus faible que la moyenne.*

Au niveau du territoire métropolitaine, un effectif de 1.724 ± (1.242,2.27) argentées est prédit en 2015 pour une biomasse de 618 tonnes. La production d'anguilles argentées du territoire français est regroupée à 60% sur les UGA Garonne (19.7%), Loire (19.7%) et Seine Normandie (19.4%). La Bretagne (13%) et la Corse (3.5%), compensent une surface en eau plus faible par les fortes densités résultant de la facilité d'accès des cours d'eaux (Figure 3).

Un réseau de rivières index a été mis en place dans le cadre du plan de gestion de l'anguille en France. Ces rivières renseignent en particulier sur la productivité en anguilles argentées des bassins de différentes tailles réparties sur la façade Atlantique et la Manche. La comparaison des effectifs produits sur ces bassins versants et des résultats d'EDA montrent que les ordres de grandeur produits par le modèle sont globalement sous-estimés d'un facteur 3 du fait de la sous estimation des surfaces en eau dans le RHT (Figure 4).

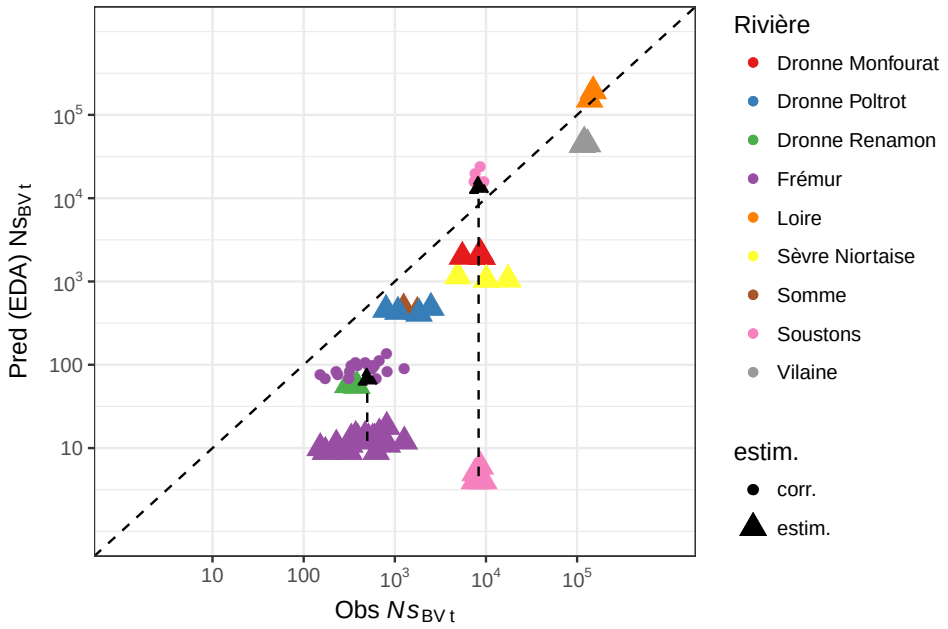

FIGURE 4 – *Comparaison des productions estimées par EDA ($\widehat{Ns}_{BV,t_a}$) et des productions des bassins versants des rivières index et des pêcheries d'argentées $\mathcal{N}s_{BV,t}$. Deux cas sont considérés, (▲) estimation de la production totale annuelle, dans le cas du Frémur et de Soustons, les estimations d'EDA (•) sont augmentées pour prendre en compte les surfaces en eau des lacs et des étangs, très importantes sur ces bassins et qui ne sont pas estimées dans le RHT.*

Part II

Report

Introduction

The european eel stock (*Anguilla anguilla*) range extends from the Baltic sea to the Mediterranea Sea. Reproduction takes place in the Sargasso sea (Schmidt, 1922; Miller et al., 2014). European eel leptocephalus larvaes cross the Atlantlic and will later transform into glass eel when they reach the continental slope (Tesch, 1980; Schmidt, 1909). The glass eel phase will, using tide currents, colonize costal areas, estuaries and possibly when conditions are favorable, progress inland during a short colonization of fresh water. The elvers then turn into yellow eels, and this phase will gradually achieve colonization of the continental freshwater habitats (Naismith and Knights, 1988; Feunteun et al., 2003). This colonisation is hampered by dams (White and Knights, 1997; Briand et al., 2006). The distribution of eels is naturally concentrated in the downstream part of water basins (Ibbotson et al., 2002). Upon reaching a size of 30 cm, eel will settle and most of them will remain confined in a reduced homerange territory for the remainder of their continental life (Laffaille et al., 2005a; Tesch and Thorpe, 2003; Imbert et al., 2010). When they reach a certain size (Svedäng et al., 1996) yellow eels will metamorphose into silver eels (Durif et al., 2006). The male silver eels mature at a lower size and age than their female counterparts, the size limit between the two sexes is about 45 cm (Tesch and Thorpe, 2003).

From the end of the 1980's, the arrival of european glass eel (*Anguilla anguilla*) have diminished to a minimum level in 2009 of about 1 to 5 % of their level before the decline. From 2010, a slight increase in recruitment has been observed, but the level of glass eel arrival remains low, between 4 and 12 % of the reference level of the 1960's-1970's (ICES, 2017). As a consequence in 2017, ICES in its advice indicates that recruitment indices remain well below the 1960-1979 reference levels, and there is no change in the perception of the status of the stock. The advice remains **that all anthropogenic impacts (e.g. recreational and commercial fishing on all stages, hydropower, pumping stations, and pollution) that decrease production and escapement of silver eels should be reduced to - or kept as close to - zero as possible**.

The EU regulation 1100/2007 establishes a management framework whose objective is to restore the eel stock. EU Member States have developed Eel Management Plans (EMPs) for their river basin districts, designed to allow at least 40% of the biomass to escape to the sea with high probability, relative to the best estimate of escapement that would have existed if no anthropogenic influences had impacted the stock.

To test wether management objectives set by the EU regulation have been met, the biomass of spawners produced by the different management units from member states must be assessed, but also the mortality rates that eel experience from anthropic source. France has to deliver a report to the commission, which contains an evaluation of management measures applied to its share of the eel stock. The report must detail

results per eel management unit EMU (Figure 1.1).

In practise, it would be extremely hard to count the real number of silver eel produced at the scale of the French metropolitan territory. Indeed, the silver eel productions of 1200 basins in France are seldom estimated and those estimate are rarely exhaustive. The estimation of the silver eel production has been made using the EDA (Eel Density Analysis) model. It uses yellow eel electrofishing data to predict densities, and a silvering model to predict the number of silver eel produced per river stretch.

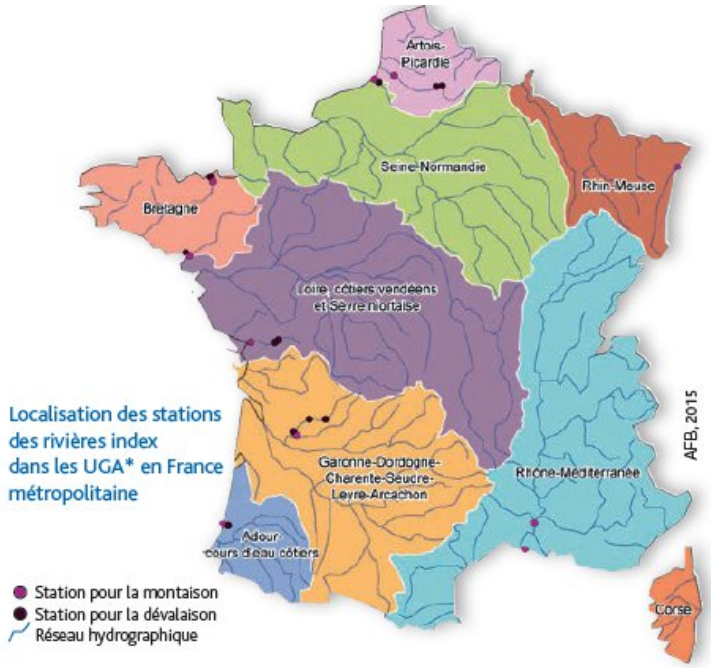

Figure 1.1 – Delimitation of the 10 french (EMUs) in metropolitan France, and localtion of index rivers (map ONEMA/Eau France)

The objective of this work is to apply EDA on the french EMUs and provide an estimation of French eel production. The modelled production will be compared to actual numbers counted from different index rivers in France.

Material and methods

2.1 A short historical overview of EDA

The EDA model was initially built EDA 1.x (EDA 1.1, EDA 1.2, EDA 1.3) in Britany and Loire-Britany to predict the impact of dams on eel density, and try to provide the best classification of obstacles (Leprevost, 2007; Hoffmann, 2008). From this work, in a preliminary attempt, the EDA 1.3 version was applied to France for the eel management plan. This version, which did not integrate the effect of obstacles, estimated a production of 12 000 t of silver eels [1].

The EDA2.x (EDA2.0 et EDA2.1) versions have explored many explanatory variables such as landover (Corine Land Cover) or the impact of obstacles.

EDA 2.0 corresponds to the application of the model to 5 european EMUs and on a virtual dataset (CREPE) in the POSE EU pilot project (Walker et al., 2011). It is based on the CCM v2.1. This method has also been applied to Ireland (De Eyto et al., 2015).

EDA 2.1 (Jouanin et al., 2012) corresponds to the model used for the second French reporting on 10 EMUs. It is based on the RHT (Pella et al., 2012). For river obstacles, it was based on the cumulated number of obstacles from the sea. EDA2.1 results estimate about 2200 t of silver eels in 2009 but the RHT water surface is only 2 114 km^2, a third of the watersurface reported in the BD Carthage database. Waterbodies, the lower part of estuaries, and wetlands are not covered.

EDA 2.2.0 (Briand et al., 2015a) uses size structure for response with size classes of 150 mm. It also uses a wider of electrofishing types, including electrofishing on river banks and point abundance sampling for deep rivers. The current version EDA 2.2.1 is just an update of the 2.2.0 model with data from 2012-2015.

2.2 Modelling strategy

The model is based on the delta-gamma approach (Stefánsson, 1996) which allows to explain a large part of the variance of abundance data especially when null values are overrepresented. The EDA model combines :

- a presence - absence model (Δ or binomial model) to determine the probability of a non-zero observed density,
- and a density model (Γ) to assess the level of abundance in non null data.

[1] 150 millions of Silver eel with an estimated weight of 0.8 kg. The total water surface was estimated at 6 727 km^2 including 3 637 km^2 for the polygon layer (with 1 500 km^2 of estuaries and 110 km^2 of lakes) and 3 090 km^2 for the vector layer of the BD Carthage

The multiplication of both models (ΔΓ model) allows then to predict the density of eel on a river segment. Each time, generalized additive models (Hastie and Tibshirani, 1990) have been used, with for the Δ model a binomial distribution and a logit link and for the Γ, model, a gamma distribution and a log link.

2.3 Dataset construction

2.3.1 Dam data

The dataset has been built from the ROE. Missing values have been modelled as data were quite heterogeneous between parts of France, and were sometimes systematically missing in some areas (Figures 2.1, 5.5) . The model uses flow, dam type and the River segment slope to predict the height of the dam (see (Briand et al., 2015a) and Annex III). The variable used in the model (h') is either the reported height of the dam (h), or

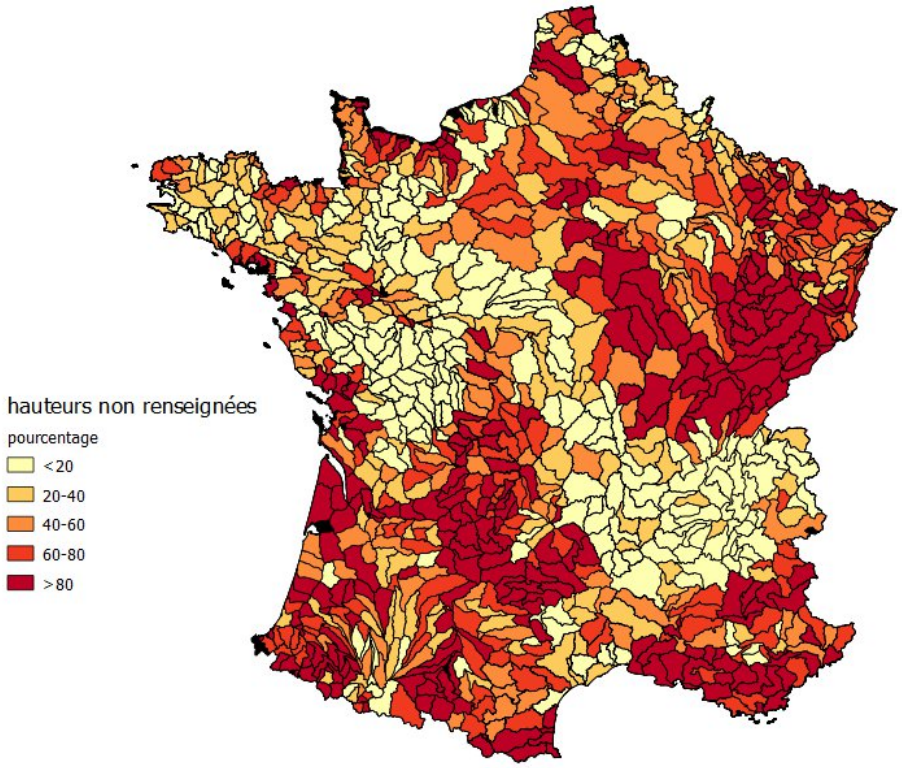

Figure 2.1 – Percentage of missing data in the ROE for dam's height.

the value predicted by Briand et al. (2015a) model ($\hat{h}$) when the height was missing in the ROE database.

The cumulated dam height ($\Sigma h'_{\lambda i}$) has been calculated from the downstream part of the streams (Equation 2.1). It is a very good descriptor of eel abundance variations in all calibrations made with EDA models (Basque country, Loire, Brittany...) (Hoffmann, 2008; Walker et al., 2011; Jouanin et al., 2012).

Cumulated distance from the sea have been calculated in a similar way by adding

the sum of individual river segments i length l : Σl_i (Equation 2.1).

$$\begin{aligned} \Sigma h'_n(\lambda) &= \sum_{i=1}^{n-1} (h'(\lambda, i)) \\ \Sigma l_i &= \sum_{i=1}^{n-1} (l_i) + \frac{l_n}{2} \\ & i \in \ parcours\ mer\ \{1 \dots n\} \end{aligned} \tag{2.1}$$

The cumulative impact might not depend solely on the cumulated heights of the dams but also their individual height: a 3m dam will have more impact than a succession of 3 dams of 1 meter. To test this assumption, a transformation has been applied to dams higher than one meter (equation 2.2) :

$$h''(\lambda) = \begin{cases} h'^{\lambda} \ si\ h' > 1 \\ h' \ si\ h' \leqslant 1 \end{cases} \tag{2.2}$$

Distance to the sea and transformed dam height are two variable tested in the model. But they are correlated. To combine them in one variable, the accessibility A_i is defined as the sum of the distance to the sea and the cumulated dam height, that an eel has to face before reaching a river segment i (Formule 2.3):

$$A_i(\lambda, \beta) = \Sigma l_i + \beta \Sigma h''_{\lambda i} \tag{2.3}$$

From the best model calibrated for EDA for other variables used in the model (see next paragraph), the coefficient combination β and λ ($\lambda \in [1, 1.2, 1.5, 2]$) providing the lowest AIC (or best goodness of fit) have been selected. The optimisation has been a step by step process, searching in turn for the best coefficient λ, then to the best β coefficient.

2.3.2 Electrofishing data

Electrofishing data come from two sources : the large majority comes from the historical BDMAP database from ONEMA and an addition temporary database BD Agglo for most data after 2015 (N=26 623). The remainder comes from a database built using eel monitoring framework data (RSA) (N=2560).

2.3.2.1 BDMAP data

BdMap data correspond to electrofishing operations using different fishing protocols (Belliard et al., 2008; Poulet et al., 2011), which are more or less suitable to describe eel abundance. The previous version of the model (version 2.1) (Jouanin et al., 2012) was only using two pass ectrofishing prospected on foot, *i.e.* complete electrofishing in shallow area to build the prediction. This selection, while allowing the best quality for calculation of the density at the scale of the station was proven biased when it came to describe the abundance in the deep part of the river. This was demonstrated in the POSE project by testing on known (but hidden to the modeller) theoretical river networks(Walker et al., 2011).

For EDA 2.2.0, the choice was made to try to include other kind of electrofishing in the model calibration. A sampling protocol variable (ω) describes the various type

of electrofishing protocols used : ω_{ful} full (two pass) electrofishing, ω_{bf} bank fishing, and ω_{dhf} deep habitat fishing (partial point surveys) (Briand et al., 2015a).

The historical dataset contains too few data before 1984 so those have been removed, but even before 1994 the number of electrofishing available remains low (Figure 2.3).

2.3.2.2 Eel specific electrofishing

Eel specfic survey data (RSA database) have been collected on index rivers (Somme, Vilaine, Soustons, Parc Marais Poitevin) or during regional eel specific surveys (see Annex III). The method used is either eel specific point sampling (eel specific abundance index ω_{eai}) (Germis, 2009b,a; Laffaille et al., 2005b) or eel specific complete fishing ω_{fue} (Feunteun, 1994). These methods differ from the standard methods by keeping the electrode for a longer duration, at least 30 seconds at a specific location (Figure 2.4).

2.3.2.3 Water surface

Densities are calculated as following:

Full fishing For either eel specific surveys ω_{fue} or standard electrofishing ω_{ful}, the water surface corresponds to the water surface of the station. Stations where water surface was reported as larger that 3000 m^2 have been removed from the dataset, while stations where the surface was too small have been manually corrected using the same station at other dates.

Bank fishing ω_{bf} The water surface corresponds to 4 times the length of the station : we consider that an anode placed in the water 0.5 m from the bank will reach an additional distance of 1.5 m from the center of the anode, and that bank fishing is done on the two banks.

Deep habitat fishing ω_{dhf} Deep habitat fishing is done by point sampling, a surface of 12.5 m^2 (1.5 m of action radius and 0.5 m of electrode move) is used as a reference in the calculation (Belliard et al., 2008). This surface was correctly reported in the database with 75 or 100 points for one station. The more standard value of 100 points has been used as a replacement in the rare cases when both the surface and the number of points were missing in the database.

Eel specific sampling ω_{eai} For eel specific abundance index, a surface of 12.5 m^2 has been used, as in the deep habitat sampling.

The surfaces are used to calculate the most accurate indice of eel density, though we know it makes little sense in the case of point sampling. In the model, the predictions are made on complete fishing and the other data serve as standardized estimates, whose variations are used to provide information on eel abundance in the downstream part of large rivers where complete fishing is not possible.

2.3.2.4 Estimation of total number in a station

The densities have been calculated using Carle and Strub (1978) (FSA package Ogle, 2017) for fishing with two pass or more. For fishing with only one pass, data have been extrapolated using using the average fishing efficiency ($\overline{ef}$). Fishing efficiency, defined as $ef = 100 * Nb_{p1}/N_{CS}$ is calculated as $\overline{ef} = 65.6$ for complete fishing (N=15 856), $\overline{ef} =$

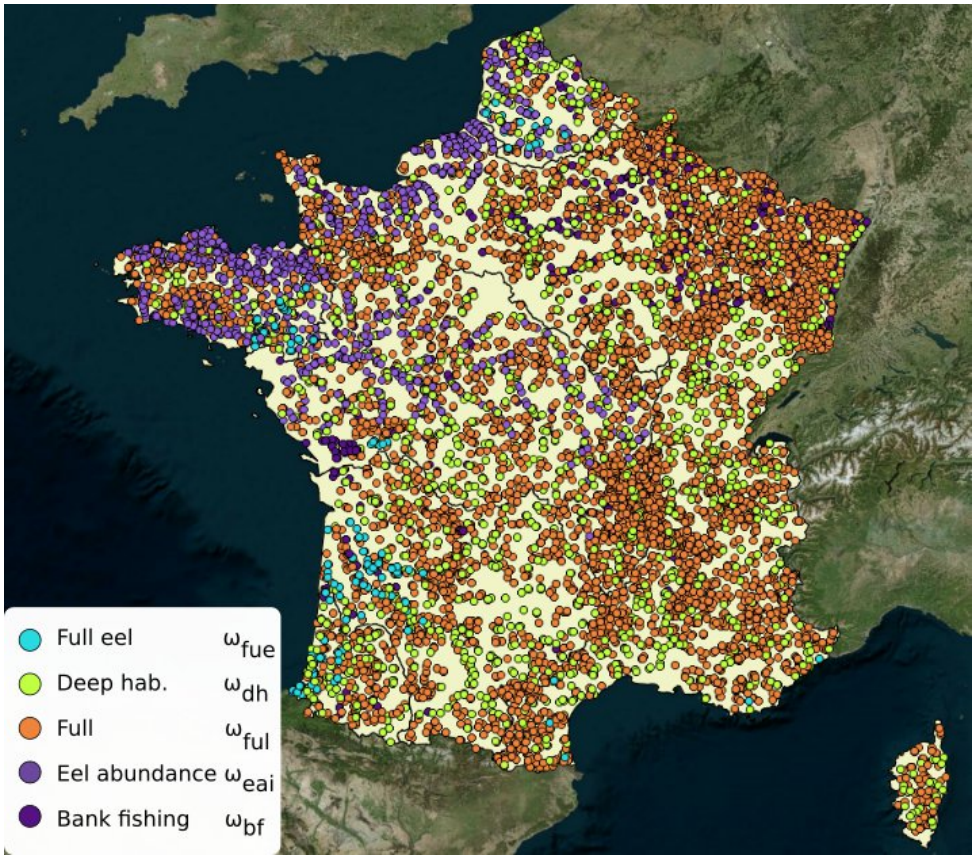

Figure 2.2 – Electrofishing types used in the model, source BdMap, BD Agglo and RSA database.

64.5 for eel specific fishing (N=445) and $\overline{ef}$ = 39.2 for bank fishing (N=2 805). Fishing with only one event are the most frequent (94%) for bank fishing, and correspond to 75% to 3% of complete fishing operations and eel specific complete fishing. A lower efficiency (40%) has been chosen for bank fishing and a common value rounded to 65% for complete fishing and eel specific fishing methods.

Table 2.1 – Number of operation and number of electrofishing stations used to calibrate the EDA2.2.1 in France. Nb ope = nb of electrofishing operations, nb ope (d>0)= number of operation with eel.

EMU	nb ope.	nb ope. (d>0)	nb stations	month	year
Adour	971	677	392	2-12	1985-2015
Artois-Picardie	822	507	406	3-12	1987-2015
Bretagne	2556	2287	1097	1-11	1985-2015
Corse	379	305	130	2-12	1988-2015
Garonne	3912	1613	1403	1-12	1985-2015
Loire	5536	2085	2484	1-12	1985-2015
Meuse	767	132	365	1-12	1985-2015
Rhin	2495	661	1268	1-12	1985-2015
Rhône-Méditerranée	6430	1086	2855	1-12	1985-2015
Seine-Normandie	5315	2934	2107	1-12	1985-2015
France	29183	12287	12504	1-12	1985-2015

2.3.2.5 Operations removed from the dataset

Batches of illegally caught glass eel seized during enforcement operations (Adour) or glass eel used for experiments (Loire) have been transported, quite often nearby electrofising locations. Some fishing operations containing unexpectedly high small eel densities, at several hundred kilometers from the sea have been discarded. They were characterized by a sharp increase in small size class numbers followed by an ageing of the eels. Those data force positive responses of delta and gamma models gam model smoothers sometimes at quite large distance from the sea, and those results can be considered as biased and not representative of what is happening in most river courses. The corresponding electrofishing stations are detailed in annex (Table 5.5).

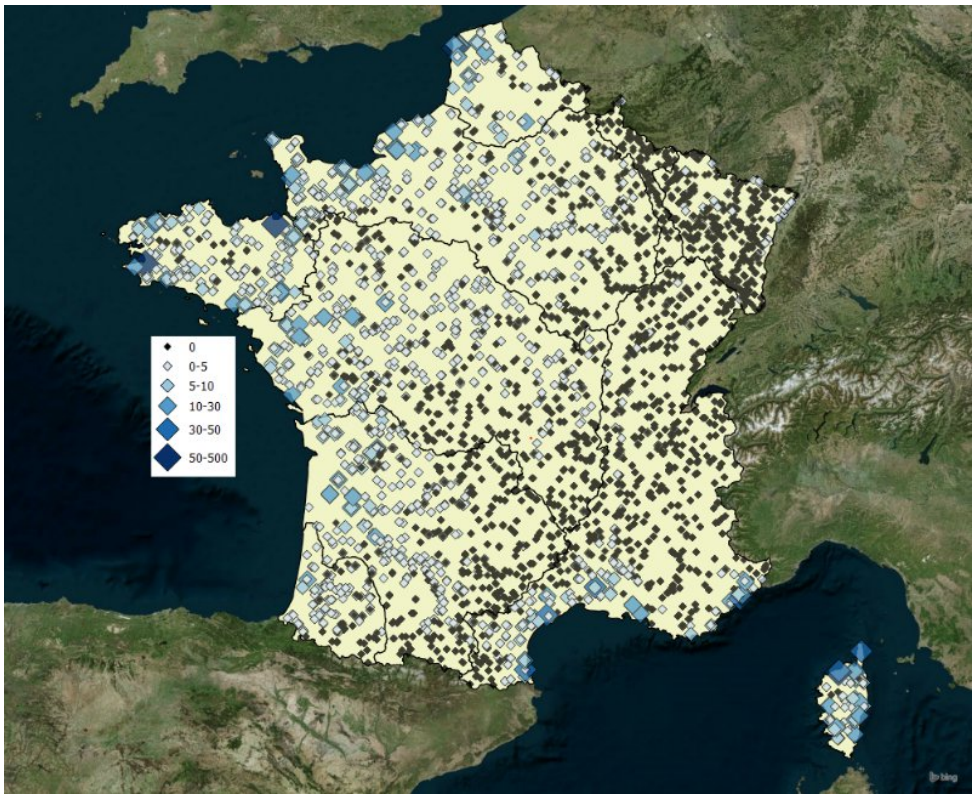

Figure 2.3 – Eel densities observed in electrofishing for 100 m^2*, source BdMap and BD Agglo. Data correspond to data selected in the model and collected from 2009 to 2015.*

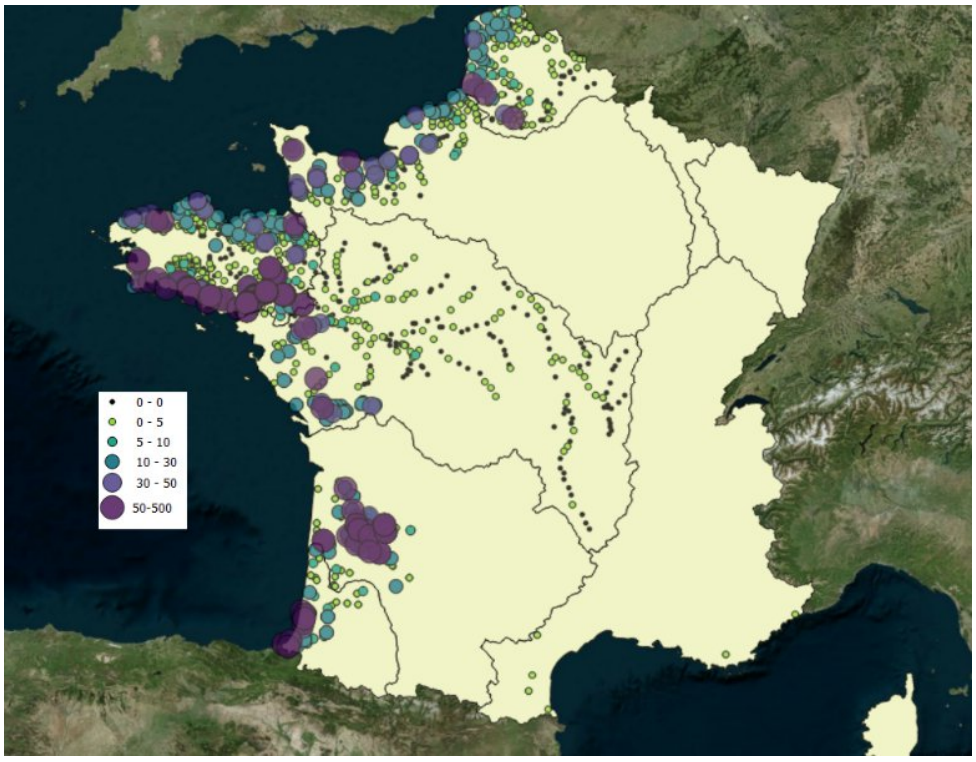

Figure 2.4 – Eel densities observed in electrofishing for 100 m^2*, eel specific surveys (RSA), all years. Data correspond to data selected in the model and collected from 1998 to 2015.*

2.4 Other variables

Most topological related variables like river width, flow, altitude and temperature come from the RHT which computes these variables at the level of the segment. Other variable like land cover have not been included after a carefull check of their possible use in previous versions of EDA.

2.5 Model calibration

The 2.1 version of the EDA model used densities as dependent variable. In the 2.2 version the eel have been separated into size class τ for each electrofishing operation. Size classes used in the model correspond to <150, 150-300, 300-450, 450-600, 600-750 and >750 mm.

Variables have been tested for co-linerarity (Figures 5.2 et 5.1, Table 5.1 Annexe III). Models have been selected according to the Akaike (AIC) criteria. The linearity of model responses have been tested and variables for which a non linear response did not bring an adjustment gain have been entered as linear responses (without spline) in the final model. For GAM the degrees of freedom have been fixed before adjustment to avoid overparametrization.

2.6 Silvering

EDA2.0 and 2.1 was considering a fixed silvering rate Π of 5% (Jouanin et al., 2012) or 2.5 % for Ireland (De Eyto et al., 2015). In the current version, the silvering probability $\Pi_{\tau,i}$ varies on each river segment. It is based on a model fitted on 1583 electrofishing operations over 797 stations in France (Beaulaton et al., 2015). After a qualitative assessment and data validation process, the silvering stage of eels has been predicted according to Durif classification Durif et al. (2006, 2009).

The mean silvering percentage per size class τ has been described using logistic regressions with the average numbers of yellow eels $\widehat{Ny}_{i,\tau}$ predicted by the EDA2.2.0 as a predictor. The processes of model calibration and the result discussion are presented in Beaulaton et al. (2015) report.

On average, the silvering rate used in EDA2.2.1 is larger than the silvering rate of 5 % used in the 2.2.0 and 2.2.1 models (Figure 2.5).

However, the 2.1 applied a silvering potential to the total density, that is, without distinction of the size classes. In contrast, the EDA2.2 model has only used eels with a size class larger than 300 mm, with a potential to become silver. These larger eels represent only 46.5 % of the total number of yellow eels.

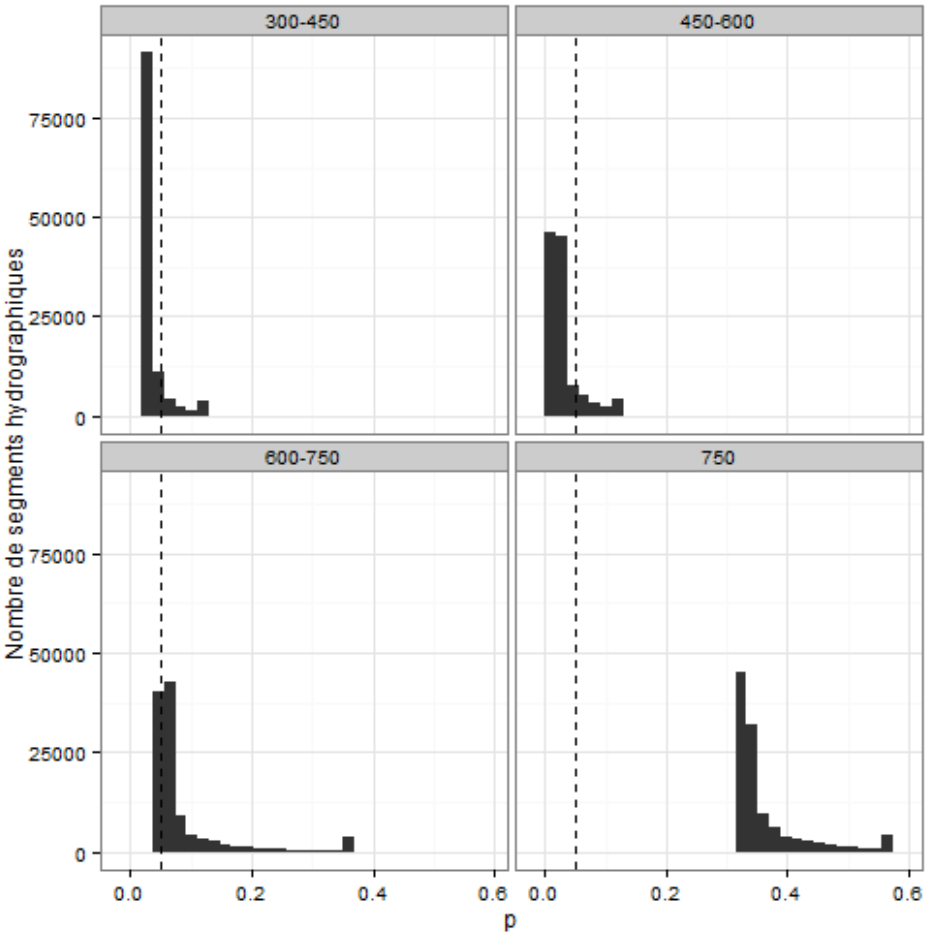

Figure 2.5 – Histograms of silvering rates predicted by Beaulaton et al. (2015) model. The silvering rate of 0.05 of Jouanin et al. (2012) model was applied to the total number of eels predicted by EDA2.0 EDA2.1 in the station.

2.7 Predictions

The number of yellow eels Ny is predicted from the model on each river segment i, from the characteristics of each segment, and assuming that the electrofishing station would cover a surface of 600 m^2 and would be prospected with a full two pass method. Densities on the electrofishing station ($\widehat{dy_i}$) correspond to the product of Δ and Γ models. The number of yellow eels ($\widehat{Ny_i}$) estimated per river segment correspond to the product of density and water surface S_i. (Formule 2.4) :

$$\begin{aligned} \widehat{Ny}_{\tau,i} =& \Delta_{\tau,i}\Gamma_{\tau,i}S_i = \widehat{dy_{i,\tau}}S_i \\ \widehat{dy_i} =& \sum_{\tau=150}^{\tau=750} \widehat{dy_{i,\tau}} \end{aligned} \tag{2.4}$$

with τ size class of eels, i the river segment.
The number of silver eels is calculated as the product of numbers in each size class with the silvering probability of this same class $\Pi_{\tau,i}$ in each River segment of the RHT (Beaulaton et al., 2015) (Formule 2.5):

$$\widehat{Ns}_{\tau,i} = \widehat{dy}_{\tau,i}S_i\Pi_{\tau,i} \tag{2.5}$$

The biomass is calculated using the Silver eel mean weight $p^-_{\tau,i}$ (Beaulaton et al., 2015) (Formule 2.6): .

$$\widehat{Bs}_{\tau,i} = \widehat{Ns}_{\tau,i} * \bar{p}_{\tau,i} \tag{2.6}$$

Size-fecundity relationships are rare for european eel, however MacNamara and McCarthy (2012) have recently proposed a relation for Irish silver eels (Formule III):

$$\mathbb{F}_\tau(\tau > 450) = \widehat{Ns}_{\tau,i} * 10^{-2.992+3.293*log_{10}\bar{l}_\tau} \tag{2.7}$$

A confidence interval on the prediction is obtained using the *confint.gam* function in package mgcv. This confidence interval is approximated as it does not account the selection of smoothing components in the model. The 95 % confidence interval of the number of yellow eels predicted by the $\Delta\Gamma$ model is calculated by multiplying the confidence intervals in both models (Formule 2.8). This calculation overestimates the true confidence interval in the model.

$$\widehat{Ny_i} \in \left(\sum_i (\widehat{\Delta_i} - 2SE(\Delta_i))(\widehat{\Gamma_i} - 2SE(\Gamma_i))S_i, \sum_i (\widehat{\Delta_i} + 2SE(\Delta_i))(\widehat{\Gamma_i} + 2SE(\Gamma_i))S_i \right) \tag{2.8}$$

with S_i water surface of the river segment. Here, we ignore uncertainties related to the prediction of water surfaces.

This report uses a threshold of 450 mm as the limit between males and females, this means that silver eels shorter than 450mm will be considered as males.

2.8 Statistic and database tools used to calibrate the model

All calculations have been made using postgreSQL and R 3.4.3 software, with in particular the use of the following packages : PresenceAbsence (Freeman and Moisen,

2008), mgcv (Wood, 2006), visreg (Breheny and Burchett, 2014), stargazer (Hlavac, 2013), sweave (R Core Team, 2013), knitr (Xie, 2014), ggplot2 (Wickham, 2009), sqldf (Grothendieck, 2017). Historical trends have been calculated using the segmented package fixing *a priori* the number and areas of breakpoints in the regression line (Muggeo, 2008).

Results

3.1 Topological variables

The heights of dams was not homogeneously recorded accross France (Figure 2.1). The amount of information seems nevertheless sufficient to characterize migratory transparency from obstacle height data (Figure 3.1 gives an overview of cumulated impact which is consistent with our expertise).Thereby, this information is better than in the previous model (2.1), which could only take into account the count of dams from the sea (Jouanin et al., 2012), as too many data concerning height was missing.

It is however necessary to model missing values to homogeneize data at the scale of the French territory The GLM model retains slope φ, flow Q and dam category (κ=dam, spillway, gates, rockfilled splillway ...). The most important variable is the type of dam (Table 3.1). A separate prediction of height is done in each EMU U (Formule 5.1).

$$log(h) \sim log(Q+1) + log(\varphi+1) + \kappa : U \tag{3.1}$$

A routing algorithm based on hierarchical tree-like structure of the network allows to calculate distance to the sea (Figure 3.1c) and the cumulated height of dams using the various transformed height variables (Figure 3.1b). In areas were multiple obstacles are reported, there might be cumulated heights larger than field altitude when predicted height of dams are used (Figure 3.1b in grey). However, this type of information also exists when using raw data from the national database ROE in areas of low altitude (Figure 3.1a in grey).

	Df	Deviance	Resid. Df	Resid. Dev	F	Pr(>F)
NULL			24649	18236.83		
$log(Q+1)$	1	455.8	24648	17780	768.11	0.0000
$log(\varphi+1)$	1	233.7	24647	17547	393.83	0.0000
U	8	123.7	24639	17423	26.06	0.0000
κ	6	2566.8	24633	14856	720.84	0.0000
$U:\kappa$	48	266.6	24585	14590	9.36	0.0000

Table 3.1 – GLM model of height according to the dam's type κ, slope φ, flow Q and EMU U.

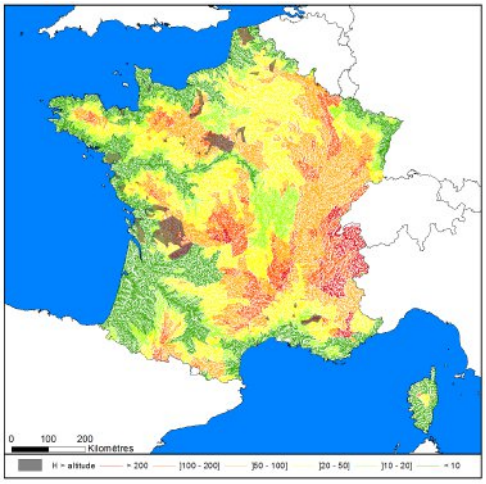

(a) Σh

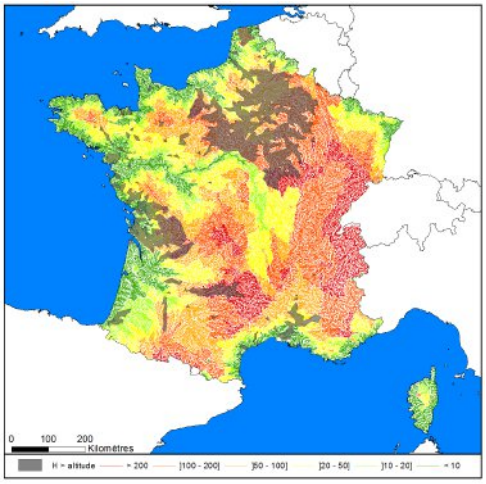

(b) $\Sigma h'$

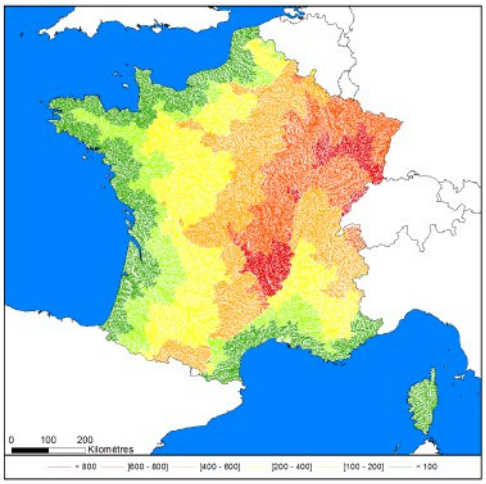

(c) Σl

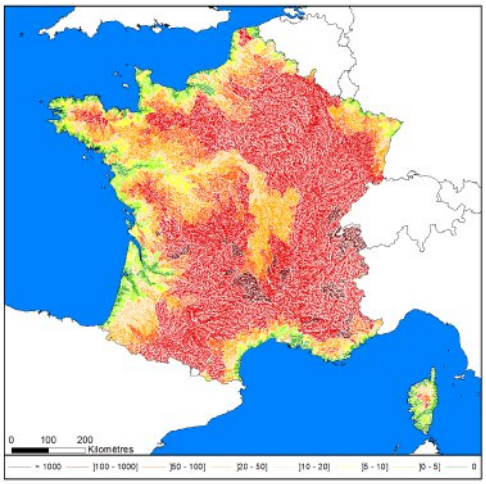

(d) $\Sigma h'^{1.5}$

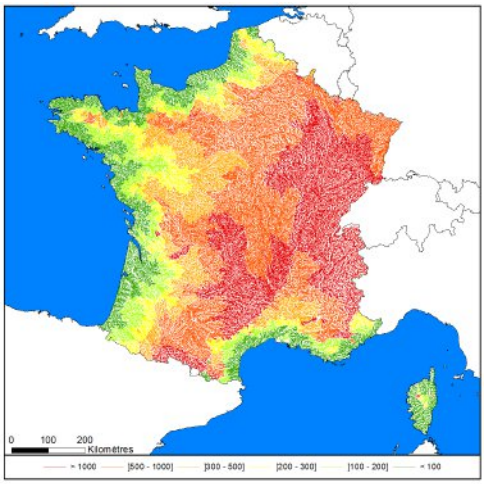

(e) A

Figure 3.1 – Maps of variables used to build Difficulty of access. Cumulated height from the sea. (a) $\Sigma h'$= cumulated values including predicted height of dams for missing values, (b) Σh= Cumulated values uncorrected. Gray shaded polygons indicate areas where the cumulated height is higher than altitude. (c) Σl= distance to the sea, (d) $\Sigma h'^{1.5}$ Sum of transformed height using a 1.5 power (see paragraph 3.5.2), (e) $A(\lambda = 1.5, \beta = 1.7)$ (formule 2.3) Difficulty of access, sum from the sea of transformed dam height and distance to the sea.

3.2 EDA adjustment

A first selection of response variables was done in EDA 2.2.0 by testing all combinations of uncorrelated variables for the Δ model (2340 combinations) and the Γ model (1260).

From this selection of candidate variables, model selection has been performed by analysing possible interactions with size class. The number of degrees of freedom in the model was not large enougth to integrate interactions between response variable and year or EMU, even if those predictions might have been interesting for the analysis. The calibration of the variables building the Difficulty of access λ (the power) and β (factor providing the relative importance of dams and distance to the sea) have been done once the model structure has been set for other variables. For time reasons, no new calibration has been done with updated data in model 2.2.1.

Models are analysed using their response curves, this means that the response is predicted by varying one parameter of the model (e.g. river width W_i) while other are fixed at pre-determined values, either their average, or a value making sense for model interpretation (e.g. Difficulty of access A=1, log(A)=0). We have chosen to illustrate the response for eels of small size, near the sea, and on small streams. Figures 3.2, 3.3, 3.4, 3.5, 3.6, 3.7, 3.8 et 3.9 take as a reference : τ (size class)=150-300 mm, θ (temperature)=18 C, A_i (Difficulty of access)=1, t (year)=2015, ω (electrofishing type)=full fishing ω_{ful}, W_i (width)=3m, U_i (EMU)=Britany, H (altitude)=0.

3.2.1 Delta model (Δ)

The best model is (formula 3.2, Table 3.2) :

$$\begin{aligned} d_{i,j} > 0 \approx & \alpha_1 ti * \tau + \alpha_2 U_i + \alpha_3 \theta_i + \alpha_4 \omega + s(Sp) + s(W_i * \tau) + \\ & s(log(A_i(\lambda = 1.5, \beta = 1.7)) * \tau) + \epsilon \ (link = log) \end{aligned} \tag{3.2}$$

t *Year, discrete (factor),*
U_i *EMU,*
θ *July temperature,*
ω *Fishing protocol,*
W_i *River width,*
A_i *Difficulty of access (see formula 2.3),*
Sp *Electrofishing station surface,*
τ *Size class, the model uses interactions with year,*
s *Polynomial smoothing function,*
$\alpha_1 \dots \alpha_4$ *Model coefficients,*
ϵ *Model residuals.*

The presence probablity is first analysed for the response to the surface of the electrofishing station Sp, july temperature θ, electrofishing method ω and EMU U (Figure 3.2). Probabilites of capture increase logically with the water surface, but stop doing so beyond 1000 m^2. Capture probabilities increase with July temperature. For fishing protocols, regression coefficient come in this order : maximum for full fishing eel ω_{fue}, then eel abundance index ω_{eai}, deep habitat fishing ω_{dhf}, full fishing ω_{ful} and finally bank fishing ω_{bf}.

EMUs in the Biscay area have a large probability of presence but suprisingly, the maximum coefficient is found in the Seine basin (in the Channel). The coefficients diminish from North (Britanny) to South (Adour (taken as a reference in Table 3.2)). They are much lower in the Rhône and Corsica basins flowing in the Mediterranean sea.

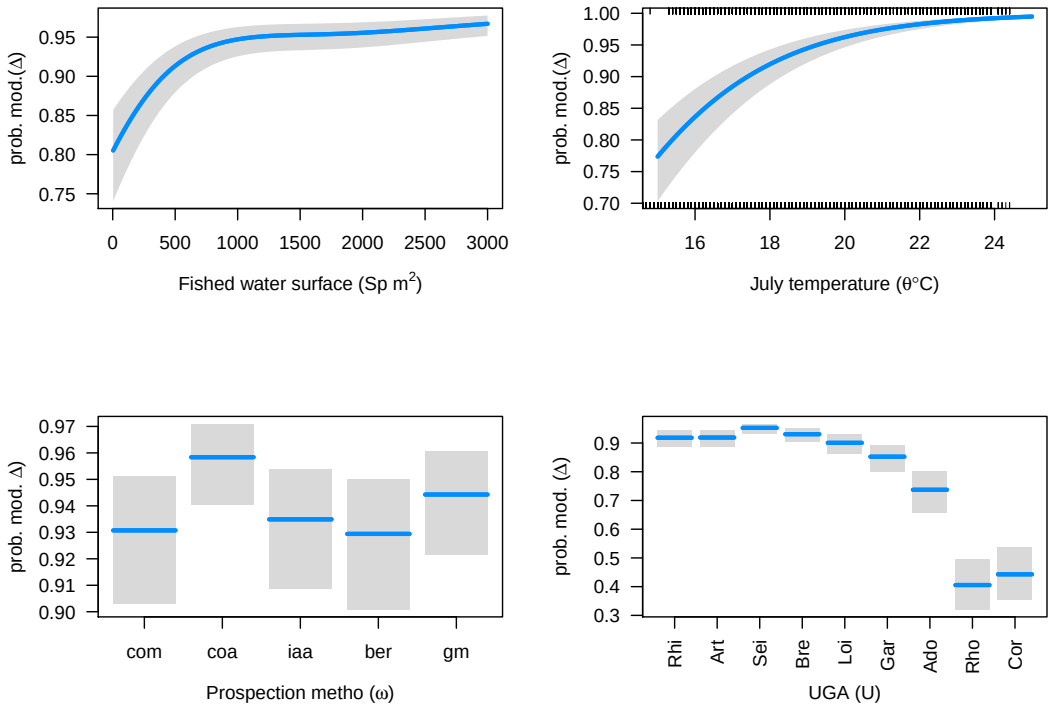

Figure 3.2 – Response curves for model Δ for the water surface of electrofishing station S_p, july temperature θ, prospection method ω, and emu U. Predictions are done in reference conditions indicated at paragraph 3.2.

The Difficulty of access A (Formula 2.3) causes a clear effect on eel presence probability for size <150mm, 150-300 mm, and 300-450 mm. The sigmoid inflexion point is located near $log(A) = 5$, which would correspond to a distance of 150 km from the sea without dams (Figure 3.3). The probabilities of presence are also lower for eels of large size (>450 mmm) and not significant for eels larger that 750 mm.

The temporal trend of presence probability per size class is constrasted (Figure 3.4.) The probability to find small eels (<150 mmm Figure 3.11a) in electrofishing increases from 1998 to 2003 then decreases. A similar breakpoint is found in 2003 in almost all series (Figure 3.11b, 3.11c). Probabilities to catch eels of 450-600 mm increase from 1985 to 1991 then diminish regularly (Figure 3.11d). A similar trend is found for the 600-750 mm size class (Figure 3.11e) but with much lower probabilities.

The presence probability shows an interaction between width and size classes. Large eels (600-750 mm and >750 mm) have a greater presence probability in wider streams. The largest increase is observed for the 450-600 mm size class (Figure 3.5).

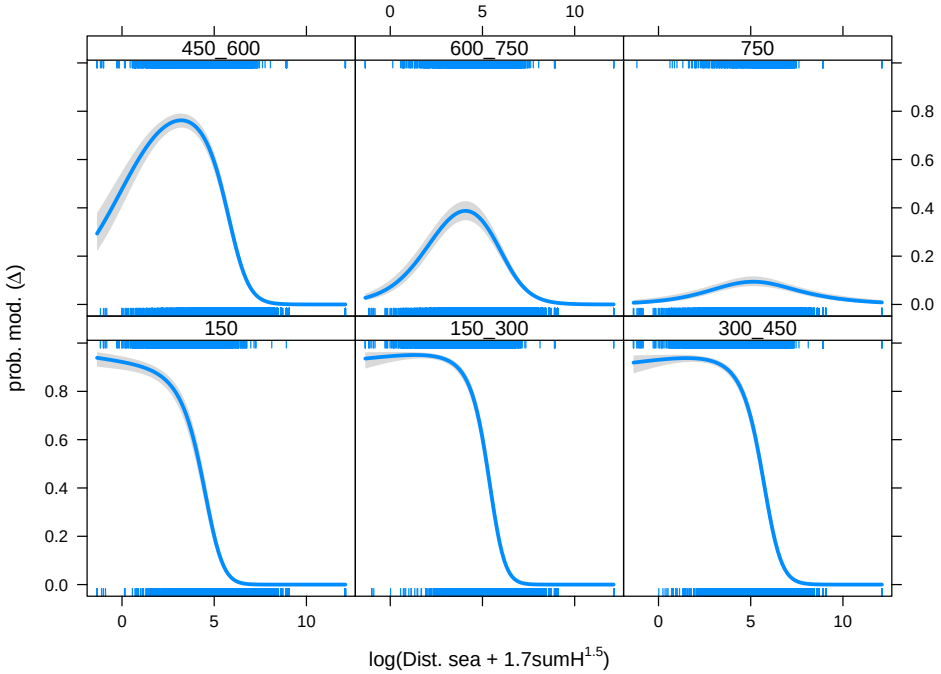

Figure 3.3 – Response curve for Δ model for Difficulty of access A (formula 2.3). The predictions correspond to other variables set to reference conditions as indicated in paragraph 3.2.

Near linear responses are obtained for size classes 150 mm, 150-300 mm and 300 mm. For the smallest size class of eel the probability is less significant (< 0.05) (Table 3.2).

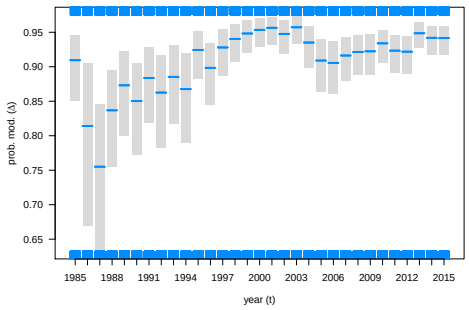

(a) <150 mm

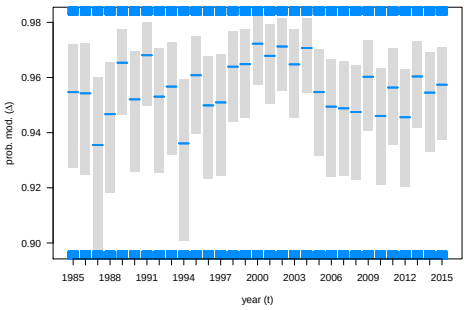

(b) 150-300 mm

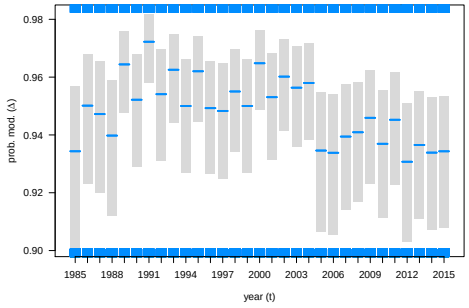

(c) 300-450mm

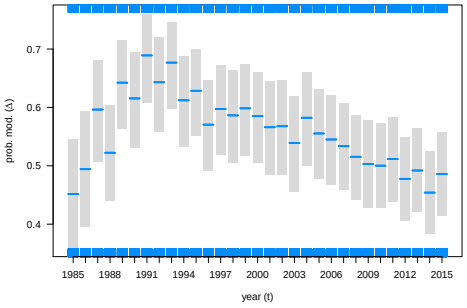

(d) 450-600mm

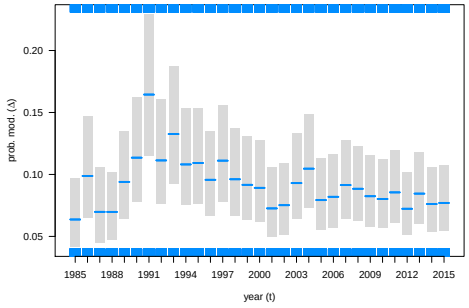

(e) 600-750mm

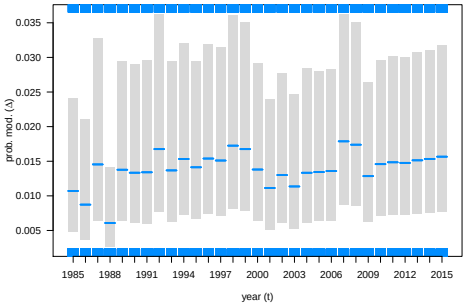

(f) 750mm

Figure 3.4 – Response curves per size class for the Δ model for year. Attention, the probability values on the y axis differ from one plot to the next. The predictions are done in reference conditions indicated in paragraph 3.2.

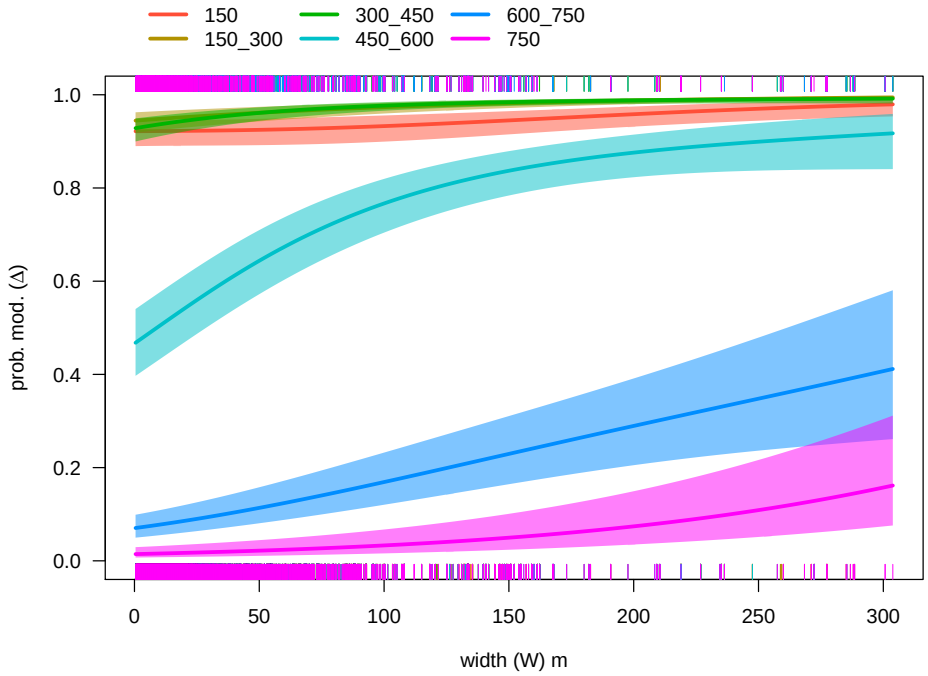

Figure 3.5 – Response curves for the Δ model for width. Predictions are made using reference for other variables as indicated in paragraph 3.2.

Table 3.2 – Coefficients for models Δ and Γ and 95% confidence intervals, U EMU (reference Adour), ω fishing method, ω_{fue} full eel fishing, ω_{eai} eel abundance index, ω_{bf} bank fishing, ω_{dhf} deep habitat fishing (reference ω_{ful} full fishing), θ temperature, H altitude, t year, τ size class, W width, A Difficulty of access. Terms using s() indicate a smoothing function, the number of degrees of freedom for the smoothing function (edf) are indicated, when edf=1 the response is linear, interaction terms (one per combination year - size), are not reported.

	Dependent variable:	
	Presence absence (Δ)	density (positive values) (Γ)
	GAM (logistic)	*GAM: Gamma (log link)*
U Art	4.044*** (0.059)	0.492*** (0.067)
U Bre	4.788*** (0.050)	0.348*** (0.053)
U Cor	0.283*** (0.073)	0.344* (0.077)
U Gar	2.058*** (0.043)	0.312*** (0.041)
U Loi	3.232*** (0.043)	0.304*** (0.045)
U Rhi	4.008*** (0.055)	0.565*** (0.063)
U Rho	0.243*** (0.048)	0.223** (0.054)
U Sei	7.178*** (0.047)	0.383*** (0.013)
ω_{fue}	1.713*** (0.048)	1.289*** (0.037)
ω_{eai}	1.069*** (0.037)	0.031** (0.035)
ω_{bf}	0.980*** (0.033)	−0.269*** (0.027)
ω_{dhf}	1.261*** (0.029)	−0.536*** (0.027)
θ	1.496*** (0.010)	0.017^{NS} (0.013)
H	–	−0.001*** (0.0001)
$t:\tau$	..	..
$\tau(150-300)$		−0.79** (0.307)
$\tau(300-450)$		−0.639** (0.299)
$\tau(450-600)$		−1.019*** (0.304)
$\tau(600-750)$		−1.907*** (0.323)
$\tau(>750)$		−2.976*** (0.408)
$s(W)\|W:\tau(150)$	.** ($edf=1.97$)	−0.008*** (0.0009)
$s(W)\|W:\tau(150-300)$	.*** ($edf=1.98$)	0.0003 (0.0005)
$s(W)\|W:\tau(300-450)$	.*** ($edf=1.98$)	0.003*** (0.0004)
$s(W)\|W:\tau(450-600)$	.*** ($edf=1.98$)	0.002*** (0.0004)
$s(W)\|W:\tau(600-750)$	.*** ($edf=1.87$)	0.0009* (0.0004)
$s(W)\|W:\tau(>750)$	.*** ($edf=1.98$)	−0.0002 (0.0006)
$s(Sp)$	.*** ($edf=2.94$)	
$s(A):\tau(150)$	.*** ($edf=1.97$)	.*** ($edf=1.98$)
$s(A):\tau(150-300)$	.*** ($edf=1.98$)	.*** ($edf=1.98$)
$s(A):\tau(300-450)$	.*** ($edf=1.98$)	.*** ($edf=1.97$)
$s(A):\tau(450-600)$	.*** ($edf=1.98$)	.*** ($edf=1.98$)
$s(A):\tau(600-750)$	.*** ($edf=1.97$)	.*** ($edf=1.86$)
$s(A):\tau(>750)$	.^{NS} ($edf=1.98$)	.^{NS} ($edf=1.00$)
Constant	0.0*** (0.415)	0.787** (0.371)
Observations	175 068	33 906
Ajusted R^2	0.423	0.221
% Explained deviance	40.9	54.2

Note: ^{NS}p>=0.1; *p<0.1; **p<0.05; ***p<0.01; edf=Estimated degrees of freedom

3.2.2 Gamma model (Γ)

The best moded writes (formule 3.3) :

$$d_{i,j}[d_{i,j} > 0] \approx \beta_1 ti * \tau + \beta_2 U_i + \beta_3 \theta_i + \beta_4 \omega + \beta_5 W_i * \tau + s(log(A_{i,\lambda=1.5}) * \tau) + \beta_6 H + \epsilon \quad (3.3)$$

t *Year (as a factor),*
U_i *EMU,*
θ *July temperature,*
ω *Prospection protocol,*
W_i *River width,*
A_i *Difficulty of access (see formula 2.3),*
τ *Size class, the model calculates interactions,*
s *Polynomial smoothing function,*
H *Altitude,*
$\beta_1 \dots \beta_6$ *Model coefficients,*
ϵ *Model residuals.*

The surface of the station which was one of the response variables used to describe the presence-absence of eels on a fishing station is not integrated into the Γ model. Indeed, it is already taken into account in the calculation of the density.

The effect of the temperature is positive as in the Δ model. Larger altitude result, as one might expect, in lower density (Table 3.2). The responses for the fishing types do not follow the order found for the Δ model :

- ω_{fue} (full fishing for eel) remains the first.
- ω_{dhf} has the lowest coefficient while it ranked second for the Δ model. So there is a high probability to find an eel during a deep habitat partial electrofishing, but densities will be low.
- ω_{eai} The eel abundance index ranks second for the Γ model.

The temperature effect it not significant in the Δ model.

Densities diminish with the Difficulty of access A. Similarly to the Δ model, the diminution is larger for smaller sizes. Interestingly, response curves for size class 450-600 mm and 600-750 mm do not have the same modal aspect as they did for the Δ model: the largest desnities are always found downstream, whatever the size of eels. Eels >750 mm are not significantly distributed according to Difficulty of access as was the case of the delta model, and the coefficient adjusted is linear (Tableau 3.2, Figure 3.7).

Annual responses for the Γ model are very different according to the size class. Sizes <150 mm, 150-300 mm show a maximum during the 2000^{th} (Figures 3.8a, 3.8b and 3.8c). Densities of smaller eels (<150 mm) increase since 2008 (Figure 3.8a). Densities of class 450-600 and 600-750 mm diminish again from a maximum at the end of the 1980's (Figures 3.8d and 3.8e).

The size class <150 mm shows the most acute response according to width with a clear decrease when streams width increase (Figure 3.9 in red). This response is different to that of the Δ model for wich probability of presence didn't depend on river width (Figure 3.5 in red). This result indicates that the small sized eels are found in large streams but that they will not correspond to high densities, probably because the propection method is not adapted to small eels. Densities of eel larger than 300mm tend to increase with stream size.

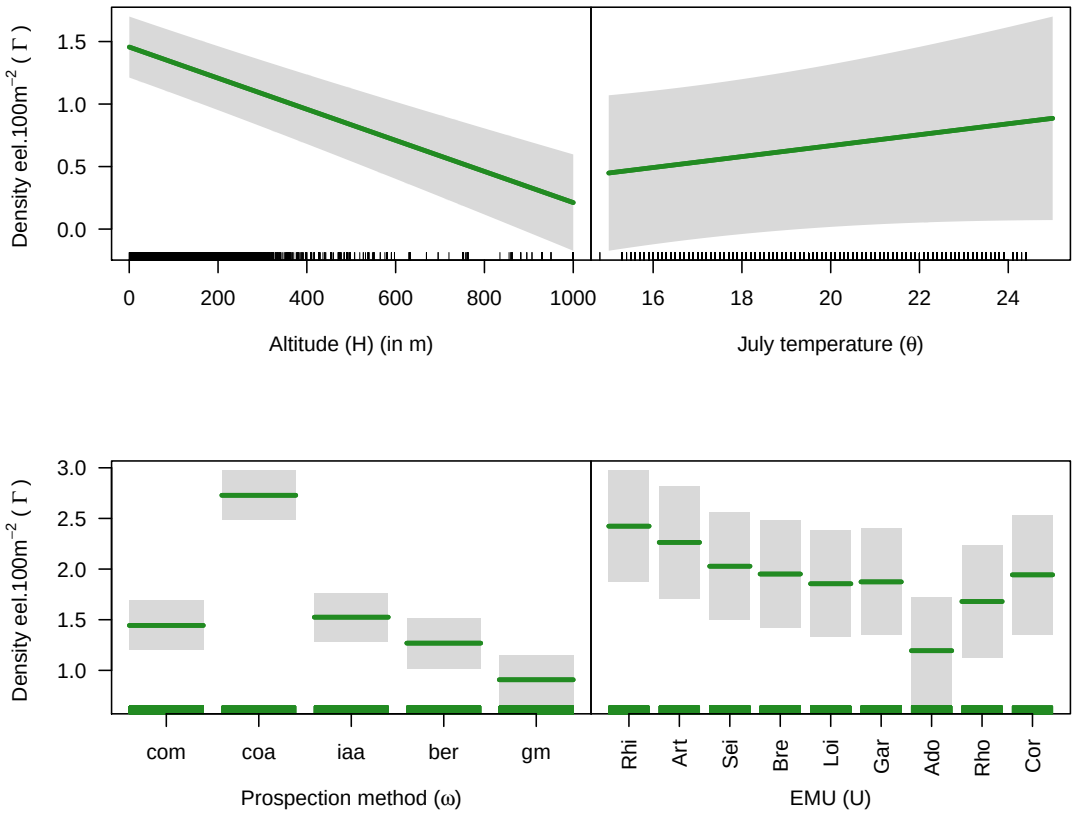

Figure 3.6 – Response curves for model Γ *for altitude, July temperature, prospection method and EMU. Predictions are made using reference for other variables as indicated in paragraph 3.2.*

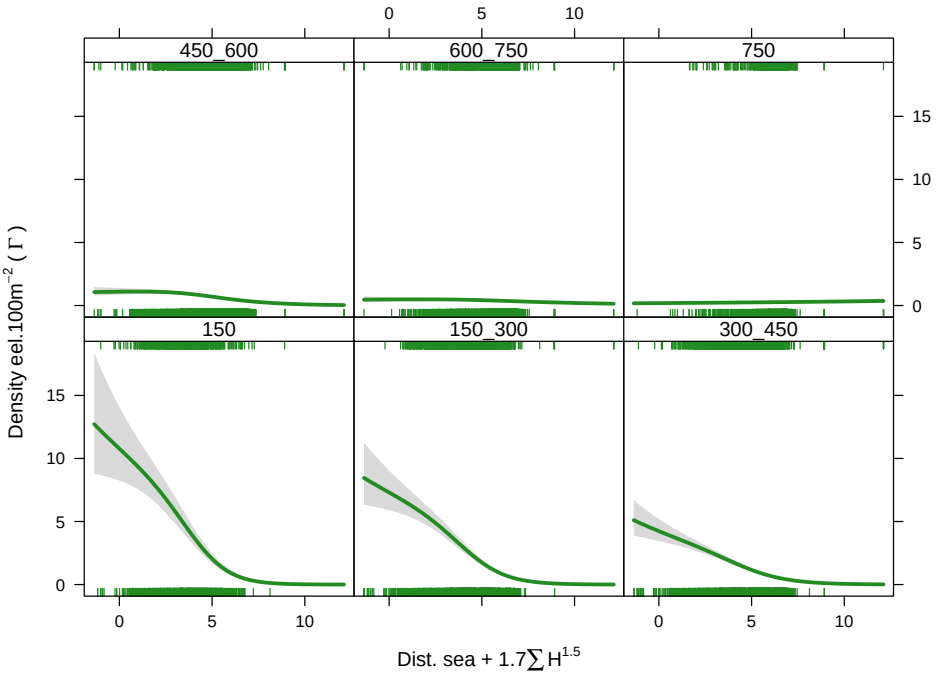

Figure 3.7 – Response curve for the Γ model for the Difficulty of access A (formule 2.3).

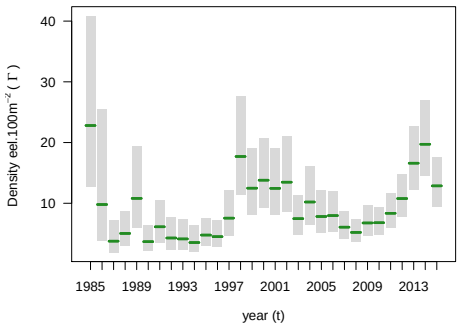

(a) <150 mm

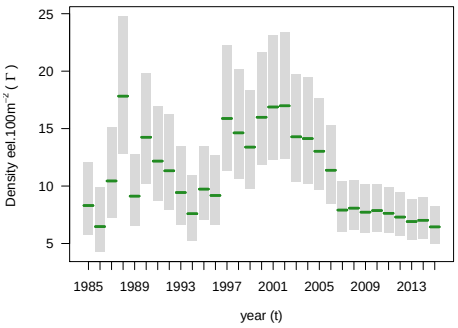

(b) 150-300 mm

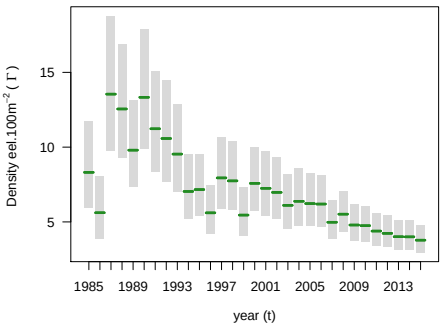

(c) 300-450mm

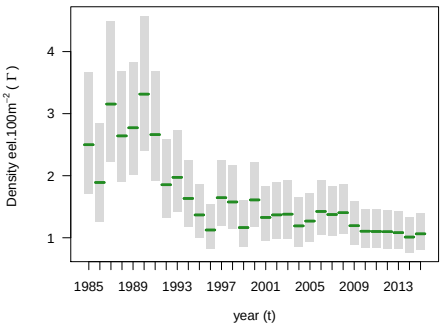

(d) 450-600mm

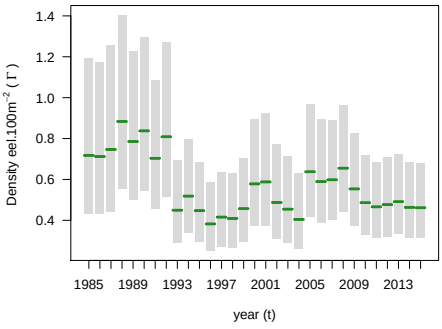

(e) 600-750mm

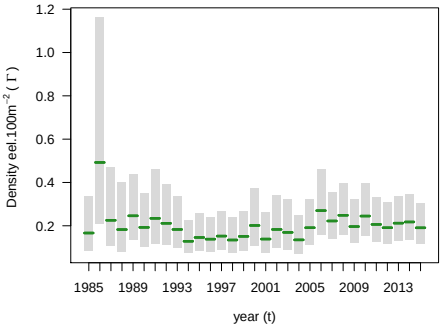

(f) 750mm

Figure 3.8 – Response curves for the Γ model according to year for each class size . Attention, the y axis displays different scales.

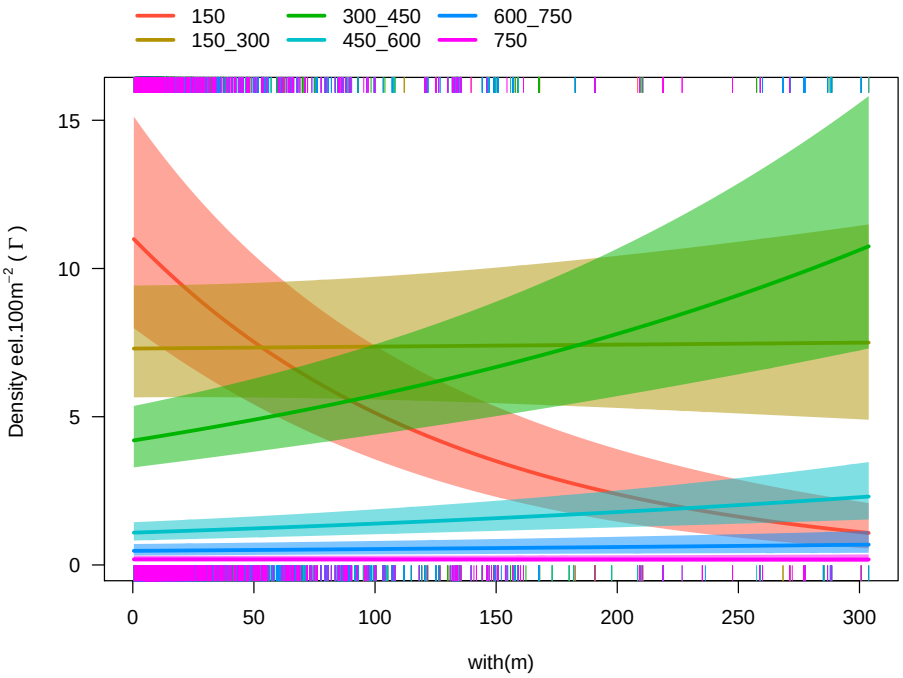

Figure 3.9 – Response curves for the Γ model for width.

3.3 Model diagnostic and prediction

3.3.1 Delta model (Δ)

The Δ model predictions are shown in Figure 3.11 and in Figure 3.12. When they reach a larger size, eels are found more upstream and the spatial variation in the colonization is mostly the consequence of dams reported in the ROE (Figure 3.12). In the calibration plot for presence/ absence, the Kappa is maximum (K=0.580) for a presence probability of about 40% (Figure 3.10). This means that at the 40% threshold, there will be a large number of (65%) stations where the actual presence is correctly predicted, without diminishing too much the number of stations where eel are absent and the absence is indeed predicted by the model (92%). Finally, at a 40 % presence probability, the model correcly predicts 87% of the stations in the calibration set.

The percentage of deviance explained by the model is 40.93%. In comparison, the 2.1 model of Jouanin et al. (2012) had a better Kappa (0.71) and a larger percentage of explained deviance 54 %. But this model was only calibrated on 9 556 operations against 175 068 lines (operation x size class) for the 2.2.1 version of the model.

The model tends to under-estimate null data in places where eel are absent (Figure 3.10, see two upper graphs, for probabilities close to zero). This means that far from the sea, or in areas affected by a large number of obstacles where the presence probability is low, the ΔΓ model runs the risk to overestimate the eel production. However, looking at the residual map there is no systematic bias either positive (observed > predicted) or negative (observed < predicted) at the exception of the Rhône basin for which predictions are probably too optimistic (All dots are black, eel are predicted as present in areas where they are actually absent 3.13a). Accounting for the migratory transparency is possibly not sufficient to account for migration difficulties on this stream in the downstream part. Presence probabilities also seem under-estimated in the Rhine.

As a whole, presence probability maps shows a progression of the distribution area as eels grow (Figures 3.11a, 3.11b and 3.11c). From 300 mm, the size at which male eels start to silver, the presence probability of eels in streams tends to diminish, but the extension of the area where eel are present at low density continues to progress from class 300-450 to 450-600mm (Figure 3.11d).

The area were eels are present will in practise [1] extend to the same level as the 450-600 mm but given the small proportion of large eels in the population, areas where the occurence probability is larger than 0.2 tend to shrink for size class 600-750 mm and 750 mm (in green Figures 3.11e et 3.11f).

3.3.2 Delta-Gamma model (ΔΓ)

The percentage of deviance explained by the Gamma model is 46%. This value is better than that obtained during the calibration of EDA2.1 (Jouanin et al., 2012). The log link of the Γ distributions allows to normalize residuals of the density model (Γ) for which only positive values have been selected. There does not seem to be any obvious flaw

[1] The scale is common to all maps and does not display probability of presence lower than 0.2, the distribution area of 750 mm size eels is thus not visible, to its largest extent, the distribution area of this size class corresponds to the distribution in Figure 3.11, as the size class 750 mm is the one depending the less on the distance to the sea in models Δ and Γ.

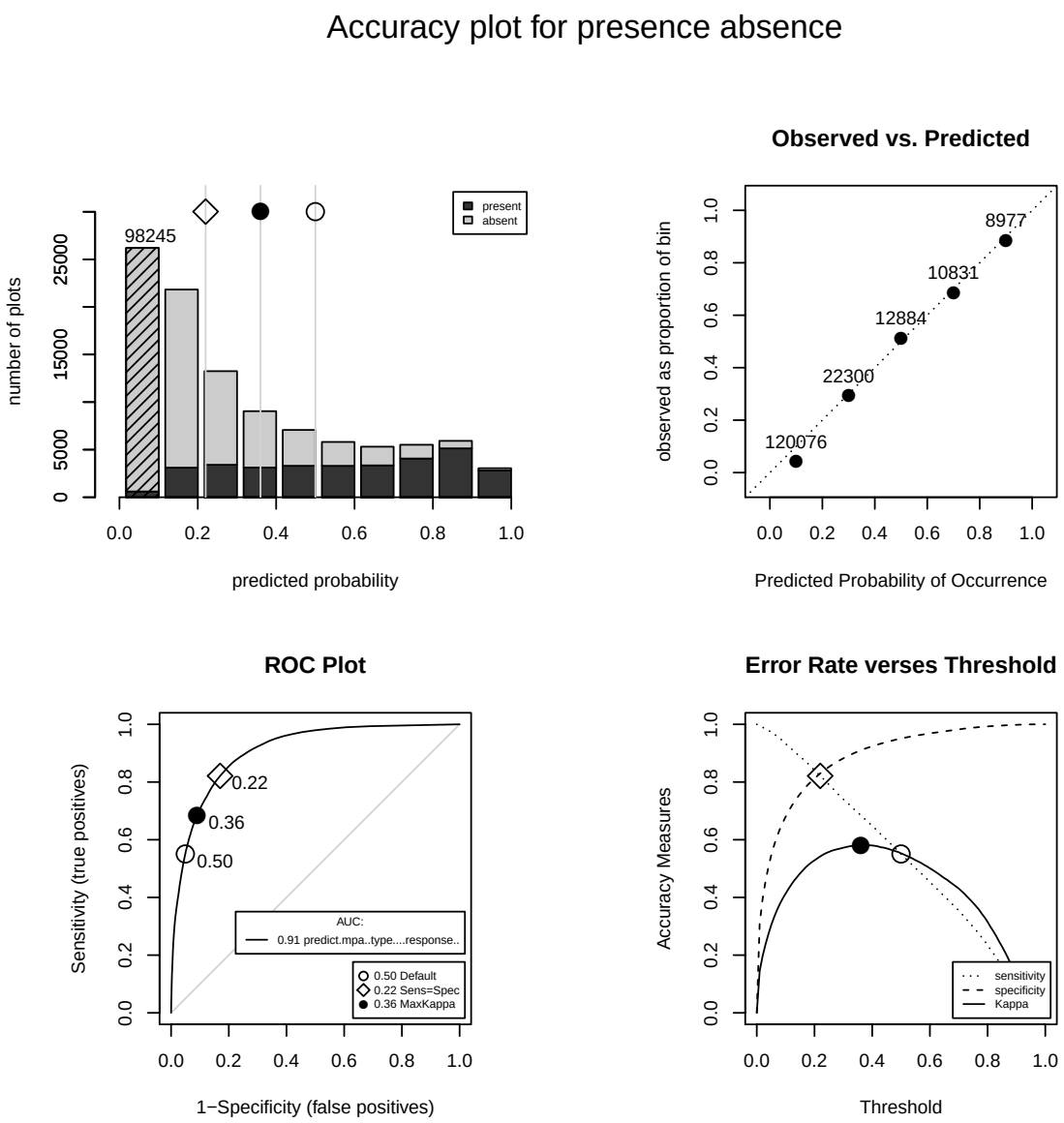

Figure 3.10 – Presence absence Δ model diagnostics. From left to right and top to bottom, (1) predicted probabilities histogram, bars ordered according to observed values (2) Calibration graph allowing to evaluate the adjustment quality, (3) Receiver Operating Curve (ROC), provides a method of evaluation of the model independent of the threshold, a good model must have a large number of true positive values while the number of false positive remains low (4) Diagram of error rate versus threshold provides specificity, sensitivity and Kappa curves according to the threshold.

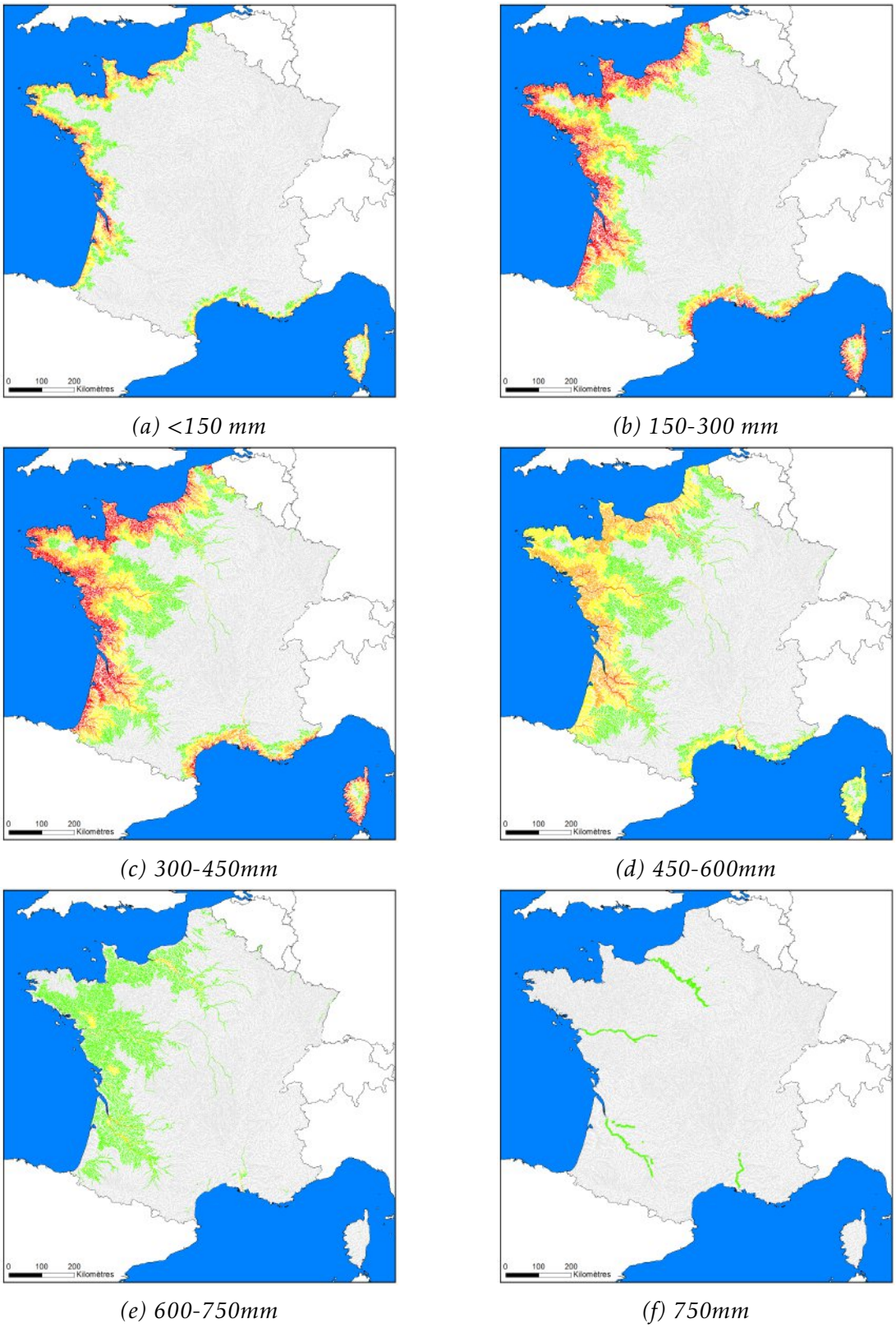

(a) <150 mm *(b) 150-300 mm*

(c) 300-450mm *(d) 450-600mm*

(e) 600-750mm *(f) 750mm*

Figure 3.11 – Presence probability of eel for the Δ model in 2015.

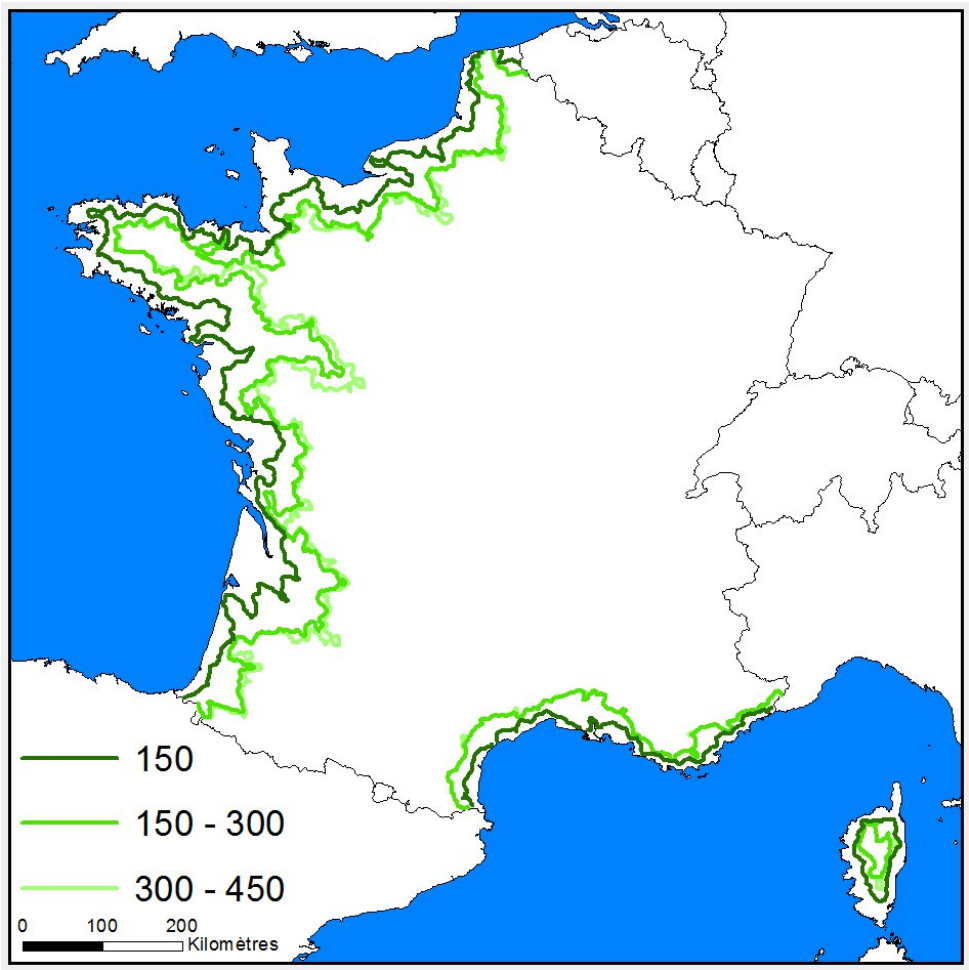

Figure 3.12 – Line delimitating areas where the probability falls below one chance on two for size class <150mm, 150-300 et 300-450mm, this corresponds to the colonisation front (Feunteun et al., 2008). Predictions are made for year 2015.

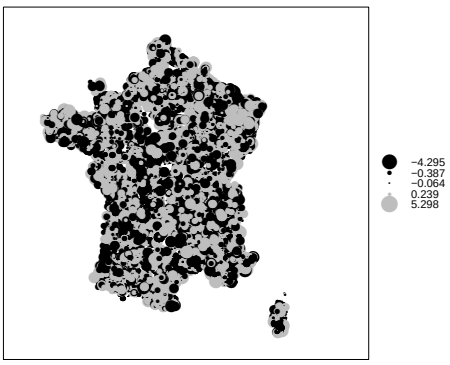

(a) Δ *model.*

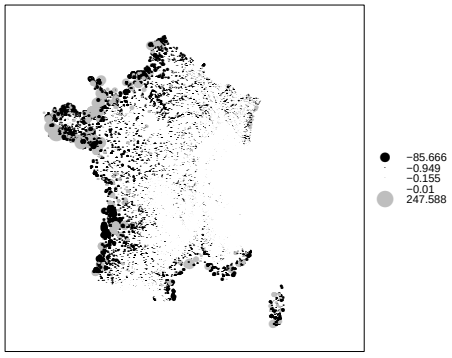

(b) Γ *model.*

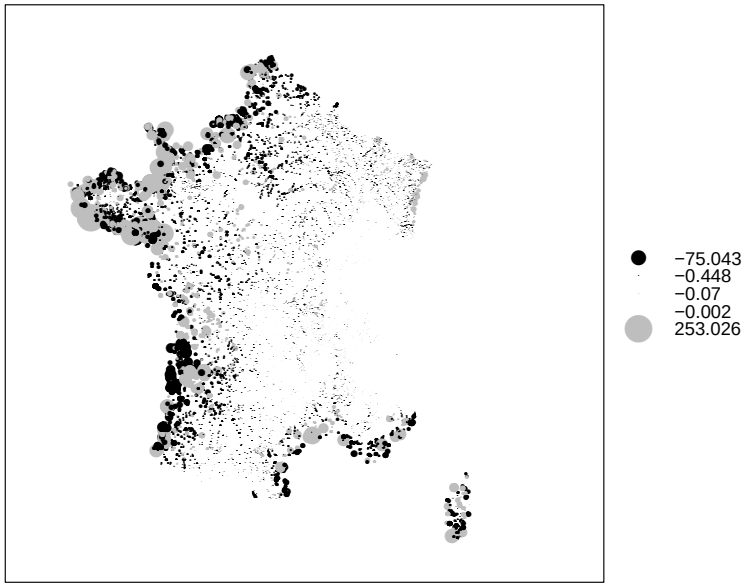

(c) $\Delta\Gamma$ *model.*

Figure 3.13 – Map of residuals (observed - predicted) obtained for models Δ*,* Γ *and* $\Delta\Gamma$*. Those residuals correspond to the sum of residuals for the 6 size class of eel for an operation. The average of residuals of different operations is then calculated for a given station.*

in the residual distribution, even if some points at a large distance from the sea will be predicted as having some eels while in practise there is no eel density (black points inland on Figure 3.13b). Generally, those points are consistent over river course [2] and indicate that the accessibility is not well accounted for.

The $\Delta\Gamma$ model has difficulties to predict densities precisely as those are strongly dependent on local stations characteristics (border and aquatic plant cover, current speed, depth, substrate), and we cannot account for those data with a large scale model. Thus the residual distribution seems inequal at the scale of the territory with large residuals (grey points) at a short distance from the coasts which correspond to points were density was large (more than 100 ind.100m^{-2}) (Figure 3.13c).

Local spots of positive residuals are found in the east of France, and near the Rhine.

[2] zoom on the residual map to see this pattern

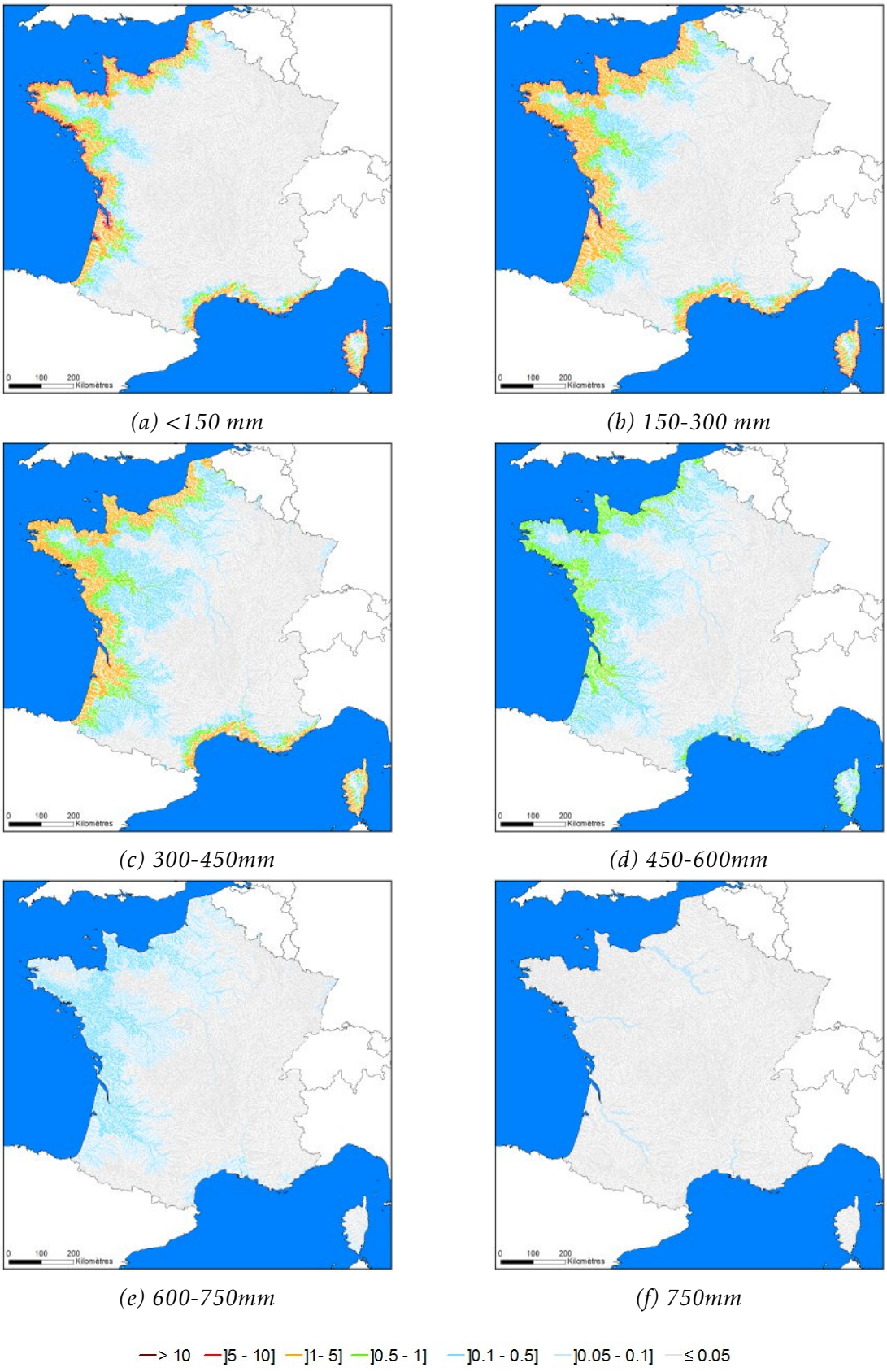

(a) <150 mm *(b) 150-300 mm*

(c) 300-450mm *(d) 450-600mm*

(e) 600-750mm *(f) 750mm*

Figure 3.14 – Yellow eel densities (in eel.100 m^{-2}) predicted per size class by the $\Delta\Gamma$ model.

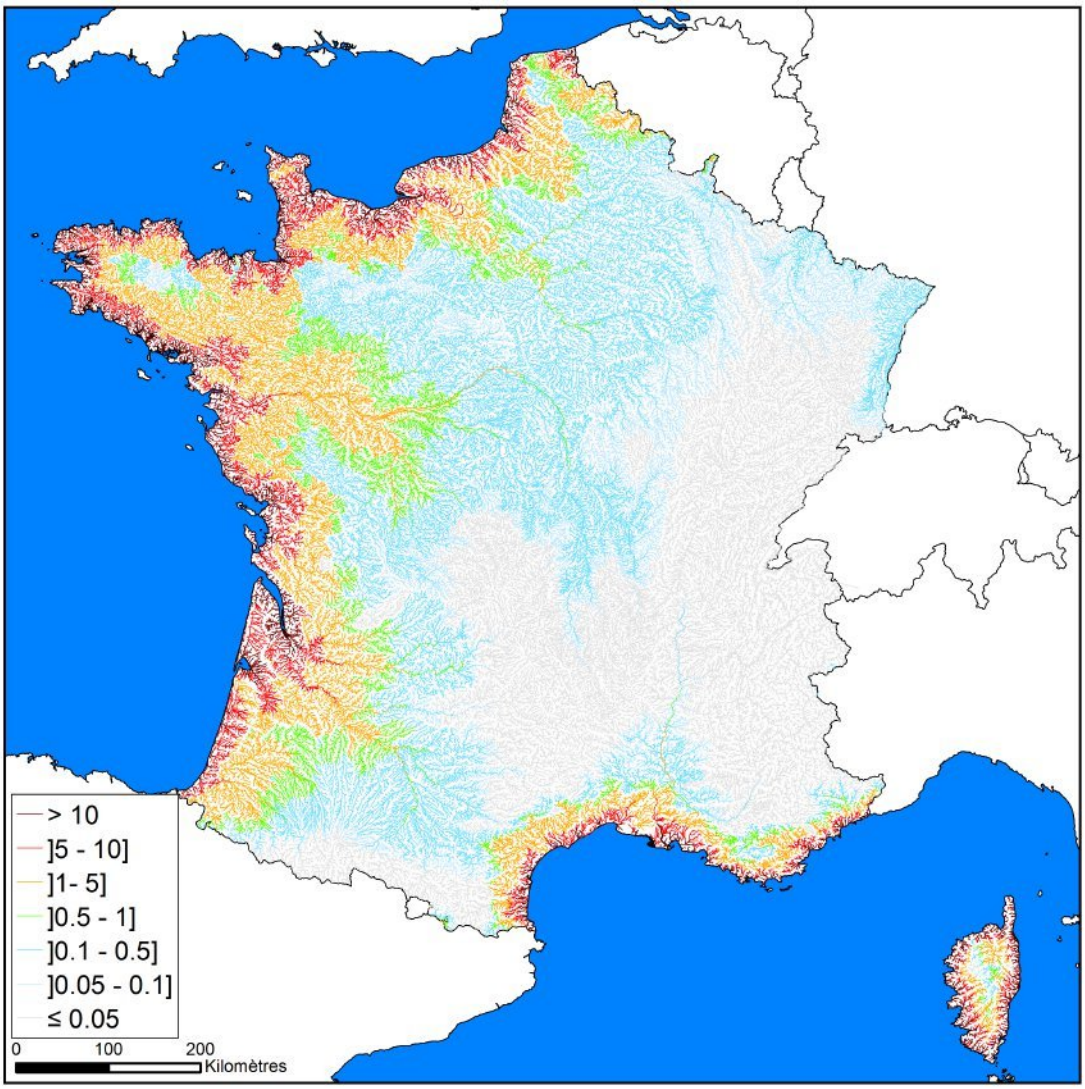

Figure 3.15 – Densities of yellow eels (in eel.100 m^{-2}) predicted in france by the $\Delta\Gamma$ model in 2015.

3.4 Temporal trends

3.4.1 Trend of yellow eel abundance per size class

The temporal trends of yellow eels of large size can be separated into a size class which will produce males (♂) and females (♀) (300-450mm) and a class (>450 mm) grouping all eels which in the end will only silver as ♀. Those two size classes (bottom Figure 3.16) provide a consistent decreasing trend.

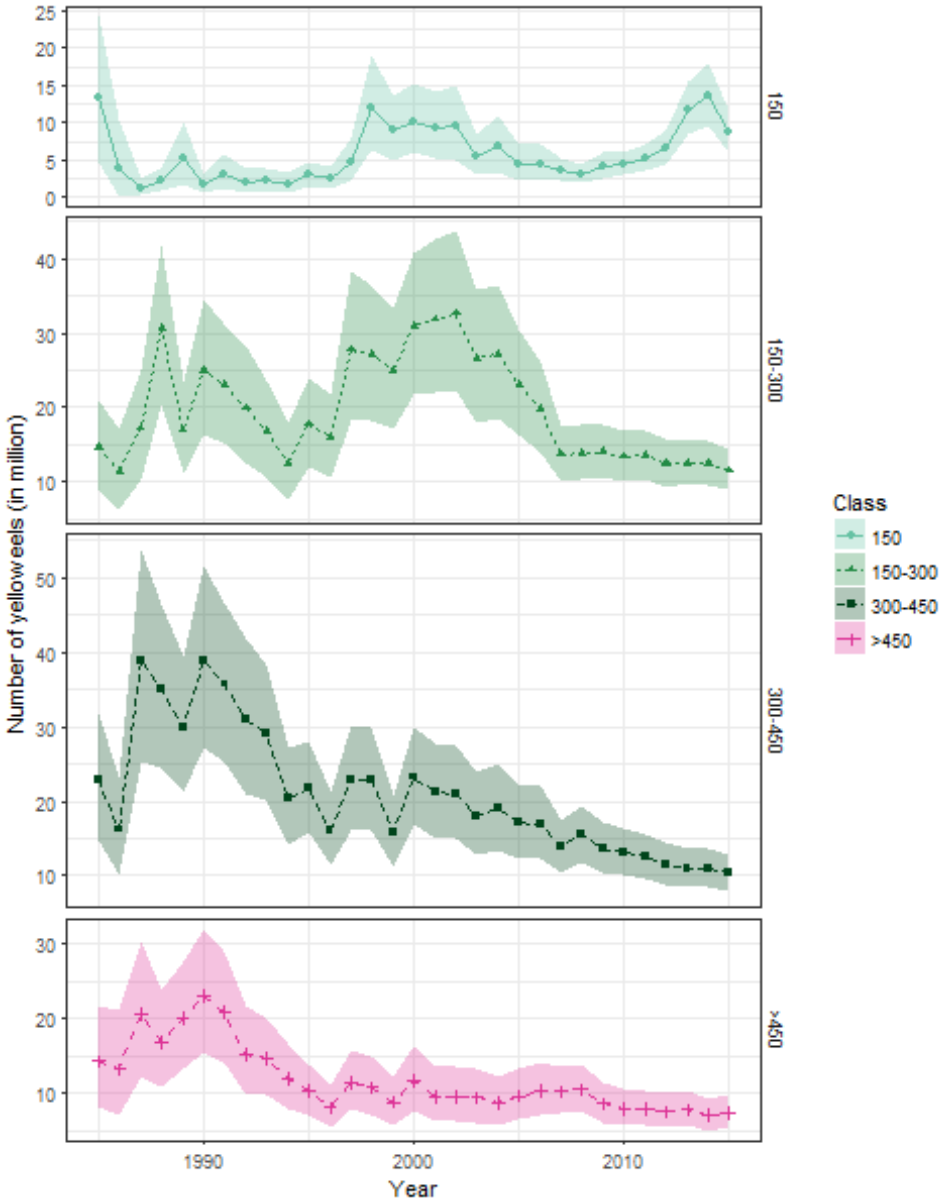

Figure 3.16 – Trend in total abundance of yellow eel in France for size classes <150mm, 150-300, 300-450mm and > 450mm. The shaded areas correspond to 95 % confidence intervals in the models.

3.4.2 Trends in silver eel abundance

The trend in Silver eel abundance is calculated from abundance per size class $Ny_{\tau,i}$ (τ> 300 mm) multiplied by the probability to silver $\Pi_{tau,i}$. From the maximum observed at the beginning of the 1990's, the trend in Silver eel production in France is decreasing. This diminution is however not continuous, and the most important downward trend has been observed from 1990 to 1995 then the segmented regression (Muggeo, 2008) selects a less decreasing trend from 1995 to 2006 before going down again from 2006 to 2015 (Figure 3.17).

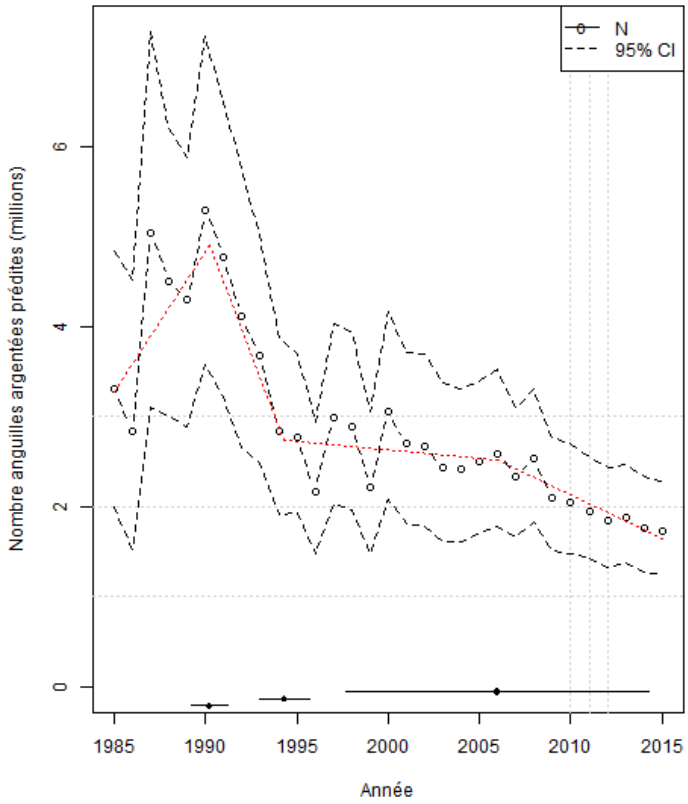

Figure 3.17 – Estimation of the number of Silver eel produced in french streams (Bpot). The confidence interval corresponds to the one reported in formula 2.8, but the uncertainty in silvering function is not accounted for. Points at the bottom of the graph represent break-points and their confidence interval at 95%. The dotted line corresponds to the segmented regression.

3.4.3 Comparison to the recruitment series

The crossed correlations between the recruitment series "Elsewhere Europe" from wgeel (ICES, 2017) and yellow eel abundance series per size class shows significant crossed correlations which are maximum for an 11 year delay for series 300-450 mm and >450 mm, a non significant positive correlation for a 4 year delay for the 150-300 mm series. The 150 mm series is not correlated positively for any delay (Figure 5.9). Figure 3.18

illustrates trends from different series including the delay. The short duration increase (blue-green circle) of the recruitment series from 1991 to 1997 could explain the increase observed four years later in the 150-300 mm series.

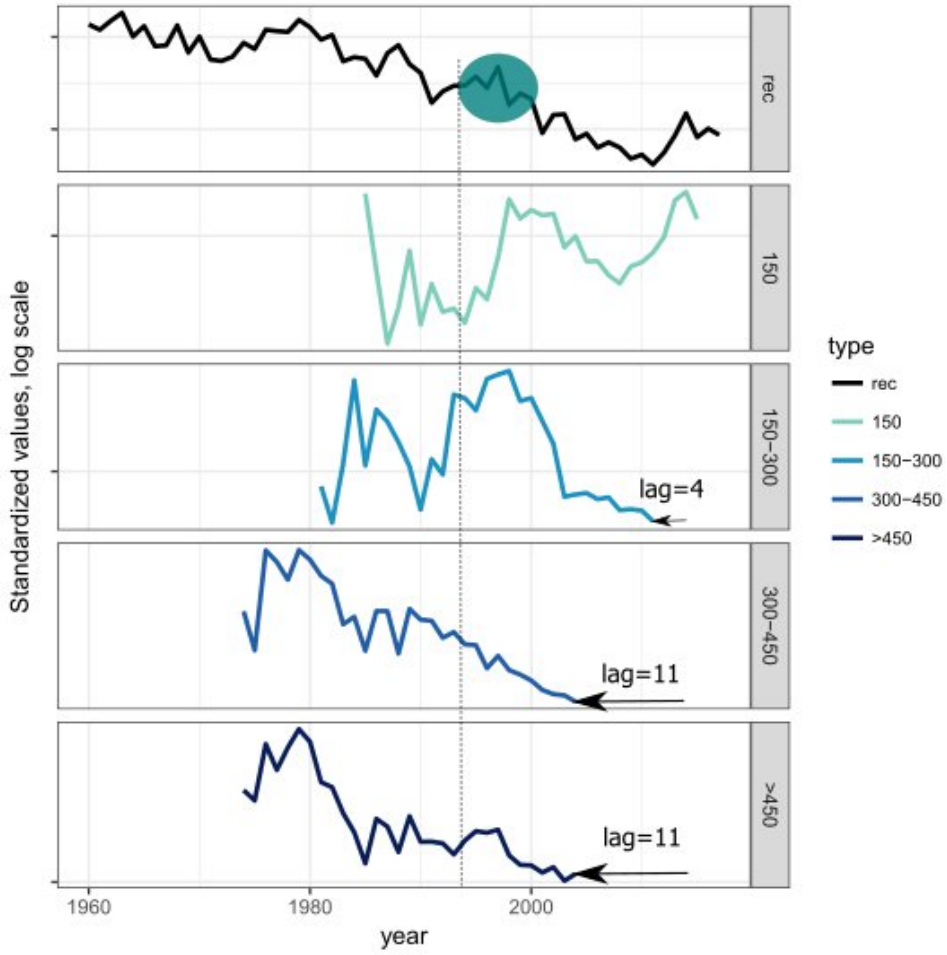

Figure 3.18 – Trend in recruitment observed for the series "Elsewhere Europe" source (ICES, 2017). This trend is compared to series >450 mm (shift 11 years), 300-450 (shift 11 years), 150-300 mm (shifted of 4 years but correlation not significant), 150 mm (no shift).

3.5 Analysis of model responses

3.5.1 Fishing type

The coefficients of the Δ model allow to compare the probability of eel capture among different fishing methods with a reference arbitrarily set to one for ω_{ful} (table 3.2). A full fishing for eel ω_{fue} has the largest probability to catch an eel and presents 60.30, 35.85, 71.34 and 74.84 % of increased chance to catch an eel than eel specific abundance index ω_{eai} , deep habitat point sampling ω_{dhf}, full fishing ω_{ful} or bank fishing ω_{bf} respectively, other conditions (distance to the sea ...) being fixed (Table 3.3).

This relation is illustrated in Figure 3.19. The probability presented is the average of catch probability of eels for the different size class. Catch probabilities fall below

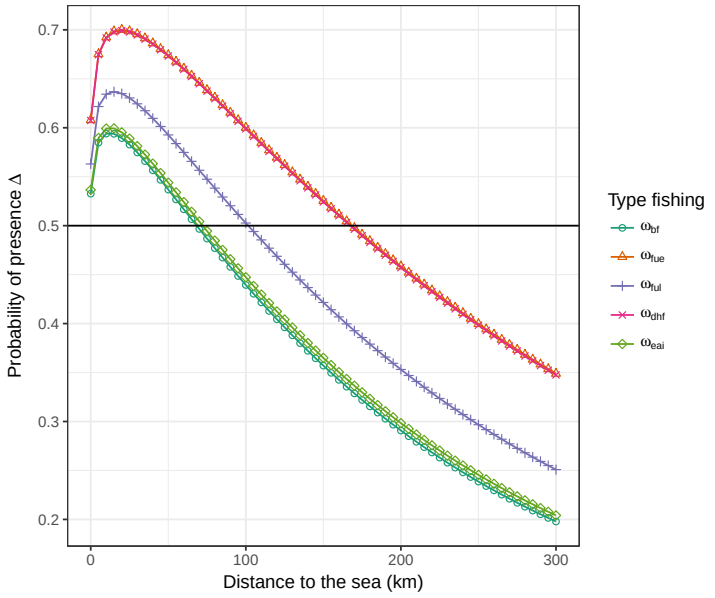

Figure 3.19 – Probability to catch at least one eel on the electrofishing station, comparison of model response for the different prospection methods. Responses are predicted for year 2015, 30 electrofishing points forω_{eai}, 70 points for ω_{dhf}, for a water surface of 600 m^2 ω_{ful} and a bank fishing length of 100m ω_{bf}. According to this choice, responses for ω_{fue} and ω_{dhf} are stacked.

0.5 (less than one in two) to catch an eel at a distance of 65 km for bank fishing ω_{bf}, 100 km for full fishing ω_{ful}, 70 km for eel abundance index ω_{eai}, 165 km for deep habitat fishing ω_{dhf} and 200 km for full fishing for eel ω_{fue}

For the Γ model, one has to keep in mind that the densities predicted only correspond to stations where eel was present. To compare eel catch among different methods, the predictions were made with the following assumptions : 30 points for ω_{eai}, 75 points for ω_{dhf}, a 600 m^2 surface for ω_{fue} and ω_{ful}. For bank fishing ω_{bf} we assume that fishing is performed on two banks on 100m length. Predictions are also made assuming that temperature is equal to the average temperature on RHT segments, a river width of 10 m and that EMU for prediction is Britany (Bretagne). Densities are predicted and expressed relatively to ω_{ful} which has been arbitrarily set to one 3.3.

Table 3.3 – Relative density coefficients for models Γ and Δ, the model coefficients corresponds to the ratio of density using full fishing ω_{ful} as a reference.

Protocol	Coefficient Γ	Relative odd ratio Δ
Deep habitat ω_{dhf}	0.585	1.261
Bank fishing ω_{bf}	0.840	0.980
Full fishing ω_{ful}	1	1
Eel abundance index ω_{eai}	1.085	1.069
Full fishing for eel ω_{fue}	3.615	1.713

These result differ from those of the delta model, deep habitat fishing have a large probability to catch at least one eel, but densities calculated using the electrode range (12.5 m^2) will always be low. The Γ model compensates for the high value in the Δ model. The coefficients for full fishing targetted for ee ω_{fue} are the highest in both models.

For deep habitat fishing ω_{dhf} and eel abundance index ω_{eai}, results are expressed as an average number of eel per point. When comparing those data with densities obtained during full fishing, one obtains a relative coefficient which only accounts for stations where at least one eel was present, as the result includes the effect of the gamma model which has been calibrated on positive abundance values. One has to multiply $\Psi_{eai \to ful}$= 11.431 to convert the index into density $d_{ful} = \Psi_{eai \to ful} \overline{N_{eai}}$ where $\overline{N_{eai}}$ is the average number of eel per point in an eel abundance index, and d_{ful} is the density obtained for a full fishing ω_{ful}.

The coefficient relying eel abundance indices $\overline{N_{eai}}$ and densities obtained during full fishing for eel d_{fue} is written accordingly $\Psi_{eai \to ful}$= 41.319.

Finally, a similar relation can be set up between a full fishing and the average number of eel per point for deep habitat fishing $\overline{N_{dhf}}$ $\Psi_{gm \to ful}$= 21.199.

3.5.2 Difficulty of access

The best adjustment is obtained by using a Difficulty of access A as a combination of cumulated height of dams to the power 1.5 (λ=1.5) and distance to the sea (Formula 2.2, Figure 3.1d,Figure 3.1e). The same model calibrated with different λ value is less performing particularly at the power of 2 which leads to a large increase in the model AIC. In other terms, the transformed height ($\Sigma h_i'(\lambda = 1.5)$) (Figure 3.1d) is more penalizing in terms of access difficulty than the corrected height ($\Sigma h_i'(\lambda = 1)$) (Figure 3.1b) so it gives more weight to large dams. Regarding the relative impact, dams of height 2, 5 and 10 m will have 3, 11 and 31 larger impacts than a 1m dam.

As a consequence of this transformation, the Vendée (south from the Loire), some coastal stream from Brittany, and most of mediterranean streams see their migratory transparency rapidly drop down. The absence of man made obstacles in the downstream part of the Loire is particularly visible on the map of transformed dam heights (3.1b).

The Difficulty of access synthetises information on dam impact and the effect of distance to the sea.

The relative weight of dams when compared to the distance to the sea, as selected in the adjsutment procedure is low, with a β coefficient of 1.7 (Formula 2.3). Rounding up, this means that a 1 m dam will translate into a density loss equivalent to a 2 km uptream progression, or that a 2 m dam corresponds to the loss of 5 river km.

Eels are particularly present at less than 100 km from the sea (74.1 % of estimated numbers), and almost absent beyond 500 km (only 1.8 % of estimated numbers). This result is true for all size-classes (Figure 3.21).

Dams have a lower effect than expected on migratory transparency with only 70.7 % of the population below 20 m of height but still less than 2.6% beyond 50 m. Eels are also predominantly in lowland areas with 92.7% of the population below an altitude of 100 m (Figure 3.20).

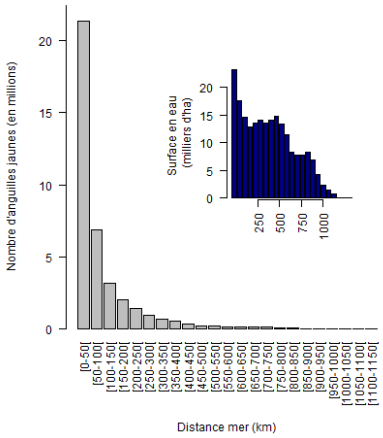

(a) Distance to the sea

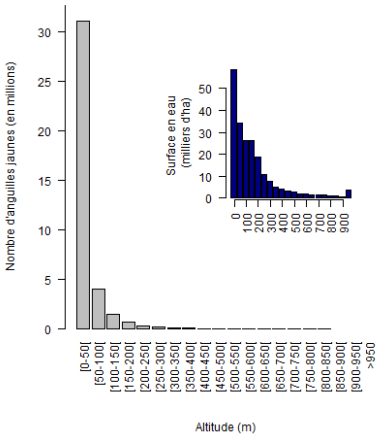

(b) Altitude

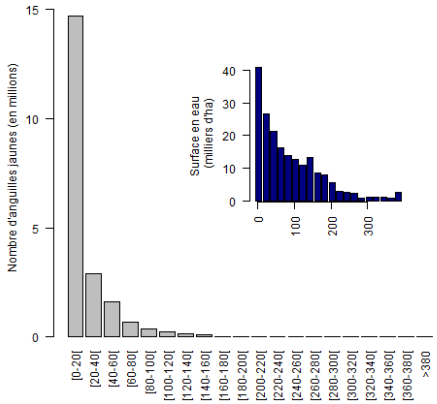

(c) Cumulated dam height

Figure 3.20 – Distribution of Silver eel production in 2015, on the RHT dataset. Results ordered as a function of model variables, ranked in discrete classes and ordered. In navy blue in the corner, the distribtuion of surfaces of the river network calculated on the RHT.

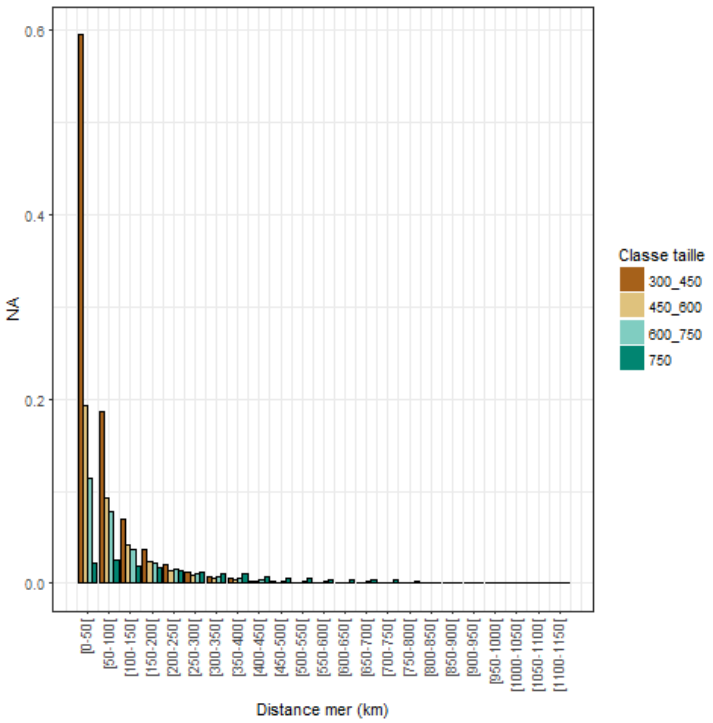

Figure 3.21 – Distribution of Silver eel predicted in 2015, on the RHT dataset. Results ordered according to distance sea class and four size class : even for large eels, the largest number of eel is produced close to the sea.

3.5.3 EMU

60% of the french Silver eel production is done on the Garonne (19.7%), Loire (19.7%) and Seine Normandie EMUs (19.4%). Brittany (13%) and Corsica (3.5%), compensate smaller water surface by high densities resulting from the easy access of water courses (Figure 3.22). The Adour EMU (5.1%) only has a small contribution to the total stock, however, the medocan lakes with a large productivity are not integrated into the EDA model. The Artois picardie EMU only produces 4% of the French production. The Rhine only has a small contribution (0.6%). Meuse data were integrated into the Rhine EMU and this might have caused an overestimation of the production in the french part of the Meuse(Figure 3.22).

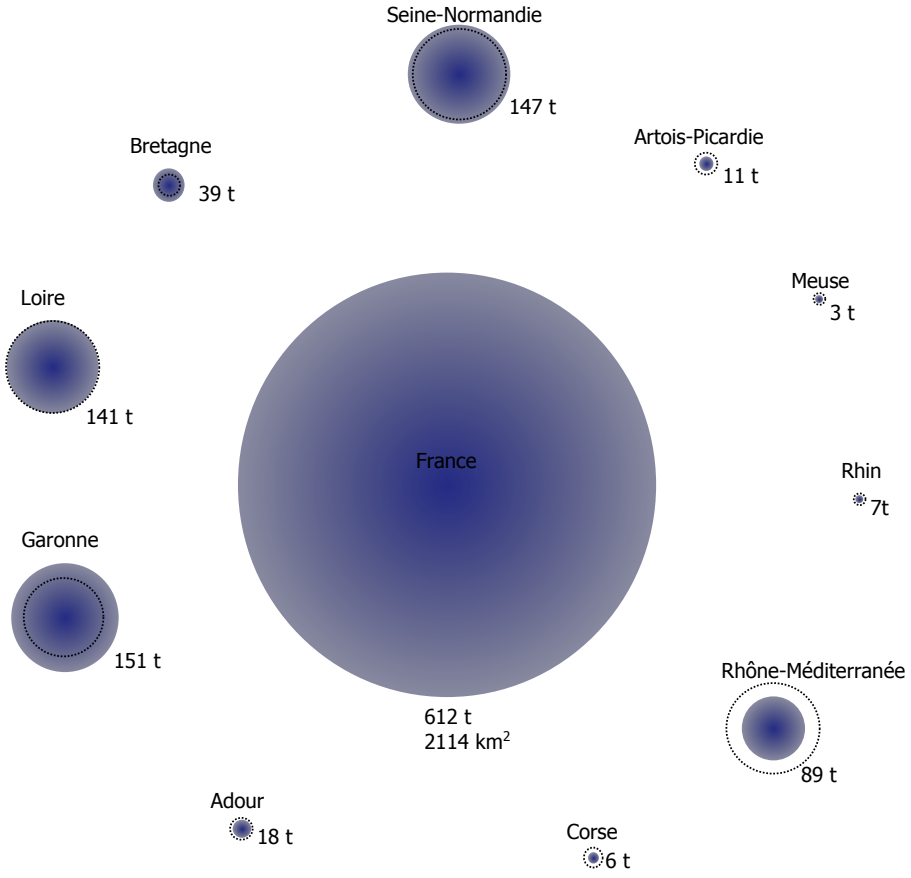

Figure 3.22 – Silver eel production, in biomass, at the scale of France, in 2015, and its repartition per EMU. The size of full circles is relative to biomass, the size of black dotted line circles is relative to the water surface estimated from RHT. EMU's for which the black circle is inside the blue circle have an eel productivity lower than average.

3.6 Silvering rates

Silvering rates calculated by Beaulaton et al. (2015) are summarized in figures 3.23. The combination of silvering rates of the the production model gives a sex-ratio calculated as the proportion of silver eels of class 300-450 mm on all silver eels, assuming that eel less than 450 mm are males (Figure 3.24). The proportion of small females is calculated as the ratio between the number off eels in class 450-600 mm among eel larger than >450 mm (Figure 3.25). Predominantly male sex ratios (in blue) are restricted to a coastal band, and this area will also produce a majortiy (>90%) of small females. Most of the eel repartition area will produce between 50 et 75 % of females. In areas of low densities, the model predicts less than 10% males.

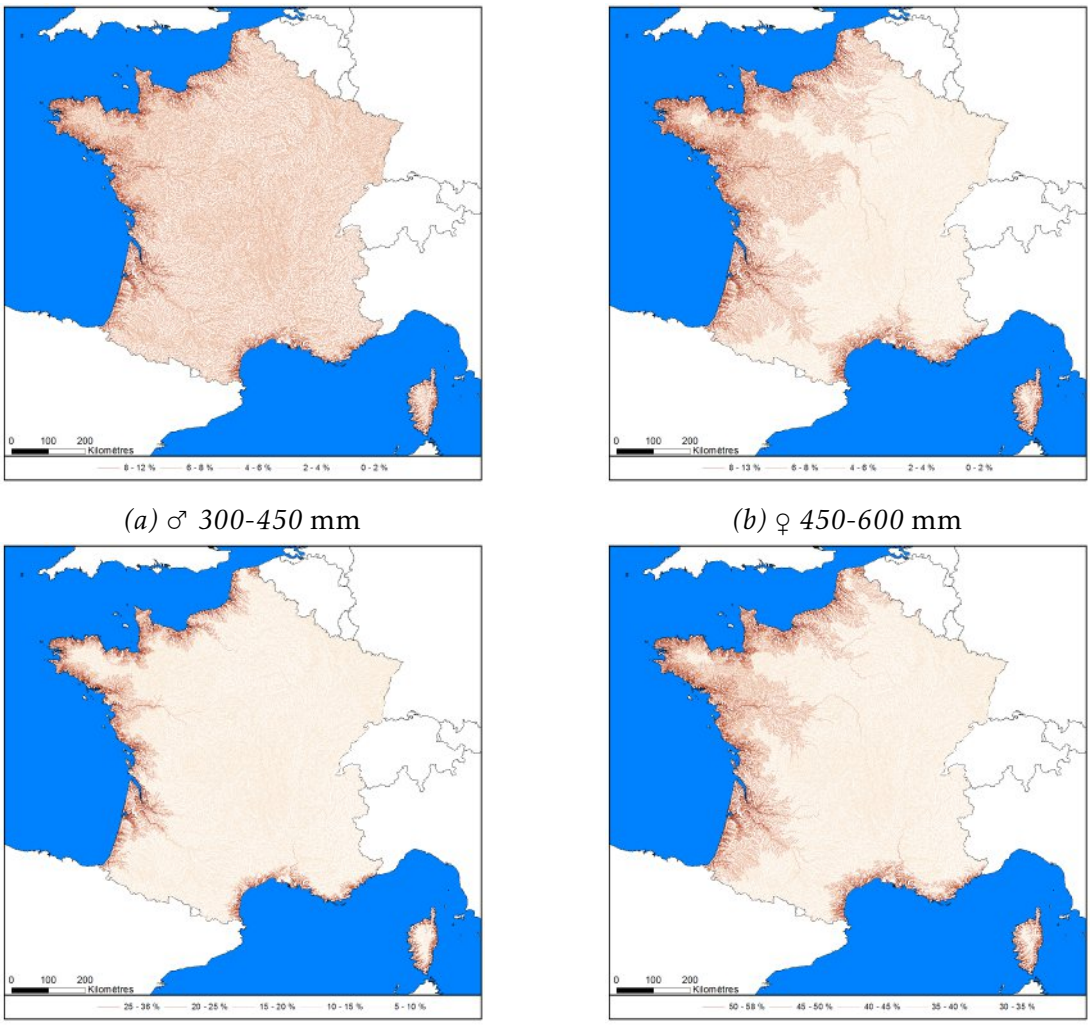

(a) ♂ 300-450 mm

(b) ♀ 450-600 mm

*(c) ♀ 600-750*mm

(d) ♀ >750 mm

Figure 3.23 – Silvering rate (Π) for eels of size 300-450 mm *(male), 450-600* mm *(small females), 600-750 (large females), ⩾ 750*mm *(very large females), warning the percentage on the y axis are not on the same scale, source (Beaulaton et al., 2015).*

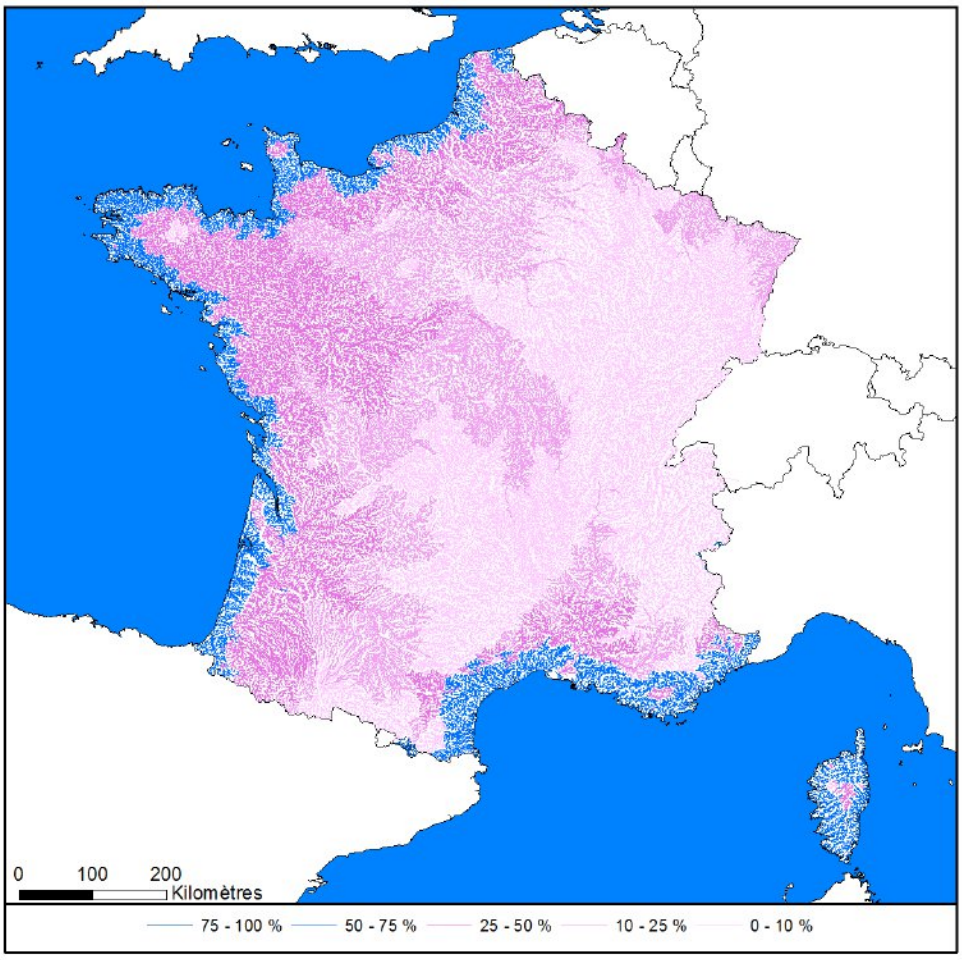

Figure 3.24 – sex-ratio of silver eels predicted per river segment using the silvering model Beaulaton et al. (2015).

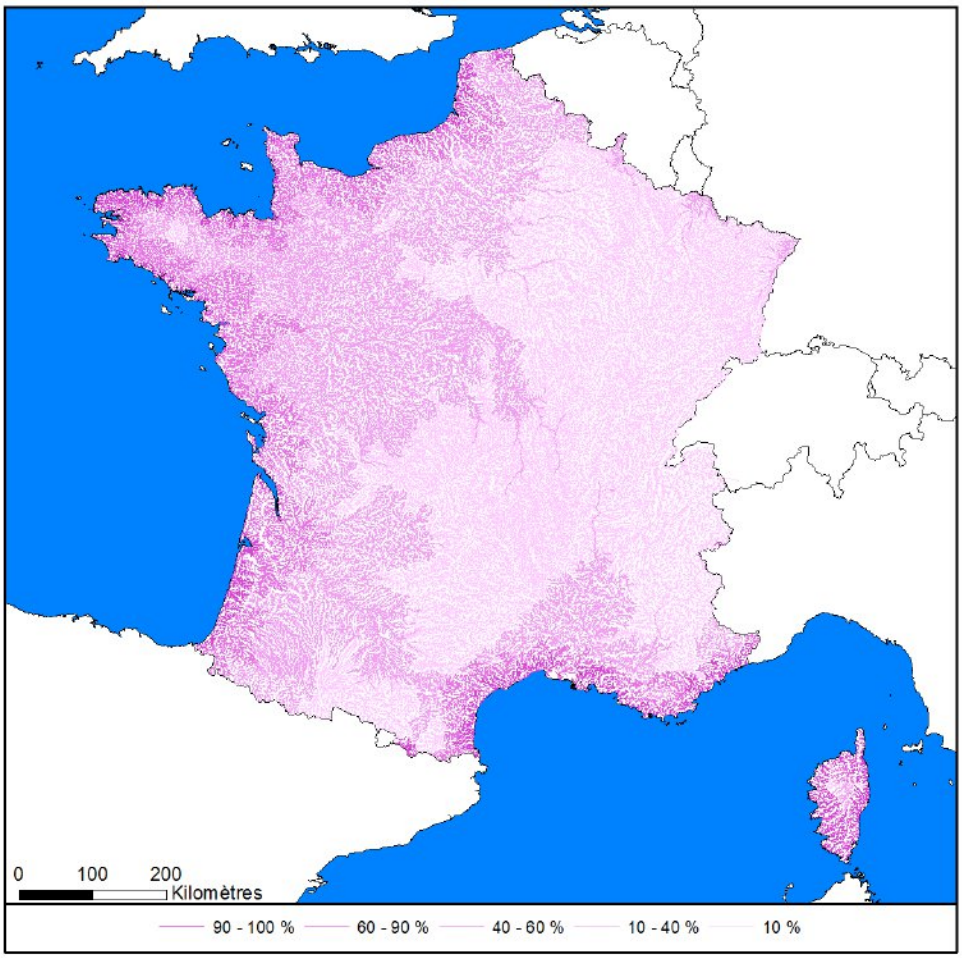

Figure 3.25 – Proportion of small females <600 mm *predicted per river segment in France using Beaulaton et al. (2015) model.*

3.7 Silver eel numbers

The repartition of silver eels produced in France shows a large production in the largest streams (Figure 3.26). However the model is based on the RHT which keeps a theoritical width for streams when those cross lakes. Surfaces of lakes, canal and marshes which contribute for a large part to the French water surfaces are not accounted for. The results of production per size class are illustrated in Figure 3.27. Productions of

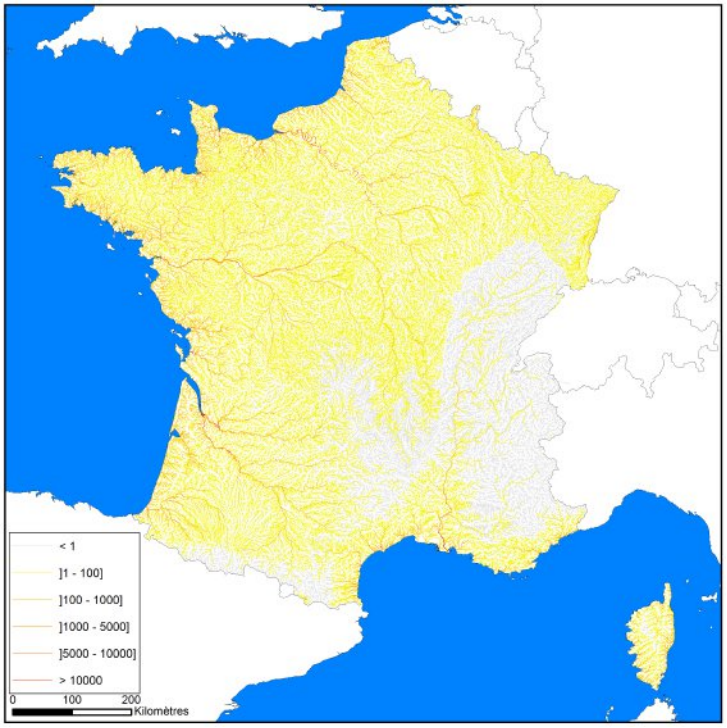

Figure 3.26 – Number of silver eel Ns produced per river segment in France.

different segments depend on how the segments were cut, a larger length will result in more eels. For each riversegment, the total number of Silver eel produced upstream (including the actual production from the riversegment) has been calculated (Figure 3.28). These number are particularly usefull when trying to evaluate the impact of hydropower plants (Briand et al., 2015b).

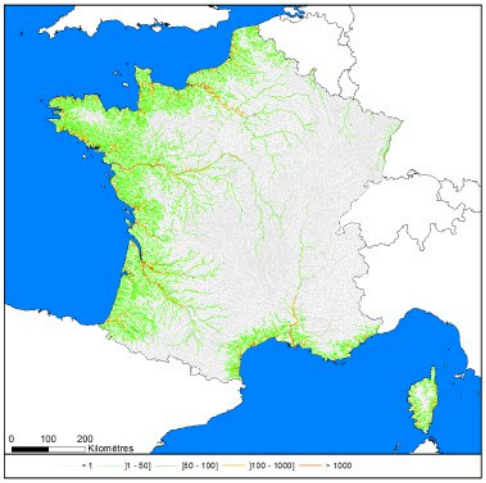

(a) ♂ 300-450 mm

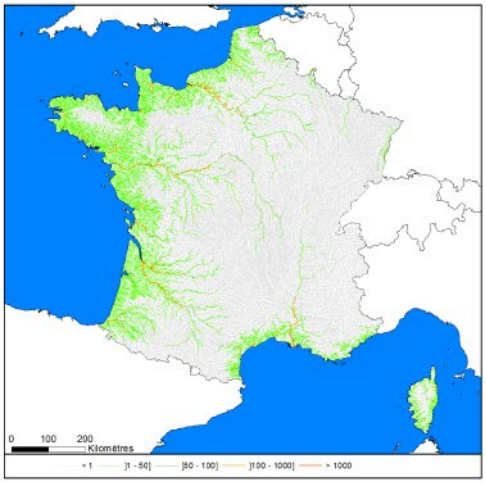

(b) ♀ 450-600 mm

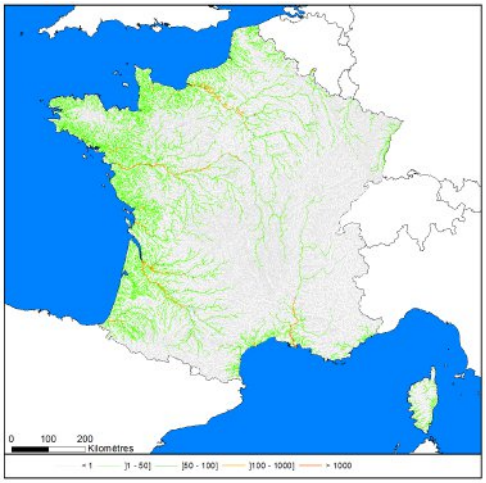

*(c) ♀ 600-750*mm

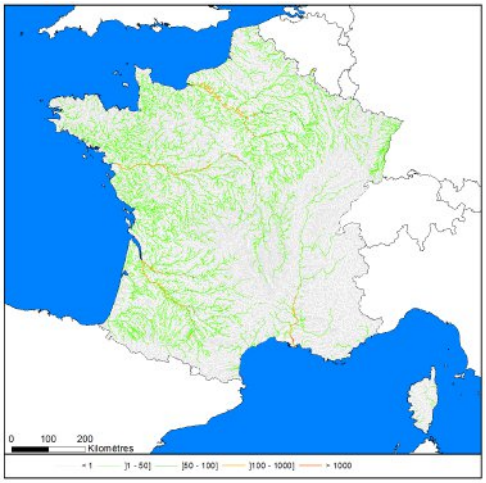

(d) ♀ >750 mm

Figure 3.27 – Number of silver eels Ns produced for size-class 300-450 mm *(male), 450-600* mm *(small females), 600-750 (large females), ⩾ 750*mm *(very large females)*

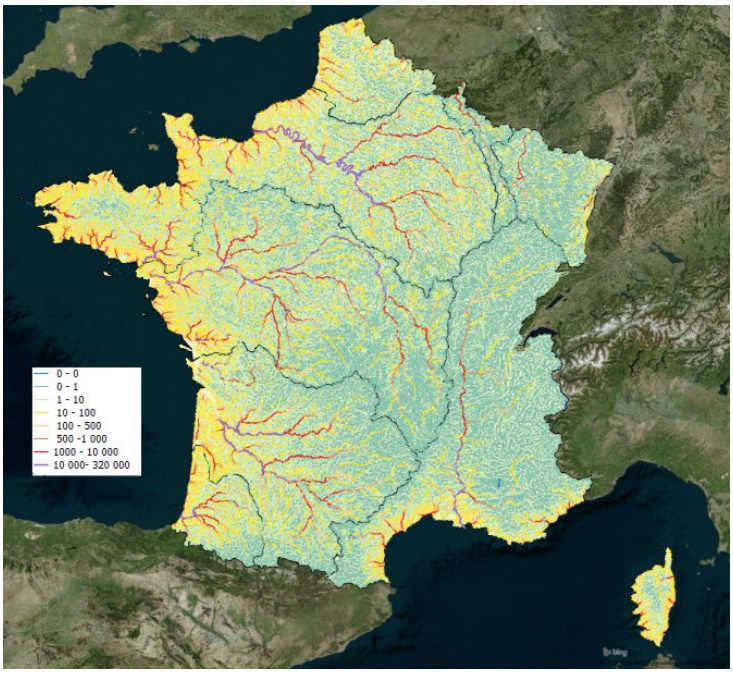

Figure 3.28 – Cumulated number of silver eel Ns produced upstream from each river segment in France, predictions for 2015.

3.8 Synthesis of results per EMU

Water surfaces predicted on RHT are reported in (Table 5.6).

Yellow eel densities correpond to the average densities predicted per riversegments (Table 3.8).

The number of yellow eel produced in France (Formula 2.4) is reported in Table 3.5.

The number of silver eels are deduced from preceeding numbers and silvering rate $\Pi_{\tau,i}$ (Formula 2.5, table 3.6).

Biomasses (Formula 2.6) are calculated using as a reference weights of 103, 291, 593 and 1298 g for the four silver eel size class (Beaulaton et al., 2015).

Table 3.4 – Average yellow eel density in eel/{100*meter*□

.

UGA	2010	2011	2012	2013	2014	2015
Adour	1.90	2.12	1.82	2.72	2.60	2.18
Artois-Picardie	2.60	2.89	2.48	3.68	3.51	2.96
Bretagne	4.72	5.25	4.60	7.19	6.95	5.66
Corse	7.06	7.88	7.08	11.75	11.50	9.04
Garonne	1.26	1.39	1.19	1.76	1.68	1.42
Loire	0.91	1.01	0.85	1.21	1.15	0.99
Meuse	0.13	0.14	0.12	0.16	0.15	0.13
Rhin	0.11	0.12	0.10	0.11	0.10	0.10
Rhône-Méditerranée	0.83	0.93	0.81	1.25	1.20	0.99
Seine-Normandie	1.44	1.59	1.38	2.07	1.98	1.65
France	1.40	1.56	1.35	2.04	1.96	1.63

Table 3.5 – Number of yellow eels (in million) predicted by EDA model

UGA	2010	2011	2012	2013	2014	2015
Adour	1.8419	2.0487	1.7036	2.3595	2.2185	1.9496
Artois-Picardie	1.3821	1.5367	1.3053	1.8989	1.8052	1.5381
Bretagne	4.2554	4.7371	4.1007	6.2439	5.9986	4.9663
Corse	1.0582	1.1816	1.0484	1.6961	1.6523	1.3177
Garonne	7.4948	8.2485	6.7912	8.9195	8.2827	7.5282
Loire	7.5551	8.2856	6.7800	8.6737	8.0051	7.3997
Meuse	0.1076	0.1133	0.0926	0.1043	0.0928	0.0940
Rhin	0.1541	0.1600	0.1324	0.1489	0.1323	0.1343
Rhône-Méditerranée	5.7747	6.3602	5.1894	6.7063	6.2326	5.6919
Seine-Normandie	7.2373	7.9405	6.6391	9.0102	8.4378	7.4997
France	36.8612	40.6123	33.7827	45.7613	42.8580	38.1195

Table 3.6 – Number of silver eel predicted by the EDA model.

UGA	2010	2011	2012	2013	2014	2015
Adour	68 426	65 901	61 167	61 384	58 474	57 499
Artois-Picardie	51 716	50 009	45 866	46 295	43 941	43 237
Bretagne	168 884	161 965	151 330	150 807	144 145	141 436
Corse	38 768	37 158	34 459	33 863	32 571	31 784
Garonne	450 459	428 086	406 165	410 274	394 208	385 042
Loire	432 914	411 792	388 644	394 569	378 760	369 780
Meuse	5 990	5 636	5 013	5 554	5 332	5 089
Rhin	10 331	9 571	8 512	9 589	9 302	8 762
Rhône-Méditerranée	378 749	361 152	340 733	340 669	327 504	320 004
Seine-Normandie	423 320	400 359	379 105	385 288	371 370	361 085
France	2 029 558	1 931 629	1 820 994	1 838 293	1 765 607	1 723 717

Table 3.7 – Biomass of silver eel (in ton*) predicted by the EDA model.*

UGA	2010	2011	2012	2013	2014	2015
Adour	18	17	16	17	16	16
Artois-Picardie	14	13	12	13	12	12
Bretagne	40	39	36	38	36	35
Corse	6	6	6	6	6	6
Garonne	164	153	144	155	149	143
Loire	167	154	145	156	151	145
Meuse	5	4	4	4	4	4
Rhin	10	9	8	9	9	8
Rhône-Méditerranée	112	105	99	105	100	97
Seine-Normandie	175	161	151	164	160	152
France	711	661	620	666	643	618

Fecundity (Formule III) has been calculated from the center of size-class : l_i 528, 671, and 842 mm for the three female size class (Beaulaton et al., 2015).

3.9 Comparison with known productions

An eel monitoring river network Index river (or index sites) has been set up for the monitoring of the French eel management plan. This sites inform in particular on the productivity of silver eels of basins of different size spread over the Bay of Biscay and Channel. To those monitoring are added some estimation of Silver eel stock based on marking recaptures set up on the silver eel fisheries of the Loire and in mediterranean lagoons [3]. The Silver eel production estimated by EDA ($\widehat{Ns}_{BV,t_a}$) at the kilometer point of the monitoring station is calculated by summing silver eel productions estimated on both the station river segment and the river segments located uptream from the station. This estimation is made for a given year t_a which corresponds to the october estimation of EDA (silvering model), for the winter downstream migration $t_a - t_{a+1}$

$$\widehat{Ns}_{BV,t_a} = \sum_{i \in BV, t=t_a} Ns_{i,t}$$

The Silver eel production on the Index river may result from the application of different methods :

- The raw number of eel captured $\mathcal{N}s_{BV,t}$ (■) is provided. In some cases (Frémur river) this number is close to the total number as the trapping device is very efficient.
- Different stock estimation methods have been used, for instance marking-recapture have been used and an estimation of the total production is provided $\widehat{\mathcal{N}s}_{BV,t}$ (▲).
- Finally in some situations, the RHT is not adapted to account for real water surface of the basin S_{obs}, as there are a large number of water impoundment (Frémur) or lakes (Soustons) upstream from the station. In that case, a corrected estimation of the production by EDA is provided (•)

$$\widehat{Ns}_{BV,t} \frac{S_{obs}}{S_{rht}}$$

Figure 3.29 and Table 3.9 give an assessment of the quality of EDA model when compared to Silver eel productions as provided by the index river monitoring program. While the order of magnitude is correct, the production seems to be most often underestimated by the model.

One of the main bias of EDA is a poor accounting of the water surface. The RHT, a theoretical network is very usefull to chain the streams, and calculate the cumulated mortality in turbines (Briand et al., 2015b). However, the examples of the Frémur and Soustons illustrate that when lakes and marshes form a large part of the river basin, the production estimated by EDA is very biased. This bias applies to the whole territory and may explain why in most cases the EDA production underestimates the true production.

[3] outside from the EDA perimeter

Table 3.8 – Productions predicted by the EDA model $\widehat{Ns}$ and calculated from observed counts in site $\mathcal{N}s$. Numbers are estimated (▲), or counted (■). The proportion per size class calculated by EDA for classes 30-45cm, 45-60 cm, 60-75 cm and >75 cm are indicated in table. The sex ratio (♂ proportion) can be read in column 30-45cm.

Site	Index site Year	$\mathcal{N}s$	$\widehat{Ns}$	EDA2.2.1 ♂	♀		
				30-45	45-60	60-75	75+
Somme	2013	1 250 ▲	475				
	2014	.	440				
	2015	1 766 ▲	431	32	17	23	28
Frémur	1996	828 ■	11				
	1997	676 ■	15				
	1999	1 271 ■	12				
	2000	815 ■	18				
	2001	392 ■	13				
	2002	372 ■	14				
	2003	571 ■	13				
	2004	333 ■	13				
	2005	565 ■	12				
	2006	602 ■	13				
	2007	515 ■	13				
	2008	473 ■	14				
	2009	320 ■	11				
	2010	228 ■	11				
	2011	152 ■	10				
	2012	625 ■	9				
	2013	238 ■	10				
	2014	173 ■	9				
	2015	315 ■	9	28	15	23	33
Vilaine	2012	130 000 ▲	44 452				
	2013	119 600 ▲	47 924				
	2014	.	43 289				
	2015	114 186 ▲	43 635	53	24	17	6
Loire	2009	150 000▲	192 404				
	2012	137 000 ▲	152 792				
	2015			34	21	23	22
Sèvre Niortaise	2013	4 897 ▲	1 154				
	2014	17 447 ▲	1 055				
	2015	10 110 ▲	1 049	36	21	23	20

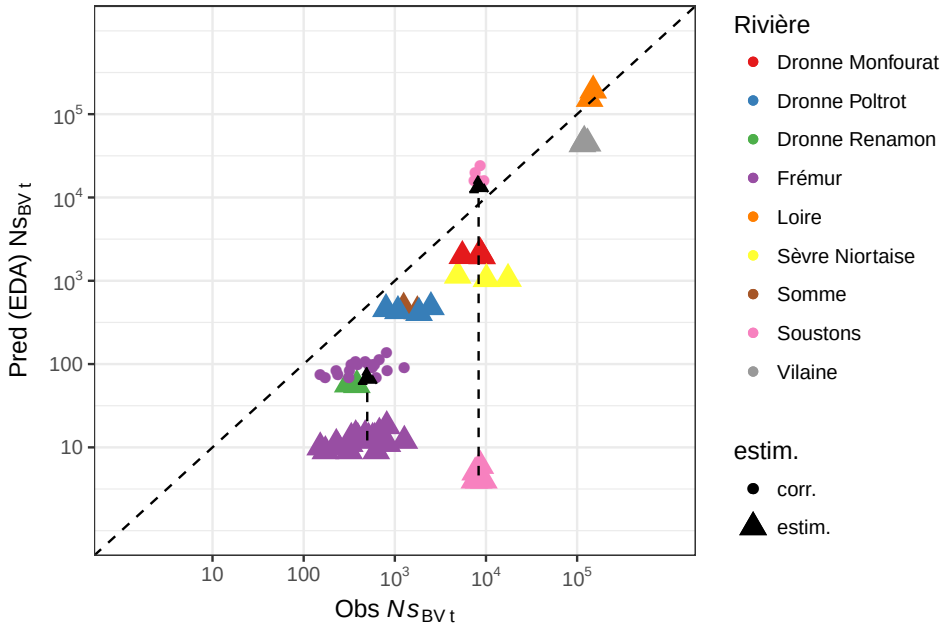

Figure 3.29 – Comparison of production estimated by EDA ($\widehat{Ns}_{BV,t_a}$), index river and fisheries estimated Silver eel run $\mathcal{N}s_{BV,t}$. ▲ estimation of the total annual production, (•) the EDA production has been raised by the surface of lakes and marshes which account for a large part of the water surface in this basin RHT.

Table 3.9 – Productions predicted by the EDA model (continued).

Site	Index site Year	$\mathcal{N}s$	$\widehat{Ns}$	EDA2.2.1 ♂ 30-45	EDA2.2.1 ♀ 45-60	EDA2.2.1 ♀ 60-75	EDA2.2.1 ♀ 75+
Dronne Monfourat	2012	9 082 ▲	1 973				
	2013	8 644 ▲	2168				
	2014	5 504 ▲	1984	37	22	22	20
Dronne Poltrot	2011	2 489 ▲	483				
	2012	1 842 ▲	411				
	2013	800 ▲	458				
	2014	1 082 ▲	433	27	15	21	37
Dronne Renamon	2013	383 ▲	56				
	2014	305 ▲	57	0	0	3	97
Soustons	2011	8 661 ▲	6				
	2012	7 461 ▲	4				
	2013	7 612 ▲	5				
	2014	8 304 ▲	4				
	2015	9 471 ▲	4	82	15	3	0

Discussion

4.1 Temporal trend in escapement

Eel production in France decline steadily (Figure 3.17). The decline was already demonstrated in earlier studies (Jouanin et al., 2012; Poulet et al., 2011; Clavel et al., 2013) If absolute numbers produced by the model must be considered with caution, the trend provided by EDA is certainly reliable. Recently the trend of the smallest eel size has increased. This increase has begun before the recruitment increase measured by ICES. When taking 2008 as a reference this increase to 2014 is of a magnitude of 4.2 which is just slighlty higher than increase of wgeel between 2011 and 2014. Different stages, and different years are involved, so we will not speculate further on this increase (Figure 3.16). Both trend go down after 2014. The large increase from 1997 to 2003 is consistent with the small increase in glass eel recruitment observed on the "Elsewhere Europe" series between 1991 and 1997 (Figure 3.18,blue circle - beware the scale is a log scale), it might also be the consequence of a change in fishing practise with a lower mesh size introduced in nets.

4.2 Search for bias in the time series

The year effect has been tested as a discrete factor in the Δ and Γ models. This transformation allows to put forward sharp cuts in time series, which hints to a change in fishing methods. This use of year as a factor allows to remove a bias in EDA2.0, which was not able to put forward small year to year variation in a simulated population due to a limitation in the number of degrees of freedom in the smoothing function (Jouanin et al., 2012, p70). In contrast a regular trend probably reflects a consistend trend in the population.

Examining the Γ model (Figure 3.8) does not show any such sharp change common to all size classes. In opposite, it shows that the responses have a large variability before the 1990s and this is probably due to the lower number of electrofishing available during this period.

The temporal trends of the Δ model show a sudden decline for the first three size classes after 2005 (Figure 3.4). The importance of this variation needs to be put into perspective by examining the scale of the graph, but it could reflect the change in the sampling strategy by ONEMA after 2005 with the introduction of a strategy to sample deep habitats. It could also to be the consequence of an increased attention brought to eels at this time. From 2013, another possible change comes with the outsourcing of electrofishing operations within the framework of the Control and Surveillance Network. This change does not appear in the global trends of the $\Delta\Gamma$ model (Figure 3.16).

Another bias is probably to put forward when analysing the small sized eel <150 and 150-300 mm, whose probability of capture increase regularly untill the 2000's. This increase could be the consequence of a change in mesh size of hand nets or an increase in the attention brough to eel during the 1990's. The large increase in density after 1998 also corresponds to the introduction of eel specific fishing, with the first electrofishing targeted on eel in the Vilaine. The other electrofishing in RSA have been introduced after 2006 or even 2010 (Figure **??**).

However it must be noticed that Jouanin et al. (2012) have also found larger number of eels from 2000 to 2005 using a dataset which only integrated full fishing operations. In addition, Hoffmann (2008) have also observed a similar increase, while the model was only calibrated locally in the Loire and in Bretagne. So there might really have been an increase at that period.

Finally, it is possible that the installation of eel passes at multiple sites at that time has resulted in an increase in the population of small eels.

The shift of 11 years for the correlation with the recruitment series (Figure 3.18) common for series of yellow eel abundance 300-450 mm and 450 mm is logical as eel of 300-450 mm and more than 450 mm follow the same trends. It remains however difficult to interpret. We would have expected a shift between the trend of the two series, as the fitting of the year effect was made independently on both size classes.

4.3 Electrofishing type

Deep habitat electofishing ω_{dhf} apply a random sampling strategy which allows to describe fish communities in large rivers but are not well adapted to the monitoring of change in fish densities and quantitative estimations (Tomanova et al., 2013). The point sampling strategy allows to explore all habitats presents on a station from the bank to the stream center. The relatively short time of fishing does not allow for a good fishing efficiency as shown by the relative efficiency of full fishing , bank fishing ω_{bf} and point sampling ω_{eai}. However, this method is probably quite efficient to detect the eel presence on a fishing station as the presence probability is quite important for this kind of fishing.

Accounting for deep habitat and bank fishing, allows to increase our dataset, from 9 556 (Jouanin et al., 2012) to 29183 fishing operations. Unlike our previous belief, the combination of different fishing methods is quite efficient to describe the eel repartition a the scale of large basins (Goodwin and Angermeier, 2003). In addition it has the advantage to remove one of the main uncertainties of the EDA 2.0 et 2.1 models : estimating the abundance of eel in deep habitat.

Indeed restricting our dataset to full fishing was leading to under-represent river segments located at a large distance from sources, which means the downstream parts of streams where eel densities are expected to be the largest (Jouanin et al., 2012, Figure 54 p105). The test of the EDA model on the CREPE theoretical river network during the POSE program has put forward the risk of a large overestimation or underestimation of densities in the downstream part of rivers. We think that as a consequence of the large geographical covering of sampling (Figure 5.3) this bias is now reduced. Still it is in this area with the largest densities that we find the largest residuals of the model. The downside of the use of specific sampling protocols is that their use is quite regional, so there might be some geographical bias introduced by the

lack of geographical cover of some sampling (i.e. lots of bank fishing in the Meuse, eel specific sampling in the Northern part of France ...).

Densities measured during standard electrofishing and during eel specific surveys may differ by a factor 10 (Bark et al., 2006; Leprevost, 2007). We find a similar result with a ratio of 3.6 between full fishing for eel and full fishing . We have chosen to use full fishing as a reference. We could have used eel specific fishing as a reference and this choice would have led four time larger biomasses of eel. In practise, eel specific fisheries increase mostly the densities of small eels which are difficult to catch with standard methods. It would thus be necessary to use a crossed effect between eel size and the fishing method in the calibration. In our expertise, eel specific fisheries also target habitats which are the most favourable to small eels (riffles) were densities are large. Still one part of the underestimation of eel productions by the model is possibly the consequence of an underestimation of eel densities by two pass electrofishing methods not specifically targeted for eels.

Full fishing and eel specific full fishing (Paragraph 2.3.2.4) have similar effiencies. A similar result was put forward by Baldwin and Aprahamian (2012) who indicate that there is no difference in fishing efficiency between the two monitoring types. Graynoth et al. (2011) show that statistical method by stock depletion (i.e. Carle and Strub) are possibly biased when they are not based on multiple pass, 3 to 5 pass. The first pass is a good descriptor of the total abundance on the station. This result is particularly true for small eels or eel species with a diurnal behaviour of hiding into the substrate. Relatively to small eels, classical electrofishing methods will probably largely underestimate true abundance. This is probably what translates into the trend of small 150 mm eels. This bias has large influence on stock estimation when the eel density is predicted from the abundance of all size classes and when a single coefficient is used to convert this biomass into Silver eel production (Jouanin et al., 2012). It is likely that our use of large eel size class to predict silver eel biomass in the 2.2 version of the model is less sensitive to that bias.

4.4 Spatial repartition of eels.

Eel densities diminish with the distance to the sea (Smogor et al., 1995; Ibbotson et al., 2002; Aprahamian et al., 2007), and the proportion of female and large sized eel increase (Vélez-Espino and Koops, 2009, fig2). The progressive intrusion of eels of increasing size into water basins has been described in the Loire by Lasne and Laffaille (2007) and is confirmed here by EDA2.2 in a larger scale study.

These authors have also put forward a diminition of large size eels >600 mm near the Atlantic ocean when compared to abundance of size class 300-450 et 450-600 mm. They have attributed this trend to a more precocious silvering of males Lasne and Laffaille (2007). This study does not find the same result, abundance decrease with distance to the sea is less sharp in large eel size classes but the model puts the majority of eels near the sea, whatever their size class (Figure 3.21).

It has not been possible to adjust separately variables describing the cumulated height of dams and the distance to the sea, as these variables are correlated. Combining the two variables into a variable describing accessibility is probably one of the ways to circumvent this bias. However, the model adjusted in this report is not optimal, as shown in underestimation of the numbers on the Frémur. Indeed, some

dams, equipped with eel passes, could have a migratory transparency that is equivalent to that of a dam of low head. This equipment probably concerns a large number of dams (> 2m) located near the sea, and explains the low adjusted impact for the dams, when we compare it to the distance to the sea.

The model would have been much more efficient if the information concerning the equipment of the passes had been used. As it stands, information on equipment was not sufficient to be used at the national level. We recommend, to inform in the national database the presence of passes allowing the passage of eel. This information must be given priority at a distance of less than 150 km from the sea. The equipment dates of these devices are also necessary to allow a time variation of the variable describing the migratory transparency.

Despite these biases, the model describes well the natural decrease of abundances with distance to the sea. However, it was necessary to identify and remove from the calibration set, the stations on which elvers or eels were transported to avoid bias adjustment. This transport greatly disrupts the structure size and density of eels, and also translates into increased fishing effort on the stations concerned. In the case of the Adour, the consideration of these stations is one of the possible explanations for the highlighting of positive trends on abundances in previous calibrations per EMU (Jouanin et al., 2012). The massive transport of glass eels over long distance, as is the case in Ireland or on the Meuse poses difficulties for the adjustment of EDA, especially when data on periods and quantities of glass eel dispersal are not recorded. As a consequence, the EDA model is probably ill fitted to describe eel populations in places where a massive transport has taken place (e.g. Germany). This might be one of the reasons of the very large residuals found on the Rhine border. The cumulated height of obstacles is also badly accounted for border streams, and this might result in systematic bias in border rivers.

Other factors such as flow rates and depth of the river account for some of the variation in eel densities (Goodwin and Angermeier, 2003; Wiley et al., 2004). In the RHT, the depth and width are calculated from the same variables, and the use of the modeled width also accounts for the depth.

To conclude with, eels are presence in a large portion of the French territory, but the area of large density (> 5 ind.100m^{-2}) remains confined to coastal areas (Figure 3.15). Most frequently, they correspond to the presence of small eels <150 mm (Figure 3.14).

4.5 Under estimation of eel production by EDA model

In most cases the production of silver eel is underestimated. This situation is different to the 2012 estimation, because at that time only the counting of eels was available, and methods to raise silver eel production from raw numbers had not been applied except in the case of the Vilaine. For the Vilaine, a more precise study of the vertical position of eels in front of the DIDSON sonar has shown that eels were using the entire water column to migrate in front of the gate, and this has doubled the estimated numbers. The situation is similar in the Sèvre Niortaise, the Soustons stream, the Drone,and the Somme. In all streams the estimations have been raised using marking recapture studies. In the case of the Loire, the production estimated from marking recapture from fishery data is about the same level as that of the EDA model but

The reasons for the difference are not clearly established. In some cases there is a clear

4.6 Importance of large eel in the reproductive stock

Eels larger than >750 mm only account for 1.17% of yellow eel numbers. As their silvering rate is much larger than other size class (on average 36.45 % against 3.54, 3.13, 8.60% for size classes 300-450, 450-600 and 600-750 mm), they represent 10.6 % of Silver eel numbers. They form 38.3% of the total biomass. Finally, fecundity also increases with size. With a free access to the sea, eels larger than 750 mm leaving French coastal areas would contribute to 43.1% of egg deposition of the territory, and probably more if we account for the success of transoceanic migration. This result does not takes into account mortalities during downsteam migration which will increase with a longer route to the sea and with eel size.

4.7 Perspectives

- Use of a stockastic component (De Leo et al., 2009).
- Better integrate dam data by a fully informed database on eel passes location and build time.
- Raise the production of basins by accounting for the true water surface as in (De Leo et al., 2009).

Bibliography

Aprahamian, M.W., Walker, A.M., Williams, B., Bark, A., and Knights, B. 2007. On the application of models of European eel (Anguilla anguilla) production and escapement to the development of Eel Management Plans: the River Severn. ICES Journal of Marine Science **64**: 1–11.

Baldwin, L. and Aprahamian, M. 2012. An evaluation of electric fishing for assessment of resident eel in rivers. Fisheries Research **123**: 4–8.

Bark, T., Williams, B., and Knights, B. 2006. The current status and temporal trends in stocks of the European eel in England and Wales. In ICES 2006. Maastricht.

Beaulaton, L., Chapon, P.m., and Briand, C. 2015. Analyse des données d'argenture acquises en France. Technical report, ONEMA, Rennes.

Belliard, J., Ditches, J., and Roset, N. 2008. Guide pratique de mise en oeuvre des opérations de pêche a lélectricité dans le cadre des réseaux de suivi des peuplements de poissons. Technical report, ONEMA.

Breheny, P. and Burchett, W. 2014. visreg: Visualization of regression models. R package version 2.1-0.

Briand, C., Fatin, D., Fontenelle, G., and Feunteun, E. 2006. Effect of re-opening of a migratory axis for eel at a watershed scale (vilaine river, southern brittany). Bulletin Français de Pêche et de Pisciculture **378**: 67:86.

Briand, C., Beaulaton, L., Chapon, P.M., Drouineau, H., and Lambert, P. 2015a. Eel density analysis (eda 2.2), estimation de l'échappement en anguilles argentées (*Anguilla anguilla*) en france. rapport 2015. Technical report, EPTB-Vilaine, La Roche Bernard.

Briand, C., Legrand, M., Chapon, P.m., Beaulaton, L., Germis, G., Arago, M., Besse, T., De Canet, L., and Steinbach, P. 2015b. Mortalité cumulée des saumons et des anguilles dans les turbines du bassin Loire Bretagne. Rapport d'étude, IAV/LOGRAMI/ONEMA/BGM/INRA, La Roche Bernard.

Carle, F. and Strub, M. 1978. A new method for estimating population size from removal data. Biometrics **34**: 621–630.

Clavel, J., Poulet, N., Porcher, E., Blanchet, S., Grenouillet, G., Pavoine, S., Biton, A., Seon-Massin, N., Argillier, C., Daufresne, M., and others 2013. A New Freshwater Biodiversity Indicator Based on Fish Community Assemblages. PloS one **8**(11): e80968.

De Eyto, E., Briand, C., Poole, R., and O'Leary, C. 2015. Application of EDA (v 2.0) to Ireland Prediction of silver eel Anguilla anguilla escapement. Report 2015. Technical report, Marine Institute, Westport, Ireland.

De Leo, G., MELIÀ, P., GATTO, M., and CRIVELLI, A. 2009. Eel population modeling and its application to conservation management. In American Fisheries Society Symposium, volume 58. volume 58, pp. 327–345.

Durif, C.M., Dufour, S., and Elie, P. 2006. Impact of silvering stage, age, body size and condition on reproductive potential of the european eel. Marine Ecology-Progress Series- **327**: 171.

Durif, C.M., Guibert, A., and Elie, P. 2009. Morphological discrimination of the silvering stages of the European eel. In American Fisheries Society Symposium, volume 58. volume 58, pp. 103–111.

Feunteun, E. 1994. Le peuplement piscicole du marais littoral endigué de Bourgneuf-Machecoul (France Loire-Atlantique). Approche méthodologique pour une analyse quantitative de la distribution spatiale du peuplement piscicole et de la dynamique de certaines de ses populations. Thèse 3ème cycle, Université Rennes I.

Feunteun, E., Laffaille, P., Robinet, T., Briand, C., Baisez, A., Olivier, J.M., and Acou, A. 2003. A review of upstream migration and movements in inland waters by anguillid eels: Toward a general theory. In Eel biology, edited by K. Aida, K. Tsukamoto, and K. Yamauchi, Springer, Tokyo, pp. 181–190.

Feunteun, E., Adam, G., Prouzet, P., and Rigaud, C. 2008. L'anguille européenne: Indicateurs d'abondance et de colonisation. Quae.

Freeman, E. and Moisen, G. 2008. PresenceAbsence: An r package for presence absence analysis. Journal of Statistical Software **23**(11): 1–31.

Germis 2009a. Méthode de pêche Électrique par Échantillonnage par point au martin pêcheur «indice dabondance anguille».

Germis, G. 2009b. Evaluation de létat de la population danguille en Bretagne par la méthode des indices dabondance anguille de 2003 à 2008. Technical report, Ouest Grand Migrateur.

Goodwin, K. and Angermeier, P. 2003. Demographic Characteristics of American Eel in the Potomac River Drainage, Virginia. Transactions of the American Fisheries Society **132**: 524–535.

Graynoth, E., Bonnett, M., and Jellyman, D. 2011. Estimation of native fish density in lowland streams by repeated electric fishing during the day and following night. New Zealand Journal of Marine and Freshwater Research **46**(2): 243–261.

Grothendieck, G. 2017. sqldf: Manipulate R Data Frames Using SQL. R package version 0.4-11.

Hastie, T. and Tibshirani, R. 1990. Generalized additive models. Technical report, Monographs on statistics and applied probability.

Hlavac, M. 2013. stargazer: LaTeX code and ASCII text for well-formatted regression and summary statistics tables. Harvard University, Cambridge, USA. R package version 4.5.3.

Hoffmann, M. 2008. Modélisation de l'impact des ouvrages sur les densités d'anguilles, dans le bassin Loire-Bretagne. Technical report, Onema.

Ibbotson, A., Smith, J., Scarlett, P., and Aprahamian, M. 2002. Colonisation of freshwater habitat by the european eel anguilla anguilla. Freshwater Biology **47**: 1696–1706.

ICES 2017. The report of the Joint EIFAAC/ICES/GFCM Working Group on Eel 310 october 2017. Technical Report ICES CM 2017/ACOM:15, ICES, Kavala, Greece.

Imbert, H., Labonne, J., Rigaud, C., and Lambert, P. 2010. Resident and migratory tactics in freshwater European eels are size-dependent. Freshwater Biology **55**(7): 1483–1493.

Jouanin, C., Briand, C., Beaulaton, L., and Lambert, P. 2012. Eel density analysis (EDA2.x) : un modèle statistique pour estimer l'échappement des anguilles argentées (anguilla anguilla) dans un réseau hydrographique. Technical report, IRSTEA, Bordeaux, FRANCE.

Laffaille, P., Acou, A., and Guillouët, J. 2005a. The yellow european eel (anguilla anguilla l.) may adopt a sedentary lifestyle in inland freshwaters. Ecology of Freshwater Fish **14**: 191–196.

Laffaille, P., Briand, C., Fatin, D., Lafage, D., and Lasne, E. 2005b. Point sampling the abundance of European eel (Anguilla anguilla) in freshwater areas. Archiv für Hydrobiologie **162**(1): 91–98.

Lasne, E. and Laffaille, P. 2007. Analysis of distribution patterns of yellow European eel in the Loire catchment using logistic models based on presence_absence of different classes. Ecology of Freshwater Fish .

Leprevost, G. 2007. Développement d'un indicateur pour caractériser l'impact migratoire sur le stock d'anguille européenne à l'échelle des bassins. Technical report.

MacNamara, R. and McCarthy, T.K. 2012. Size-related variation in fecundity of European eel (Anguilla anguilla). ICES Journal of Marine Science: Journal du Conseil p. fss123.

Miller, M.J., Bonhommeau, S., Munk, P., Castonguay, M., Hanel, R., and McCleave, J.D. 2014. A century of research on the larval distributions of the atlantic eels: a re-examination of the data. Biological Reviews .

Muggeo, V.M. 2008. Segmented: an R package to fit regression models with broken-line relationships. R news **8**(1): 20–25.

Naismith, I. and Knights, B. 1988. Migrations of elvers and juvenile european eels, anguilla anguilla l., in the river thames. Journal of fish biology **33**: 161–175.

Ogle, D.H. 2017. FSA: Fisheries Stock Analysis. R package version 0.8.13.

Pella, H., Lejot, J., Lamouroux, N., and Snelder, T. 2012. Le réseau hydrographique théorique (RHT) fran\ccais et ses attributs environnementaux. Géomorphologie (3): 317336.

Poulet, N., Beaulaton, L., and Dembski, S. 2011. Time trends in fish populations in metropolitan France: insights from national monitoring data. Journal of Fish Biology **79**(6): 1436–1452.

R Core Team 2013. R: A Language and Environment for Statistical Computing. R Foundation for Statistical Computing, Vienna, Austria.

Schmidt, J. 1909. Remarks on the metamorphosis and distribution of the larvae of the eel (anguilla vulgaris, turt.). Meddelester fra Kommissionen for Havundersøgesler, serie Fiskeri Copenhagen **III**(3): 1–17.

Schmidt, J. 1922. The breeding places of the eel. Philosophical Transactions of the Royal Society **211**: 179–208.

Smogor, R., Angermeier, P., and Gaylord, C. 1995. Distribution and abundance of American eels in Virginia streams : test of null models across spatial scales. Transactions of the American Fisheries Society **124**(6).

Stefánsson, G. 1996. Analysis of groundfish survey abundance data: combining the GLM and delta approaches. ICES Journal of Marine Science: Journal du Conseil **53**(3): 577–588.

Svedäng, H., Neuman, E., and Wickström, H. 1996. Maturation patterns in female European eel: age and size at the silver eel stage. Journal of Fish Biology **48**: 342–351.

Tesch, F. 1980. Occurrence of eel anguilla anguilla larvae west of the european continental shelf, 1971-1977. Environmental Biology of Fishes **5**(3): 185–190.

Tesch, F.W. and Thorpe, J.E. 2003. The eel. Blackwell Science, Oxford, UK.

Tomanova, S., Tedesco, P.A., Roset, N., Berrebi dit Thomas, R., and Belliard, J. 2013. Systematic point sampling of fish communities in medium-and large-sized rivers: sampling procedure and effort. Fisheries Management and Ecology **20**(6): 533–543.

Vélez-Espino, L.A. and Koops, M.A. 2009. A synthesis of the ecological processes influencing variation in life history and movement patterns of American eel: towards a global assessment. Reviews in Fish Biology and Fisheries **20**(2): 163–186. doi: 10.1007/s11160-009-9127-0.

Walker, A., Andonegi, E., Apolostolaki, P., Aprahamian, M., Beaulaton, L., Bevacqua, D., Briand, C., Cannas, A., De Eyto, E., Dekker, W., De Leo, G.A., Diaz, E., Doering-Arjes, P., Fladung, E., Jouanin, C., Lambert, P., Poole, R., Oeberst, R., and Schiavina, M. 2011. Pilote projects to estimate potential and actual escapement of silver eel. Technical report, DEFRA.

White, E. and Knights, B. 1997. Dynamic of upstream migration of the european eel, anguilla anguilla (l.), in the river severn and avon, england, with special reference to the effect of man-made barriers. Fisheries Management and Ecology **4**: 311–324.

Wickham, H. 2009. ggplot2: elegant graphics for data analysis. Springer New York.

Wiley, D., Morgan, R., and Hilderbrand, R. 2004. Relation between physical habitat and american eel abundance in five basins in Maryland. Transactions of the American Fisheries Society **133**: 515:526.

Wood, S.N. 2006. Generalized Additive Models: An Introduction with R. Technical report.

Xie, Y. 2014. knitr: A comprehensive tool for reproducible research in R. In Implementing Reproducible Computational Research, edited by V. Stodden, F. Leisch, and R.D. Peng, Chapman and Hall/CRC. ISBN 978-1466561595.

Glossary

ω_{bf} In large or deep stream, or in marshes, electrofishing is performed from the banks of the river). 19, 28, 35, 48, 49, 66, 79

ω_{dhf} In large or deep stream, a point abundance sampling method described as "pêche partielle par points" in Belliard (2008). 19, 28, 32, 35, 48–50, 66, 79

ω_{eai} Eel abundance index electrofishing method. Point abundance sampling, performed in wadable streams, with portable equipment using AC current (Germis, 2009) . 19, 28, 32, 35, 48–50, 66, 79

ω_{fue} Full electrofishing for eel. Electrofishing made with two pass with direct current (DC), the electrode is kept for at least 30s at one point. The whole surface of the stream is prospected) . 19, 28, 32, 35, 48, 49, 79

ω_{ful} Full electrofishing. Electrofishing in wadable streams with two pass) . 6, 19, 28, 35, 48–50

Akaike Information Criterion The Akaike Information Criterion (1973) is a criteria allowing to select the best model, it is a tradeoff betwee the the goodness of fit and the number of independent parameters used in the model. 18, 23

Bbest Silver eel biomass corresponding to recruitment which would have survived if only natural mortality occured, and without glass eel transport. 1

Bcurrent The biomass of silver eel which escape to the sea to perform the spawning migration, corresponds to the year of evaluation. 1

BD Agglo Database of electrofishing from AFB. This version contains data after 2012. 4, 20, 22

BD Carthage Hydrographical reference system for French streams. This geographical database from water agencies and the environment ministry covers 525 000 km of streams. 16

BdMap Database of electrofishing from ONEMA. Historical data used in the model were exported in 2014 and contain data updated to 2012, the most recent data come from another database. 4, 18, 20, 22

Bpot Silver eel spawner biomass produced on the river network before any downstream migration mortality occurs. 47

CCM Catchment characteristation and modelling is a pan-European river database. Based on digital elevation data, it is a hierarchical structured and allows to model the streams in an area from the Atlantic to the Ural. 16

Difficulty of access The difficulty of access A to river segment i is a linear combination of (1) migratory transparency expressed as the sum of transformed power of dam height from the sea, (2) distance to the sea. 4, 27–30, 32, 34, 35, 50, 73, 74

EMU Eel management unit, adminitrative unit which sets the geographical level of reporting by EU countries for the Eel Management Plans. Initally based on Water Framework Directive district, they are adapted by european countries to fit the national eel management. In France Loire and Brittany form two separate EMUs of one same district, because migratory fishes are managed by different regional instances. Some countries have chosen to report at the national level, some others at the regional level, mose are using WFD districts. 14–16, 21, 26, 28, 30, 33, 49, 52, 68, 74

ERS Electrofished River Segment, corresponds to RHT river segments which have been fished at least once, The ERS dataset is used to calibrate the model. 76, 78

GAM General Additive Model, GLM including a quadratic form in the response curves which allows to adjust a non linear response to some terms in the model. In this report, the adjustment is done using the mgcv package, which also allows to calibrate the degrees of freedom in the smoother, which is related to the number of breakpoint points in the response curve. 23

GLM Generalized Linear Model, GLM model corresponding to a generalization of simple linear regression . This approach allows, among other things, to get an error distribution for the response variable that is different from a normal distribution. 26

Index river Index sites located in the different EMUs of the national territory, whose objective is to describe eel population. Recruitment, yellow eel standing stock and silver eel escapement are monitored, both qualitatively and quantitatively. Those sites provide data to compare with the current estimated eel numbers by EDA. 15, 61

ONEMA Office national de l'eau et des milieux aquatiques. 18, 65

RHT the RHT (réseau hydrographique théorique - hydrographical theoretical network) is a physico-chemical database associated with all streams in France which have been divided in river segments. It is built on digital elevation data corrected to fit the French streams. It is hierarchically structured (Pella 2012) . 12, 16, 25, 51, 52, 57, 59, 61, 62, 74, 76, 78, 84, 85

River segment Elementary unit of the RHT. 17, 25

ROE Référentiel des Obstacles à l'écoulement, a database with all man made obstacles, the models uses an extraction from 19 mai 2014, it has not been updated in 2017. Data concerning "bridges" et "dikes" have been removed from the dataset as those types most often do not create an obstacle to eel migration. 5, 17, 26, 38, 82

RSA Eel specific surveys (réseau de suivi anguille), eel monitoring framework collected both on index rivers, and in the frame of specific protocols applied to collect eels in some french regions. 4, 18–20, 22, 66

Silver eel Subadult eel, which at the end of the continental life, will experiences physiological modifications. Those will prepare it to the marine migration towards the Sargasso Sea. This stage migrates downstream in the rivers to the sea. 4, 14, 16, 25, 47, 51–54, 57–59, 61, 62, 67, 68, 85

Part III

Annexes

Annex 1: Equations

Estimated height of dams ($\hat{h}$) (Formula 5.1):

$$\hat{h} \approx exp(log(Q+1) + log(\varphi+1) + damtype : EMU) \tag{5.1}$$

Corrected height (h') for dams (Formula 5.2):

$$h' = \begin{cases} \hat{h}\ si\ h = \varnothing \\ h\ if\ h\ exists \end{cases} \tag{5.2}$$

With h height of dam, h' height corrected by the model, $\hat{h}$ value estimated by the model.

Cumulated height and distance to the sea ($\Sigma h'_{\lambda i}$ and Σl_i) up to segment i (Formula 2.1):

$$\Sigma h'_{\lambda i} = \sum_{i=2}^{n} (h'_{h' \in i})^{\lambda}$$

$$\Sigma l_i = \sum_{i=1}^{n-1} (l_i) + \frac{l_n}{2}$$

$$i \in course\ to\ sea\ \{1 \dots n\}$$

In the previous equation, to avoid to give more weight to small dams we also have

$$h'_{\lambda} = \begin{cases} h'^{\lambda}\ si\ h' > 1 \\ h'\ si\ h' \leqslant 1 \end{cases}$$

With l length of the river segment, λ coefficient tested for the impact of dams $\lambda \in [1, 1.2, 1.5, 2]$

Difficulty of access (A) to segment i (Formula 2.3):

$$A_i = \Sigma l_i + \beta \Sigma h'_{\lambda i}$$

With α coefficient relying the relative impacts of sea distance (km) to the cumulated height of dams (m).

Number of yellow eels for each RHT segment, calculated from model $\Delta\Gamma$ (Formula 2.4):

$$Ny_{,i} = \Delta_{\tau,i}\Gamma_{\tau,i}S_i = d\hat{y}_{i,\tau}S_i$$
$$dy_i = \sum_{\tau=150}^{\tau=750} dy_{i,\tau}$$

Where τ is the eel size class, i the river segment.

Number of silver eels for each RHT segment, calculated from model $\Delta\Gamma$ (Formula 2.5):

$$Ns_{,i} = d\hat{y}_{i,\tau}S_i\Pi_{\tau,i}$$

Silver eel biomass (Formula 2.6):

$$\widehat{Bs}_{\tau,i} = \widehat{Ns}_{\tau,i} * \bar{p}_{\tau,i}$$

Fecundity (Formule III) (MacNamara and McCarthy, 2012):

$$\mathbb{F}_\tau = \widehat{Ns}_{\tau,i} * 10^{-2.992+3.293*log_{10}\bar{l_\tau}}$$

Δ **moel**

$$d_{i,j} > 0 \approx \alpha_1 ti * \tau + \alpha_2 U_i + \alpha_3 \theta_i + \alpha_4 \omega + s(Sp) + s(W_i * \tau) + s(A_{i,} * \tau) + \epsilon$$
$$\epsilon \sim N(0, \sigma),\ \lambda \in [1, 1.2, 1.5, 2]$$

Γ **model**

$$d_{i,j}[d_{i,j} > 0] \approx \beta_1 ti * \tau + \beta_2 U_i + \beta_3 \theta_i + \beta_4 \omega + \beta_5 W_i * \tau + s(log(A_{i,}) * \tau) + \beta_5 H\epsilon$$
$$\epsilon \sim N(0, \sigma),\ \lambda \in [1, 1.2, 1.5, 2]$$

t Year (as a factor),
U_i EMU,
θ July temperature,
ω Prospection protocol,
W_i River width,
A_i Difficulty of access (see formula 2.3),
Sp Electrofished station surface,
τ Size class, the model calculates interactions,
s Polynomial smoothing function,
H Altitude,
$\alpha_1 \dots \alpha_4$ Model coefficient,
$\beta_1 \dots \beta_6$ Model coefficient,
ϵ Model residuals

Annex 2: Comparison ERS-RHT

The ERS data are compared with the river structure network to check for representativity of the electrofishing dataset.

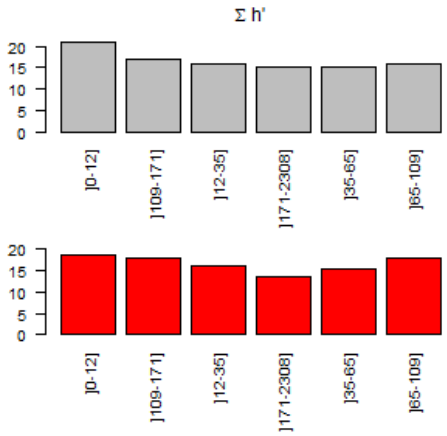

(a) Corrected dam heights (m)

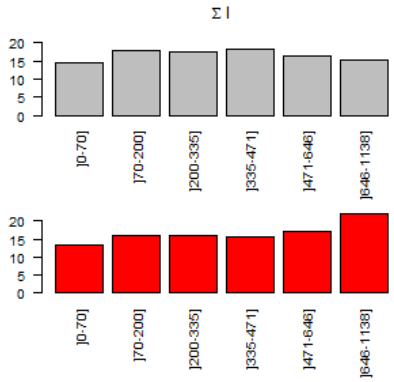

(b) Distances to the sea (km)

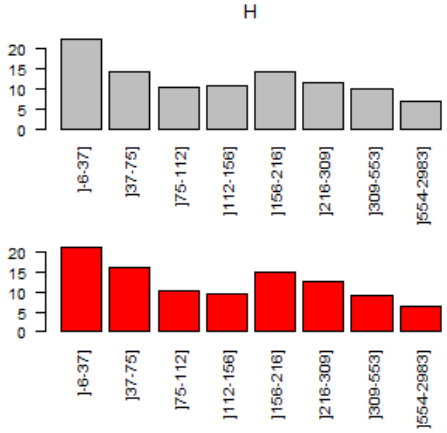

(c) Altitude (m)

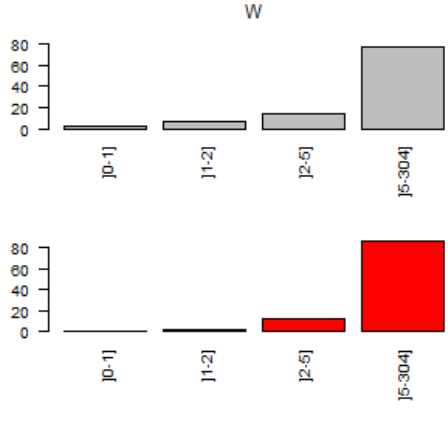

(d) Width (m)

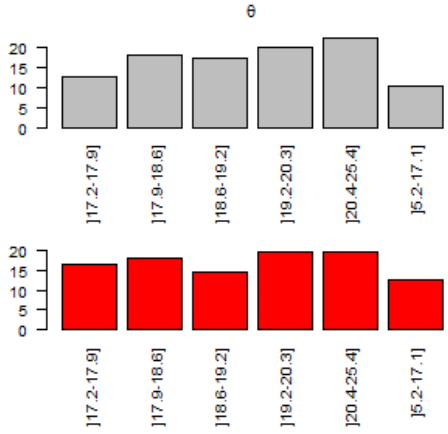

(e) July temperature (C)

Figure 5.1 – For various topological variables used in the model, comparison of the ratio of water surface from one class to the total surface for the ERS dataset ■ and RHT ■.

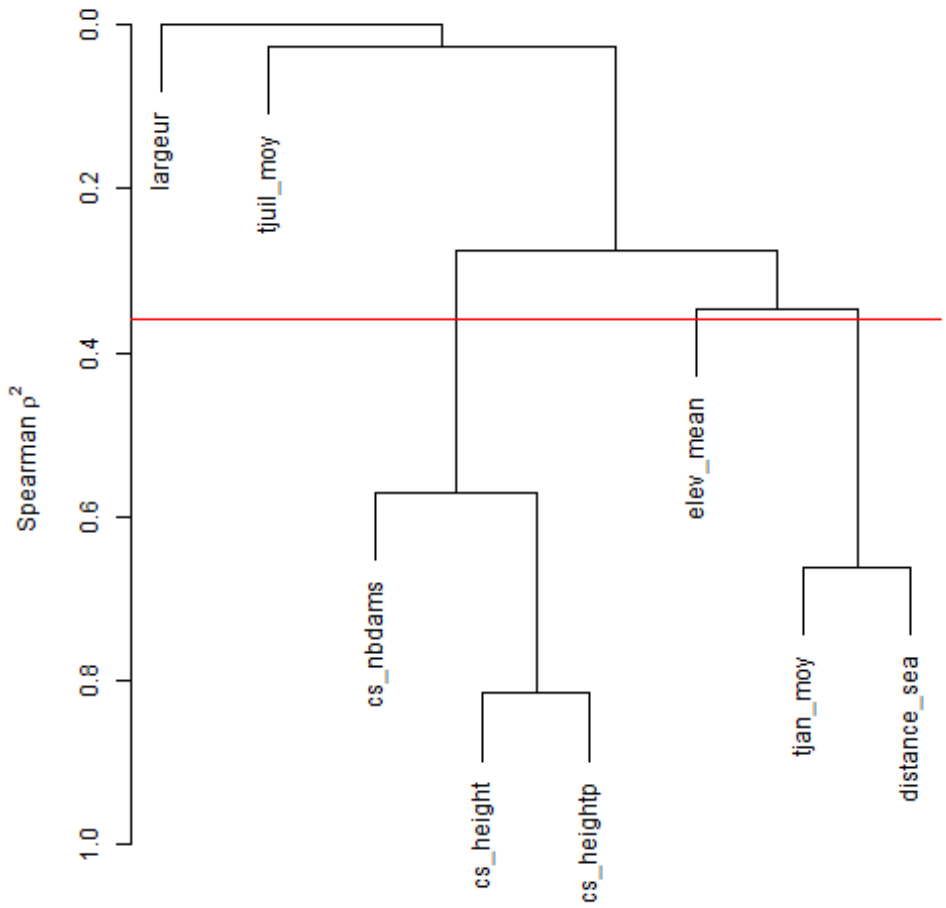

Figure 5.2 – Hiercarchical clustering of the main continuous variables used in the model according to their collinearity.

Table 5.1 – χ^2 test comparing the percentage of water surface for topoligical variables of the model cut in classes for two datasets ERS segments with an electrofishing station used in the model, and RHT.

	Class	RHT $\frac{\sum(S_j)}{\sum(S)}$	ERS $\frac{\sum(S_j)}{\sum(S)}$
	]0-70]	14.6	13.4
	]70-200]	17.8	16.1
Σl	]200-335]	17.6	15.8
p= 0.905	]335-471]	18.3	15.7
	]471-646]	16.3	17.2
	]646-1138]	15.4	21.8
	]-6-37]	22.5	21.1
	]37-75]	14.0	15.9
	]75-112]	10.3	10.3
H	]112-156]	10.8	9.5
p= 1	]156-216]	14.3	14.9
	]216-309]	11.3	12.5
	]309-553]	9.9	9.3
	]554-2983]	6.9	6.5
	]17.2-17.9]	12.4	16.3
	]17.9-18.6]	17.9	18.1
θ	]18.6-19.2]	17.3	14.3
p= 0.944	]19.2-20.3]	19.8	19.3
	]20.4-25.4]	22.4	19.6
	]5.2-17.1]	10.2	12.4
	]0-1]	2.2	0.2
W	]1-2]	6.5	1.7
p= 0.172	]2-5]	14.5	12.4
	]5-304]	76.8	85.6
	]0-12]	21.1	18.8
	]109-171]	17.1	18.0
$\Sigma h'$	]12-35]	15.9	16.2
p= 0.996	]171-2308]	15.2	13.7
	]35-65]	15.0	15.5
	]65-109]	15.7	17.8

Annex 3: Data source for eel specific surveys

Most eel specific survey data have been collected by fishermen associations for fishing and protection of aquatic environment (FD). Other structures working specifically on migratory fishes have also coordinated the work or done the surveys.

Artois Picardie FD59, FD62, FD80;

Seine Normandie SEINORMIG +FD14, FD14, FD27, FD50, FD76;

Bretagne BGM + FD22, FD29, FD35, FD44, FD56, EPTB Vilaine;

Loire et côtiers Vendéens Parc inter-régional du Marais Poitevin + FD17, FD79, FD85 (+ ONEMA IRSTEA) Garonne, Dordogne : MIGADO;

Adour MIGRADOUR;

Rhône Méditerranée ONEMA / BDMAP;

The eel specific survey database follows a simple structure with stations (containing geographical information), operations (common to all table), specific operation results as following.

- op_{epab}. Point abundance sampling (EPA) made from boat (ω_{dhf}).
- op_{epap}. Point abundance sampling (EPA) on foot (ω_{dhf}).
- op_{iaa}. Point abundance sampling (standardized method- eel abundance sampling) (ω_{eai}).
- op_{inv}. Two pass electrofishing for eel (ω_{fue}).
- op_{pcbgb}. Bank electrofishing, from boat (ω_{bf}).
- op_{pcbgp}. Bank electrofishing, from the river bank (ω_{bf}).

And finally a table for eel specific results (Figure 5.4).

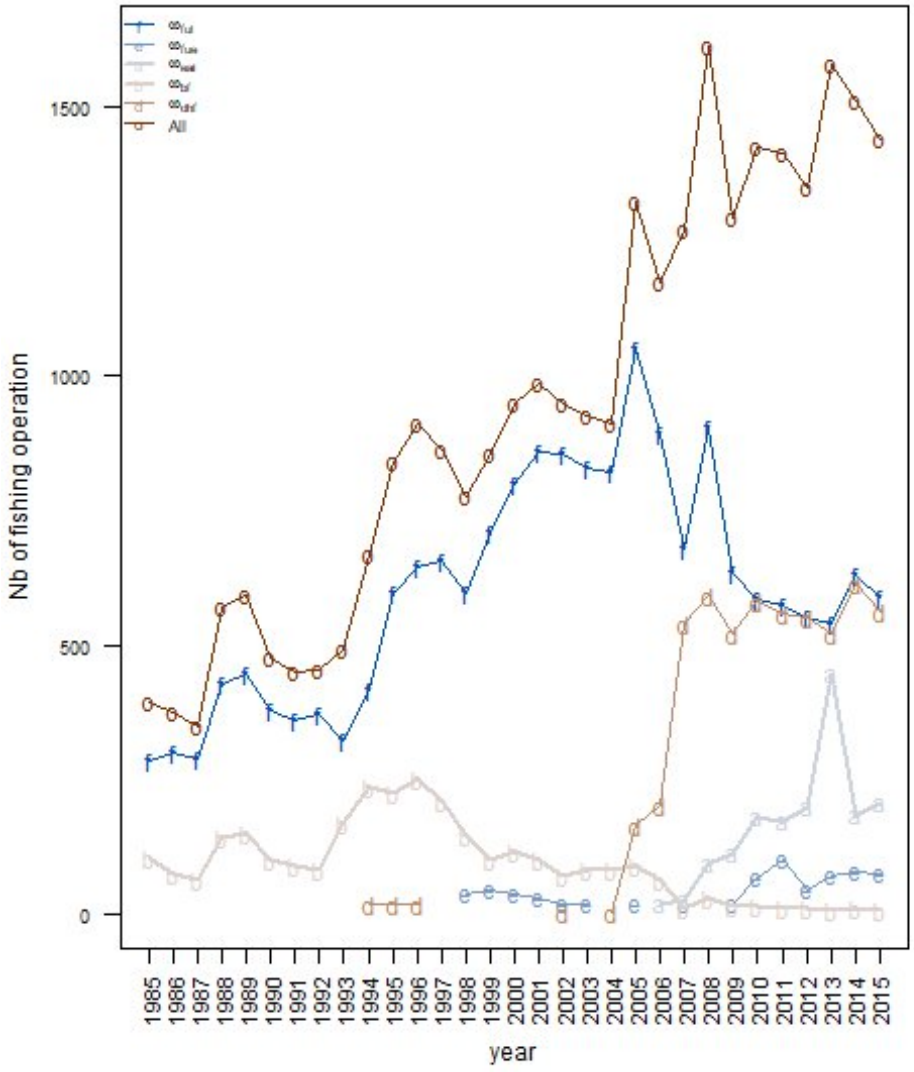

Figure 5.3 – Repartition of electrofishing data, per type of data used in the model, source BDMAP (ONEMA) and eel specific surveys (RSA). The map corresponds to data collected from 2010 to 2016.

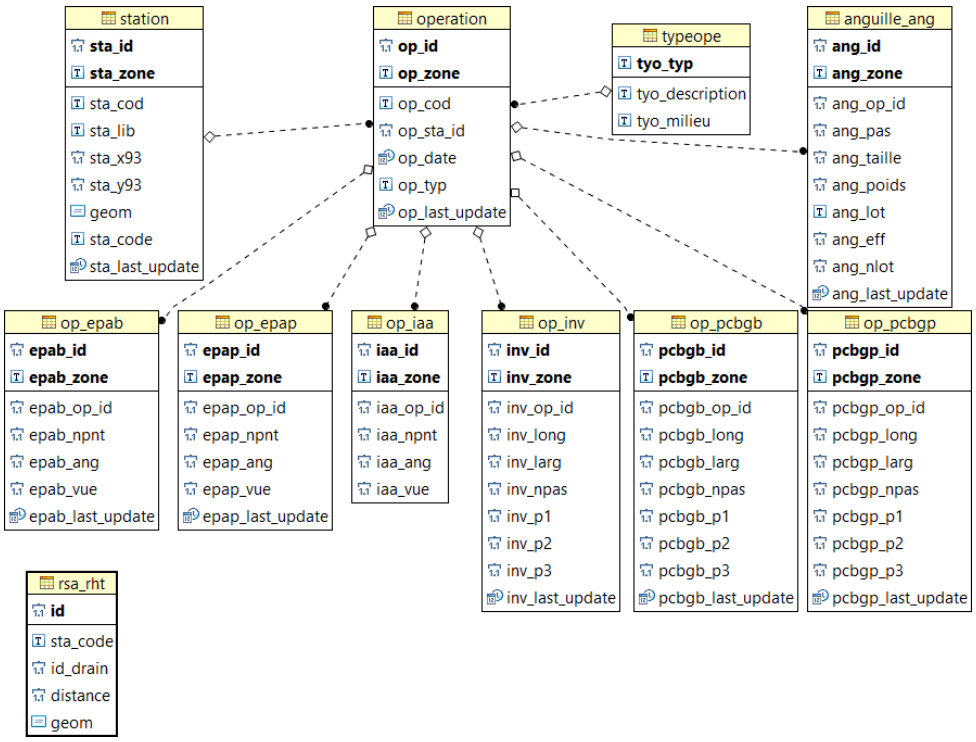

Figure 5.4 – Eel specific survey database diagram

Annex 4: Data for dams

Table 5.2 – Dam height predicted per type of obstacle, by model 5.1

EMU	Dam	Spillway	Gates	Rocks	Other	Unknown
Art	3.93	1.46	0.95	0.72	1.14	1.38
Rhi	2.79	1.30	0.86	0.69	1.81	2.35
Loi	3.44	1.24	1.12	0.98	1.10	1.03
Gar	5.20	1.42	1.12	0.59	0.90	1.11
Sei	2.61	1.39	1.29	0.68	0.82	1.24
Ado	2.85	1.51	0.72	0.86	1.31	1.82
Rho	3.69	1.53	1.12	0.84	0.56	0.27
Bre	3.26	1.40	1.08	0.98	1.14	1.45
Cor	2.68	1.39	0.78	0.70	1.05	1.35

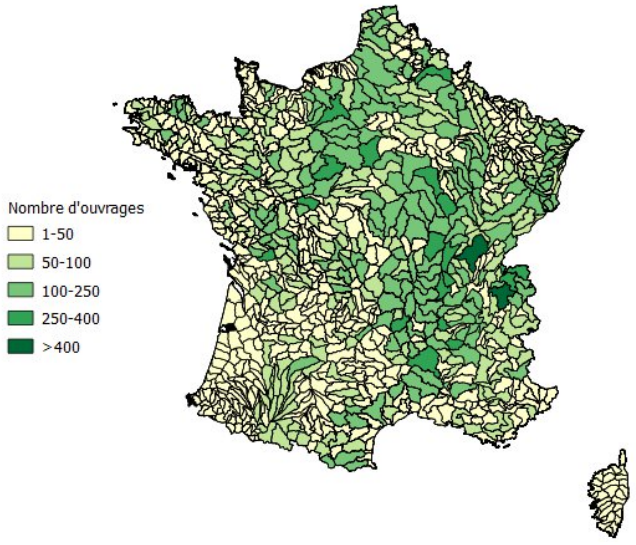

Figure 5.5 – Number of dam per sub-catchment in the ROE, version from may 2014.

Annex 5: Model response variables

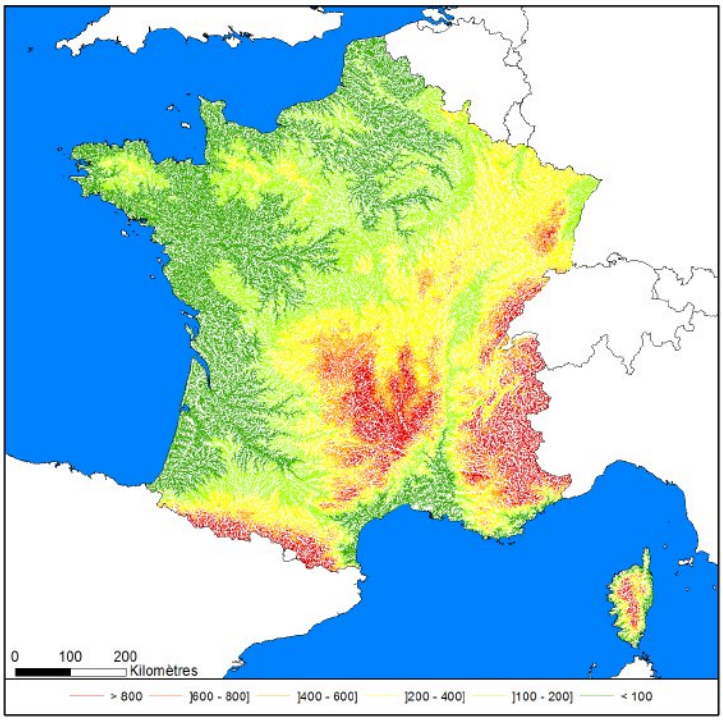

Figure 5.6 – Map of elevations H used in the model.

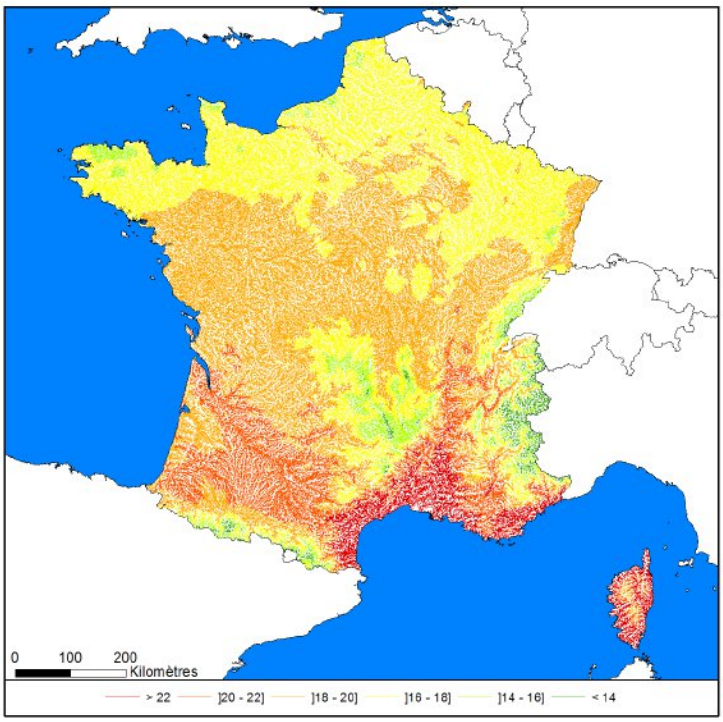

Figure 5.7 – Map of July temperatures θ used in the model, source RHT.

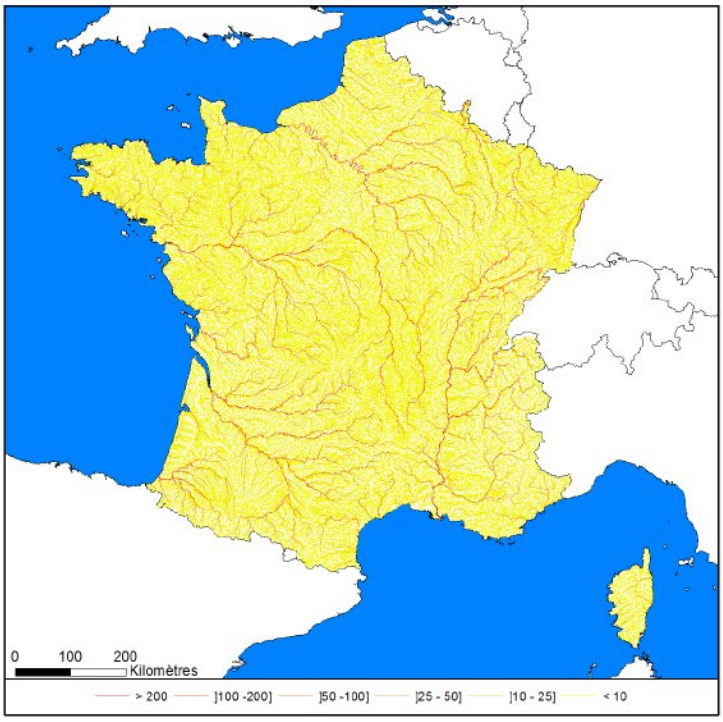

Figure 5.8 – Map of river width W used in the model, source RHT.

Annex 6: Predictions without dams

The number of silver eels is predicted by setting the height of dams to zero. The difference between this number and the production with dams is used in the national reporting to account for habitat effect.

Table 5.3 – Number of silver eels predicted by EDA on the RHT for a prediciton without dams.

EMU	2010	2011	2012	2013	2014	201
Adour	78 810	83 017	65 792	70 099	63 746	64 02
Artois-Picardie	65 034	68 557	54 125	57 540	52 571	52 56
Bretagne	190 001	200 700	158 273	168 256	153 398	153 60
Corse	41 242	43 928	34 031	35 745	33 015	32 67
Garonne	519 462	539 010	435 583	472 194	427 962	429 36
Loire	470 935	486 822	394 575	428 367	389 169	389 64
Meuse	7 939	7 748	6 585	7 365	6 898	6 69
Rhin	11 223	10 550	9 214	10 456	10 032	9 51
RhÃ´ne-MÃ©diterranÃ©e	479 995	503 607	400 856	429 239	390 448	391 33
Seine-Normandie	476 338	490 247	398 338	433 180	395 216	394 04
France	2 340 979	2 434 185	1 957 373	2 112 442	1 922 455	1 923 46

Table 5.4 – Biomass of silver eels ton predicted by EDA2.2.1 on the RHT river network for a prediction without dams.

EMU	2010	2011	2012	2013	2014	2015
Adour	0	0	0	0	0	0
Artois-Picardie	0	0	0	0	0	0
Bretagne	0	0	0	0	0	0
Corse	0	0	0	0	0	0
Garonne	0	0	0	0	0	0
Loire	0	0	0	0	0	0
Meuse	0	0	0	0	0	0
Rhin	0	0	0	0	0	0
RhÃ´ne-MÃ©diterranÃ©e	0	0	0	0	0	0
Seine-Normandie	0	0	0	0	0	0
France	1	1	1	1	1	1

Annex 7: Cross-correlations with recruitment trends

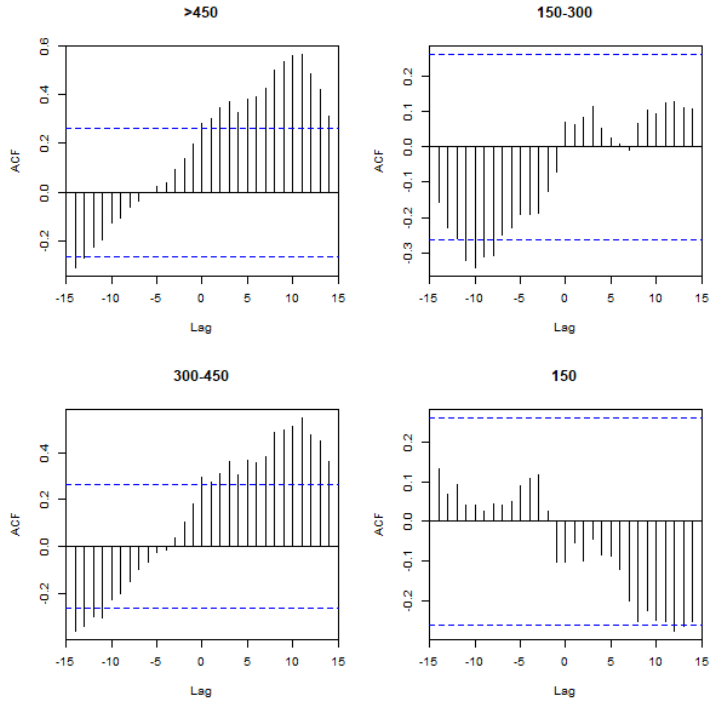

Figure 5.9 – Cross correlation between the "Elsewhere Europe" recruitment time series from ICES and yellow eel abundance time series. The correlation is significant and maximum for an 11 year shift for series >450 mm *and 300-450* mm*, the correlation is maximum and non significant for series 150-300* mm*, and the series 150* mm *is not correlated positively to recruitment.*

Annex 8: Missing electrofishing stations

Table 5.5 – Electrofishing station removed from the dataset.

EMU	Station	Distance sea (km)
Seine-Normandie	bn_85	175
Garonne	gdl_10	232
Rhin	02540017	708
Loire	04030012	661
Loire	04180035	480
Loire	04180047	447
Loire	04410033	371
Loire	04450013	475
Adour	0532B006	223
Adour	05401004	175
Adour	05641005	118
Adour	05641043	113
Rh?ne M?diterran?e	06660102	86

Annex 9: Water surface

Table 5.6 – Water surface calculated on RHT km^2.

UGA	Surface
Adour	85.03
Artois-Picardie	46.46
Bretagne	83.37
Corse	14.80
Garonne	402.17
Loire	474.57
Meuse	42.30
Rhin	86.52
Rhône-Méditerranée	532.08
Seine-Normandie	347.07
France	2114.37